Characterization of OC field radiometers

Ilmar Ansko
Tartu Observatory, ESTONIA

Venice 2024

Spectroradiometry

Radiometer converts the incident radiation (light) into electrical signals (voltage, current, charge) and/or digital numbers.

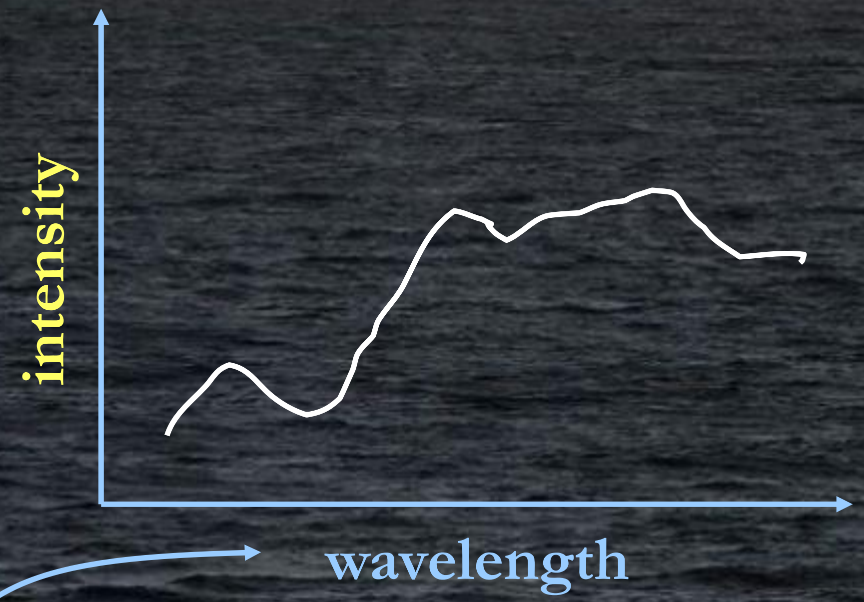

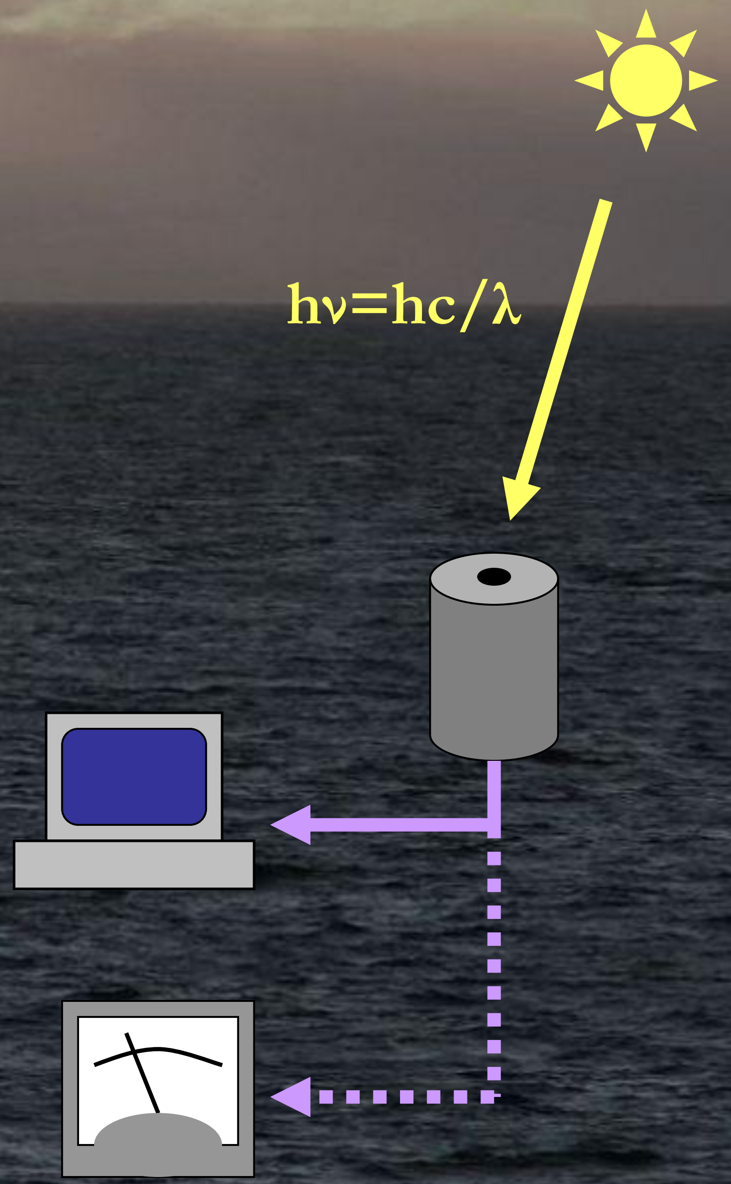

Spectroradiometer (=hyperspectral radiometer)

calibrated

Multispectral radiometer

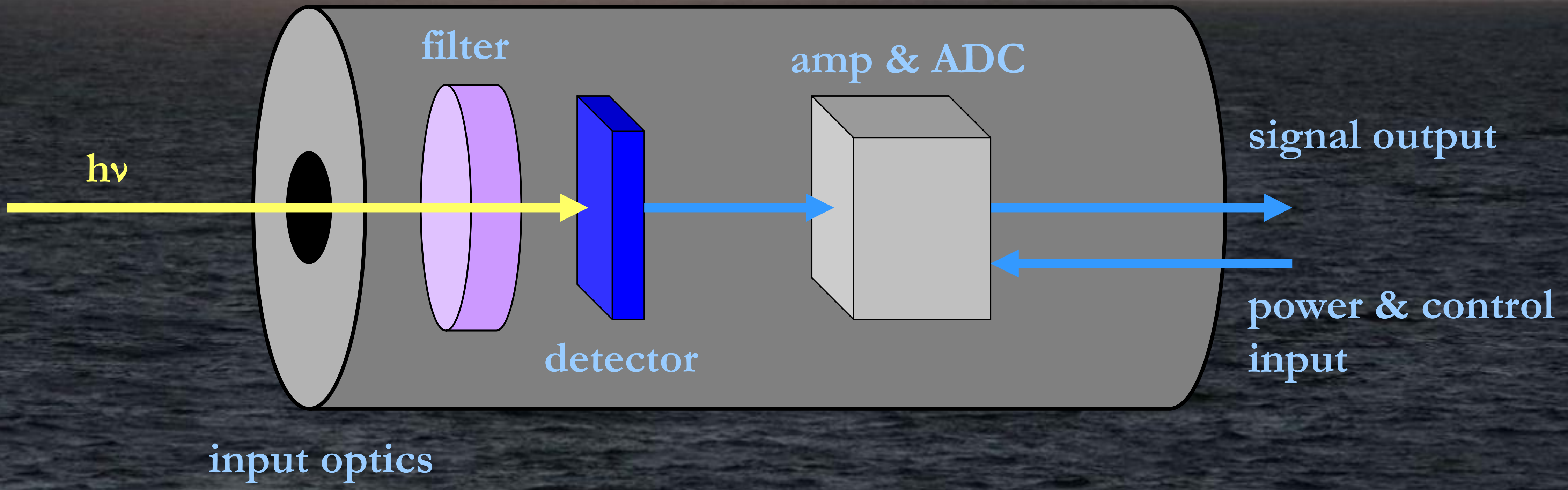

Hyperspectral radiometer

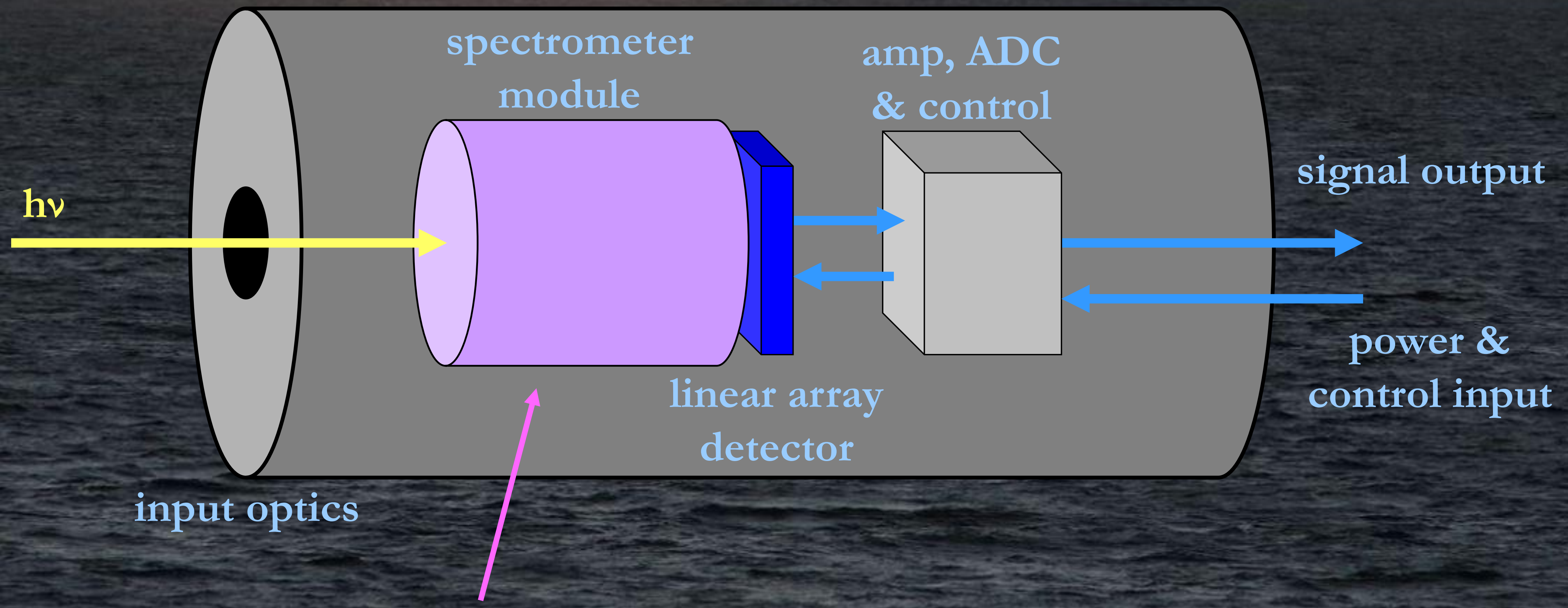

Zeiss, Ocean Optics, Avantes, Hamamatsu, Ibsen, Wasatsch, …

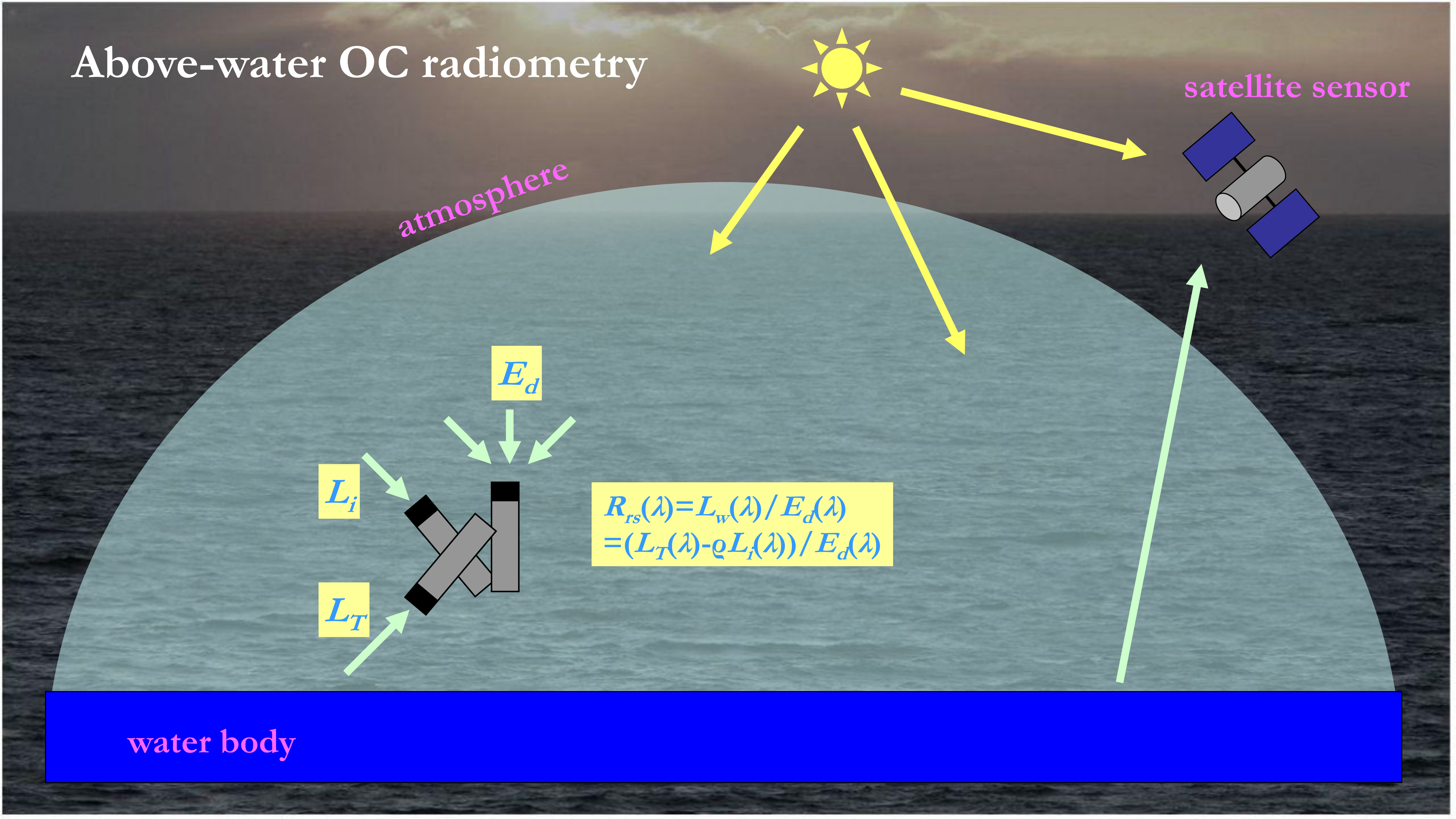
Above-water OC radiometry
satellite sensor
atmosphere
E_d
L_i
L_T
$R_{rs}(\lambda)=L_w(\lambda)/E_d(\lambda)$
$=(L_T(\lambda)-\varrho L_i(\lambda))/E_d(\lambda)$
water body

Radiometric quantities

The basic quantity in radiometry is optical power (=radiant flux), measured in watts; 1 W= 1 J/s.

"optical" in OC radiometry means ≈(300..1000) nm.

Spectral representation: power is measured separately for each wavelenght (hyperspectral radiometry).

Integral representation: power is integrated over certain wavelength range (multispectral radiometry).

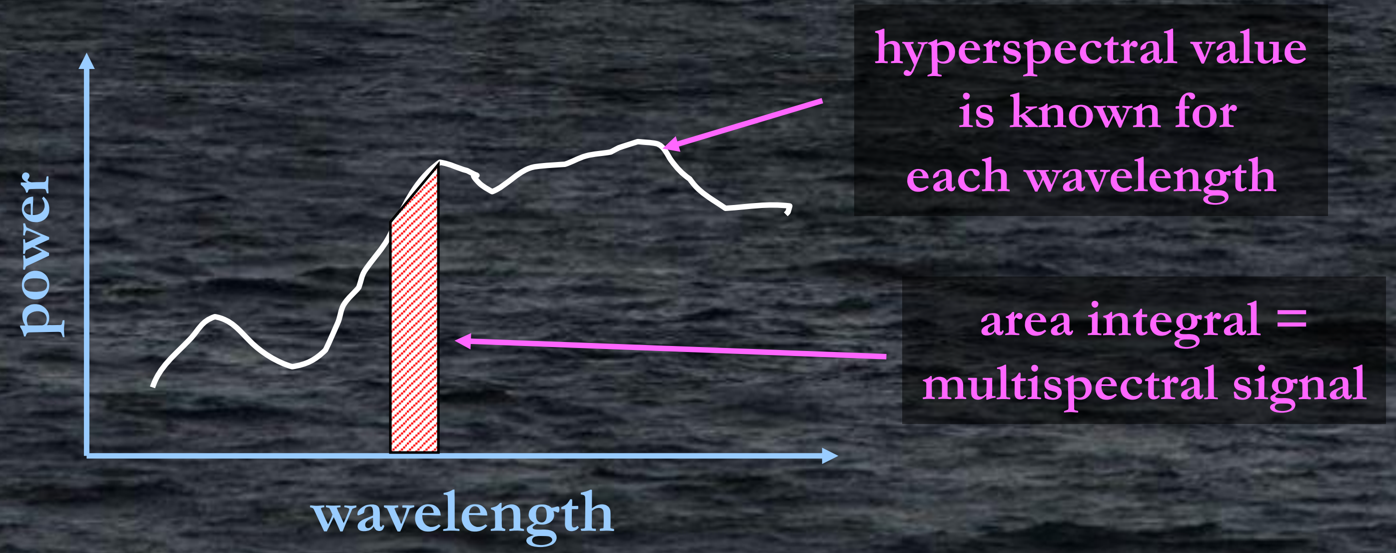

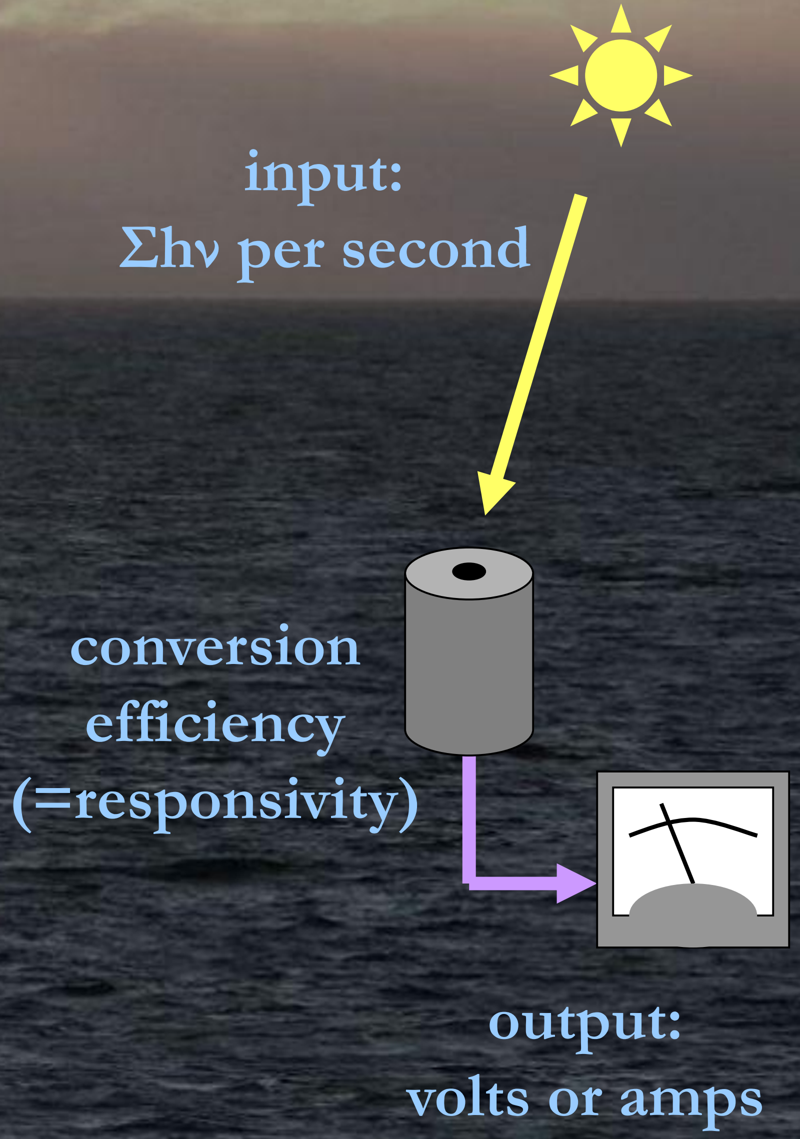

Radiometric quantities: radiance and irradiance

Radiance $L(\varphi,\theta,\lambda)$: power, emitted from the unit area of the source into unit solid angle.
Unit: $W\cdot m^{-2}sr^{-1}$ or $W\cdot m^{-2}sr^{-1}nm^{-1}$

Irradiance $E(\lambda)$: total power, emitted from the unit area.
Unit: $W\cdot m^{-2}$ or $W\cdot m^{-2}nm^{-1}$

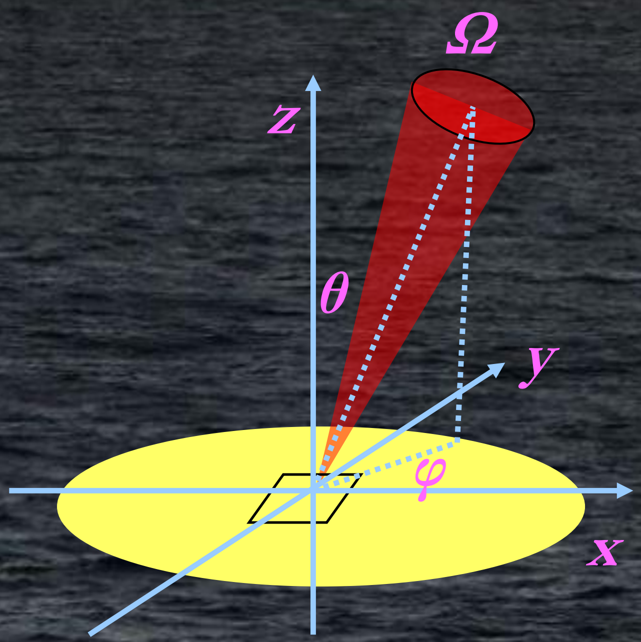

$$E(\lambda)=\iint L(\varphi,\theta,\lambda)\,\mathrm{d}\varphi\,\mathrm{d}\theta$$

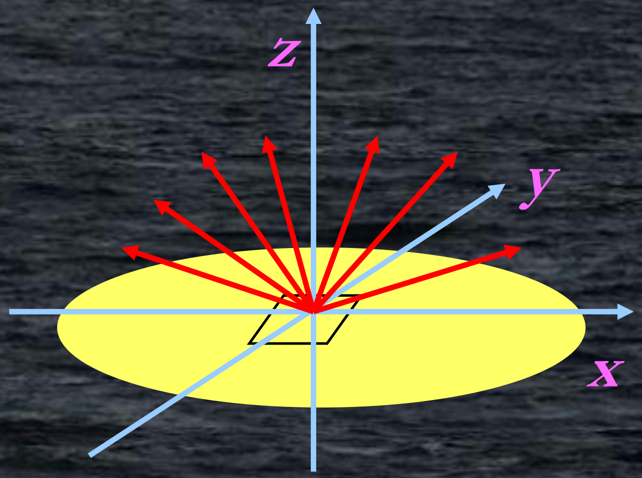

For hemisphere: $\Omega=\iint \mathrm{d}\varphi\,\mathrm{d}\theta=2\pi\ sr$

Special case: Lambertian surface

Radiance $L(\varphi,\theta,\lambda)$ does not depend on the polar angles φ,θ:
the surface is perfectly diffuse (e.g. white snow, Sun's surface):
$E(\lambda)=\iint L(\varphi,\theta,\lambda)\mathrm{d}\varphi\mathrm{d}\theta=\pi L(\lambda)$
Diffuse (Lambertian) targets are widely used for calibration and characterization purposes.

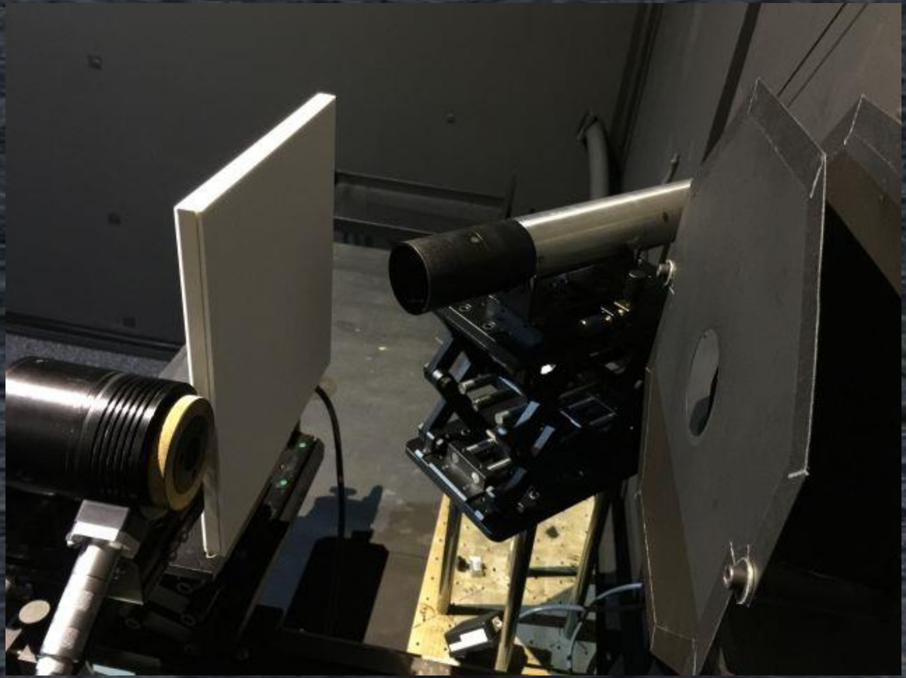
diffuse reflectance target


integrating sphere

Radiance and irradiance sensors

Radiance sensor accepts light from narrow solid angle.
Calibrated in radiance units.

Iradiance sensor accepts light from the full hemisphere.
Calibrated in irradiance units.

Radiance and irradiance sensors

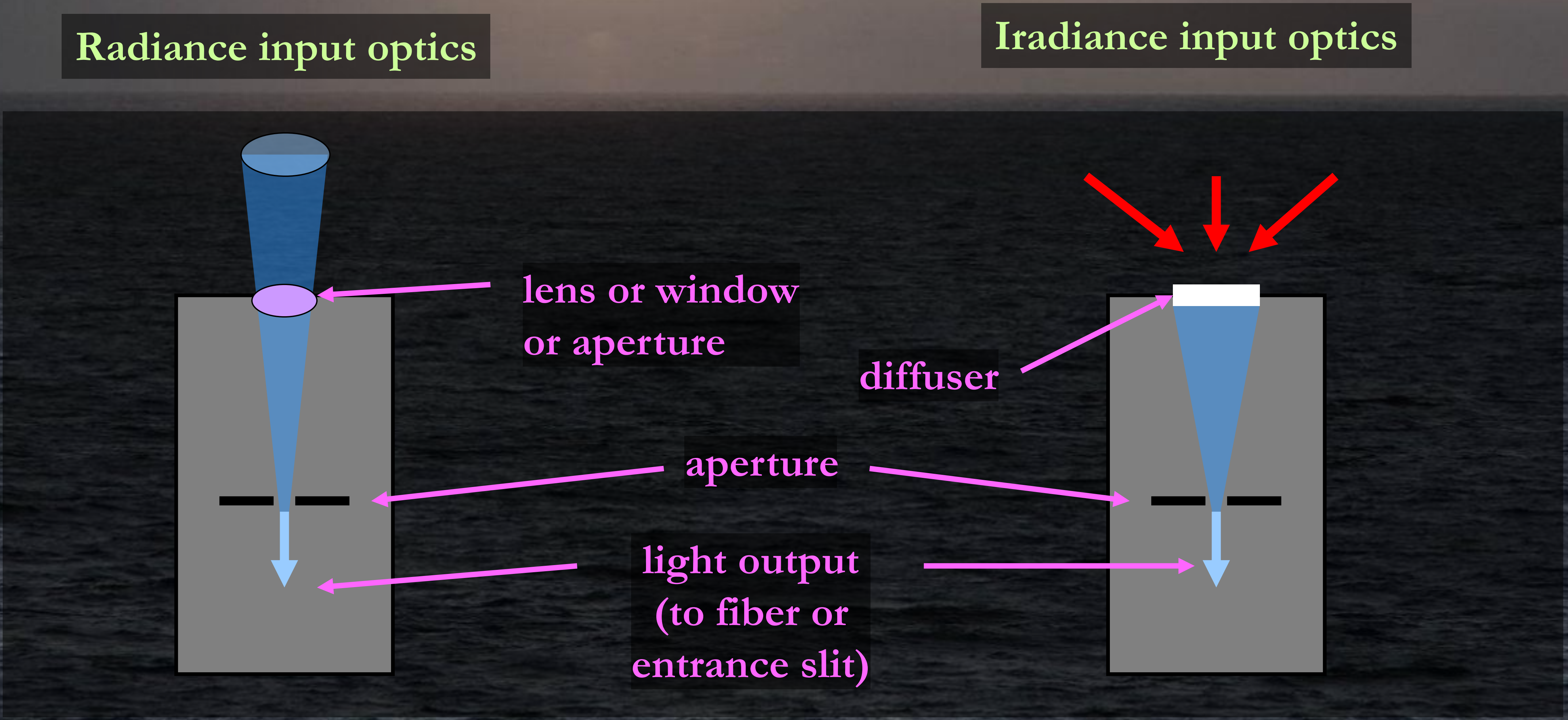

Instrumental parameters

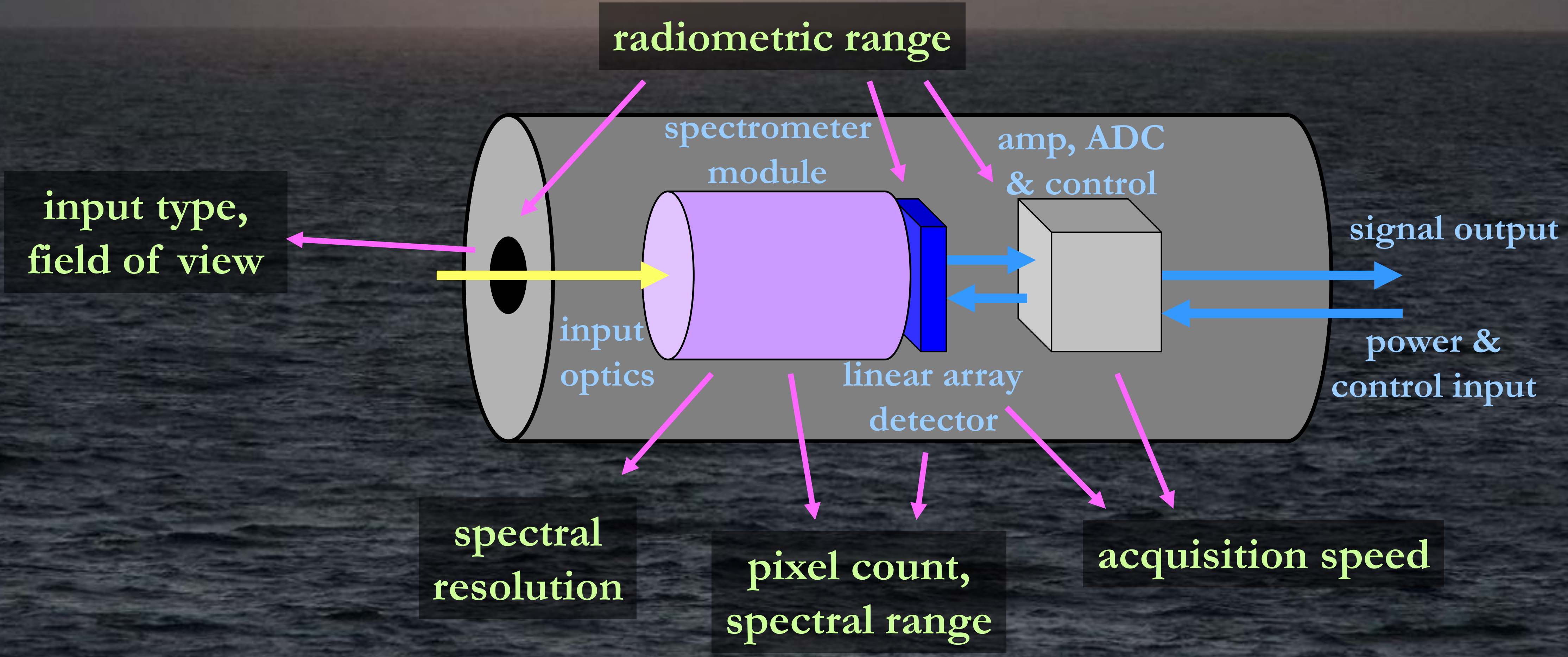

Other: temperature range, power consumption, waterproofness, weight, dimensions, cost, software options ...

Radiometers for OC

Multispectral: sat, cimel, …

Hyperspectral: ramses, sat, wisp, dalek, SR-3500

TriOS RAMSES & Satlantic/Sea-Bird HyperOCR

TriOS RAMSES family

Satlantic/Sea-Bird HyperOCR family

TriOS RAMSES & Satlantic/Sea-Bird HyperOCR

Parameter	HyperOCR	RAMSES	Unit
weight	1.2	0.9	kg
digital interface	RS232	RS232	-
supply voltage	+9..+18	+8..+12	V
power consumption	4	0.85	W
depth rating	250	300	m
temperature range	-10..+50	+2..+40	°C
field of view	9	7	°
integration time	4 8192	4..8192	ms
wavelength range	305..1100	305..1100	nm
wavelength step	3.3	3.3	nm
wavelength accuracy	0.3	0.3	nm
spectral bandwidth	9.5	9.5	nm
pixel count	256	256	-
NER @ 500 nm	1.4	0.5	$\mu Wm^{-2}nm^{-1}sr^{-1}$
radiance responsivity @ 500 nm & 1 ms	1.8	13	$\mu W^{-1}m^{2}nmsr$
mininum sampling interval	0.5	1	s
internal shutter	yes	no	-
thermal control	no	no	-
internal temperature sensor	yes	no	-

Above-water measurement setup with RAMSES

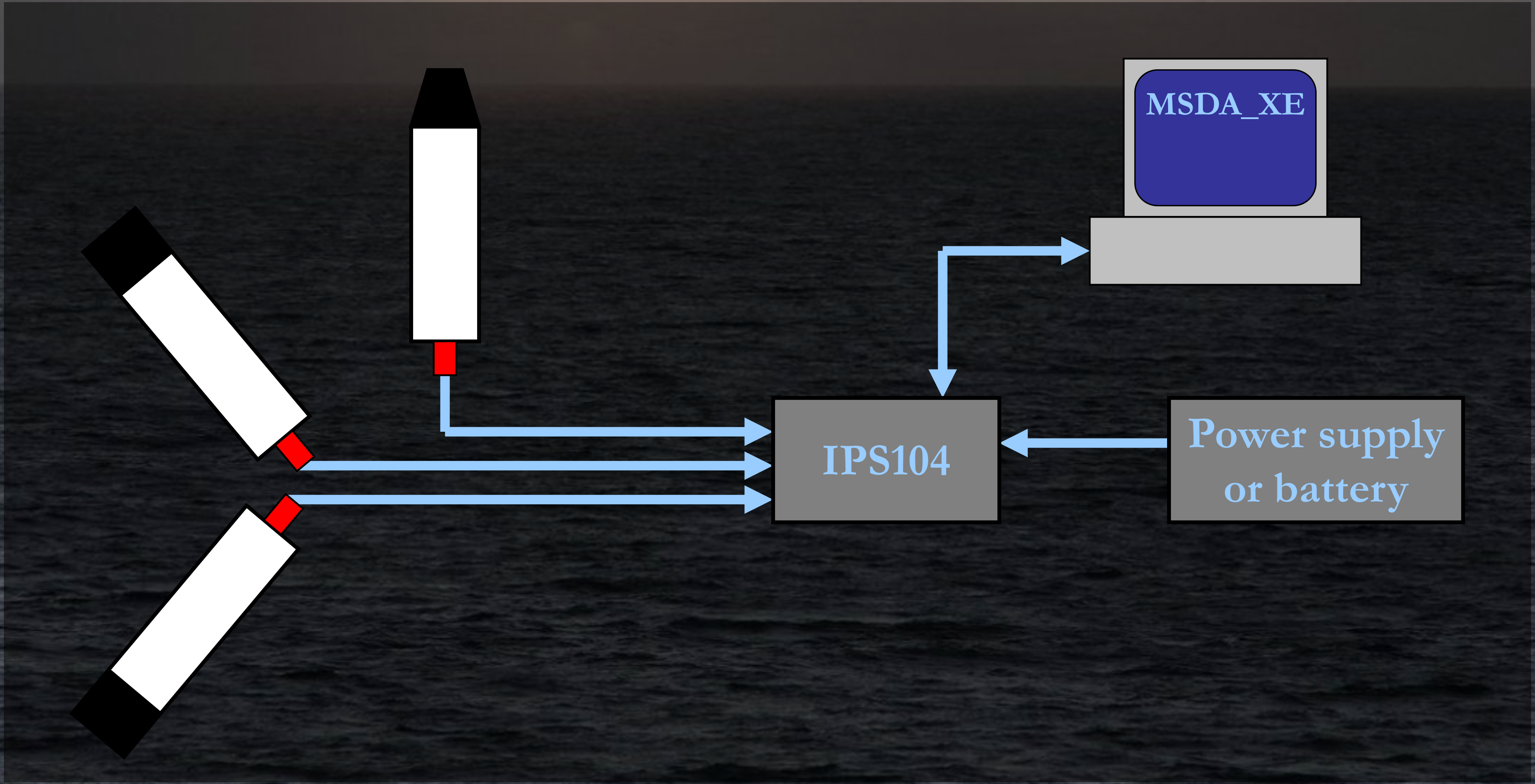

Output data

RAMSES

Data acquisition and file conversion: "MSDA_XE", records binary (MS ACCESS) or ASCII datafiles.

All 256 pixel values are recorded, pixel number 0..255 shown in datafiles.

Temperature data only availabe for second generation (G2) devices.

HyperOCR

Data acquisition: "SatView", records binary datafiles.

Binary-to-ASCII datafile conversion: "SatCon".

Varying subrange of pixels is recorded and converted.

Pixel number is not shown in datafiles.

Contains temperature data.

!!! Be careful when working with spectral data: pixel shift can easily happen !!!

MSDA_XE example datafile

serial number

date & time

comment

integration time

256 pixel numbers and raw readings

```
[Spectrum]
Version              = 1
IDData               = DB43_2007-10-10_10-47-55_599_050
IDDevice             = SAM_8166
IDDataType           = SPECTRUM
IDDataTypeSub1       = RAW
IDDataTypeSub2       =
IDDataTypeSub3       =
DateTime             = 2007-10-10 10:47:55
PositionLatitude     = 0
PositionLongitude    = 0
Comment              =
CommentSub1          =
CommentSub2          =
CommentSub3          =
IDMethodType         = SAM Control
MethodName           = SAM_8166
RecordType           = 0

[Attributes]
CalFactor = 1
IDBasisSpec =
IDDataBack = DLAB_2006-05-04_09-11-52_144_774
IDDataCal = DLAB_2006-05-04_09-59-07_917_979
IntegrationTime = 128
PathLength = +INF
Temperature = +NAN
Unit1 = $05 $00 Pixel
Unit2 = $03 $05 Intensity counts
Unit3 = $f0 $05 Error counts
Unit4 = $f1 $00 Status
[END] of [Attributes]
[DATA]
 0 6 0 0
 1 3941 0 0
 2 5479 0 0
...
 255 1353 0 0
[END] of [DATA]
[END] of [Spectrum]
```

Example spectra

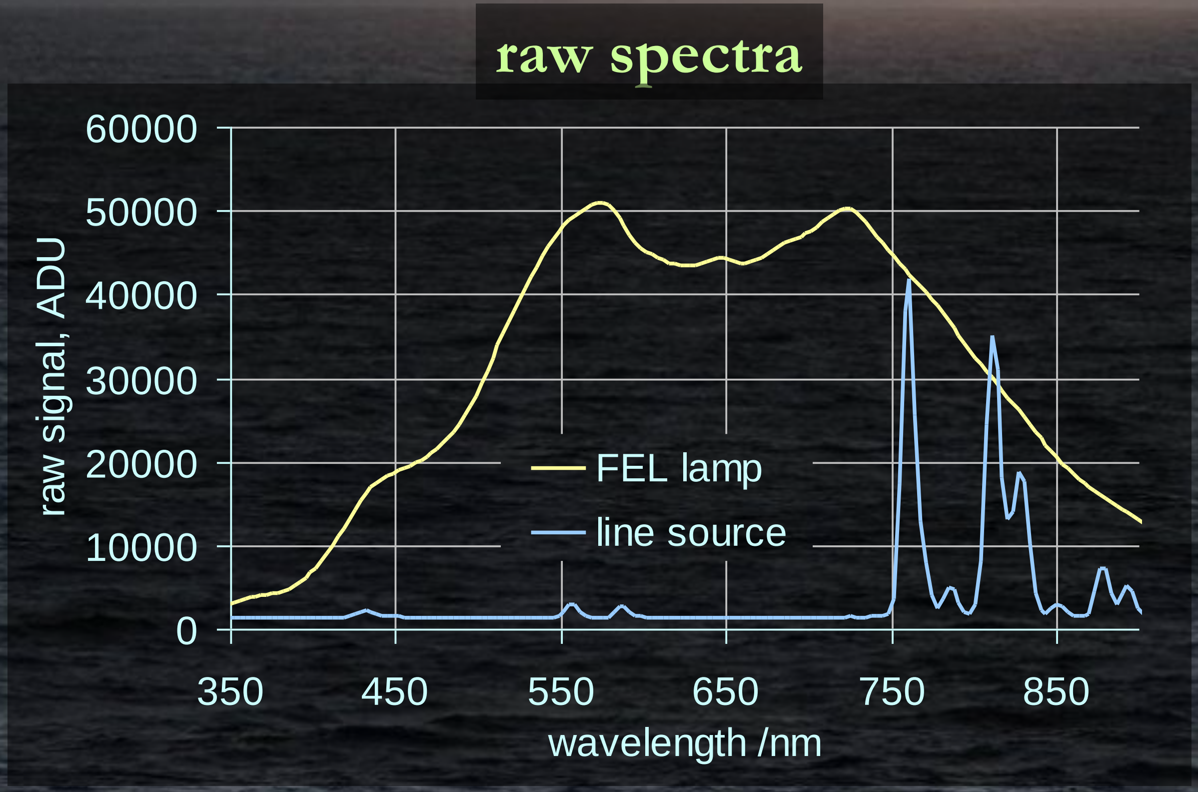

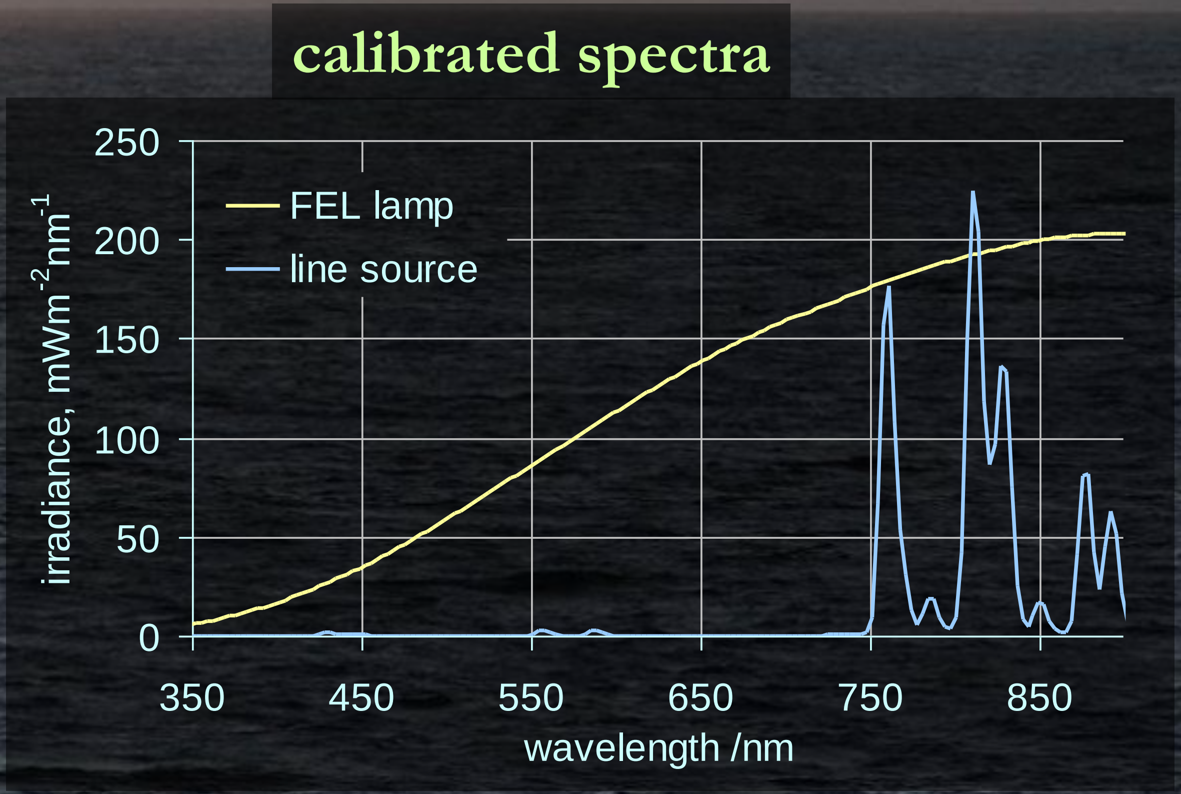

More instrumental parameters

Radiometric responsivity
Long term stability
Radiometric non-linearity
Dark signal
Signal-to-noise ratio
Wavelength scale
Spectral straylight
Thermal sensitivity
Angular response
Polarization sensitivity
Other:

- Accuracy of integration times
- Temporal response
- Immersion factors
- Pressure effects

Characterization and correction

Characterization is determination of the optoelectronical, mechanical and environmental properties of the radiometer.

Characterization takes mostly place in the laboratory by using dedicated light sources, environmental conditions and measurement procedures.

Characterization result: a correction factor or formula with uncertainty. This result belongs to the radiometer regardless of the measurement task.

The uncertainty of the characterization result depends on the capabilities of the radiometer and the characterization method.

The characterization result is used to correct any (laboratory or field) measurement carried out with the radiometer.

The characterized instrumental property will interact with the measurement conditions: the spectral and angular distribution and intensity of the radiation, temperature etc.

The magnitude and the residual uncertainty of the final correction depends on these conditions.

Test spectra and field conditions

The characterization results shown below belong to the real radiometers.
Due to the interaction between the characterization results and the field conditions, we need to define the example field spectra in order to evaluate the final corrections and residual uncertainties.

The example field conditions:

SZA	45 °
calibration temperature	20 °C
field temperature	30 °C
DOLP	0.4 (L_i)
	0.75 (L_T)
maximum raw signal	30000 ADU

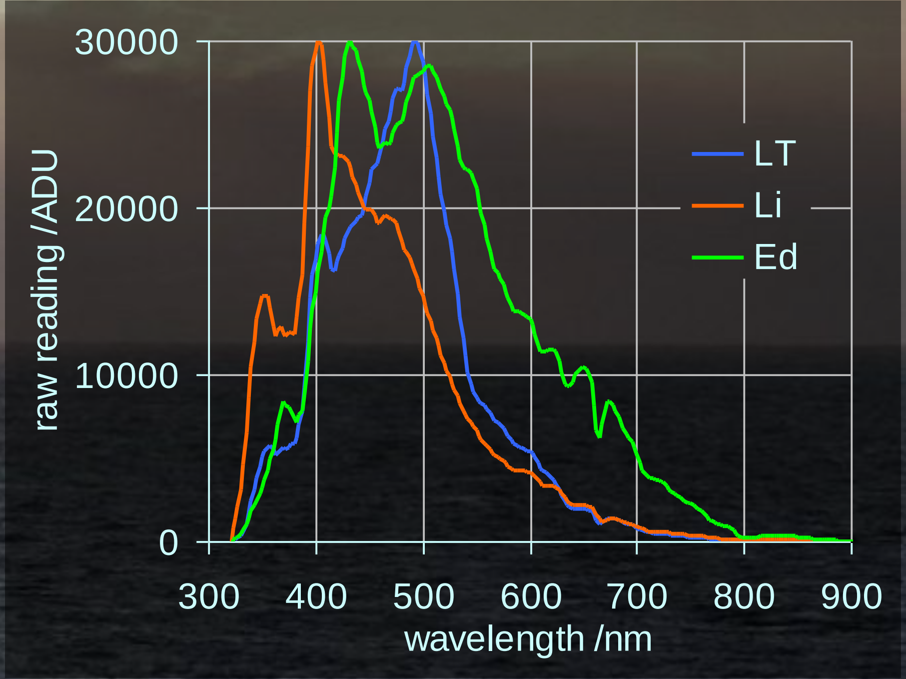

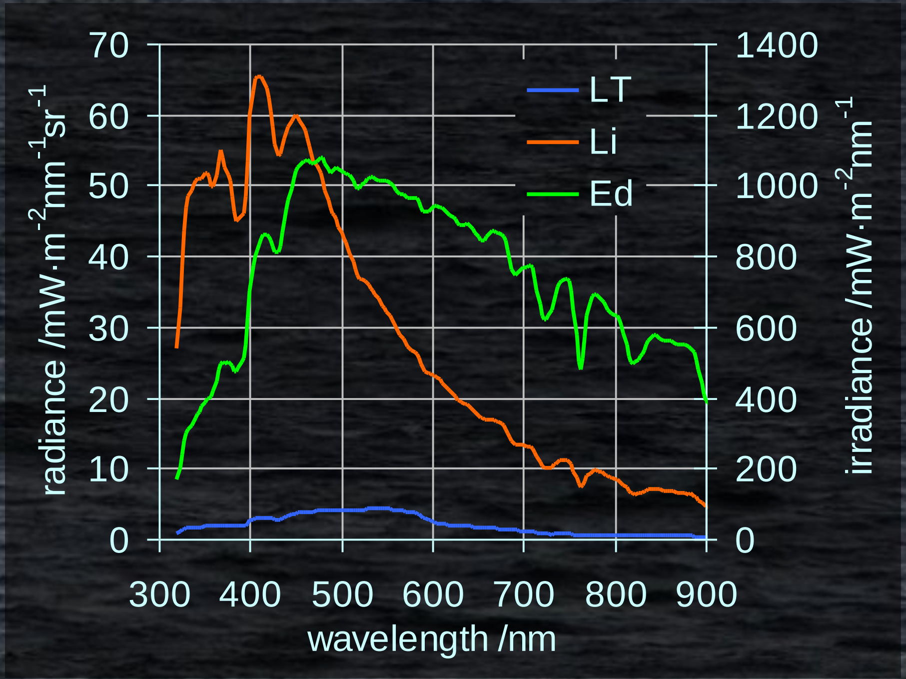

Radiometric responsivity

Responsivity shows the ability of the radiometer to convert the input radiant power into output electrical/digital signal.
Responsivity depends on the wavelength.

RAMSES

irradiance responsivity=output signal/irradiance [1/(mW·m^{-2}nm^{-1})]

radiance responsivity=output signal/radiance [1/(mW·m^{-2}nm^{-1}sr^{-1})]

HyperOCR

irradiance responsivity=irradiance/output signal [μW·cm^{-2}nm^{-1}]

radiance responsivity=irradiance/output signal [μW·cm^{-2}nm^{-1}sr^{-1}]

Radiometric calibration setup for irradiance

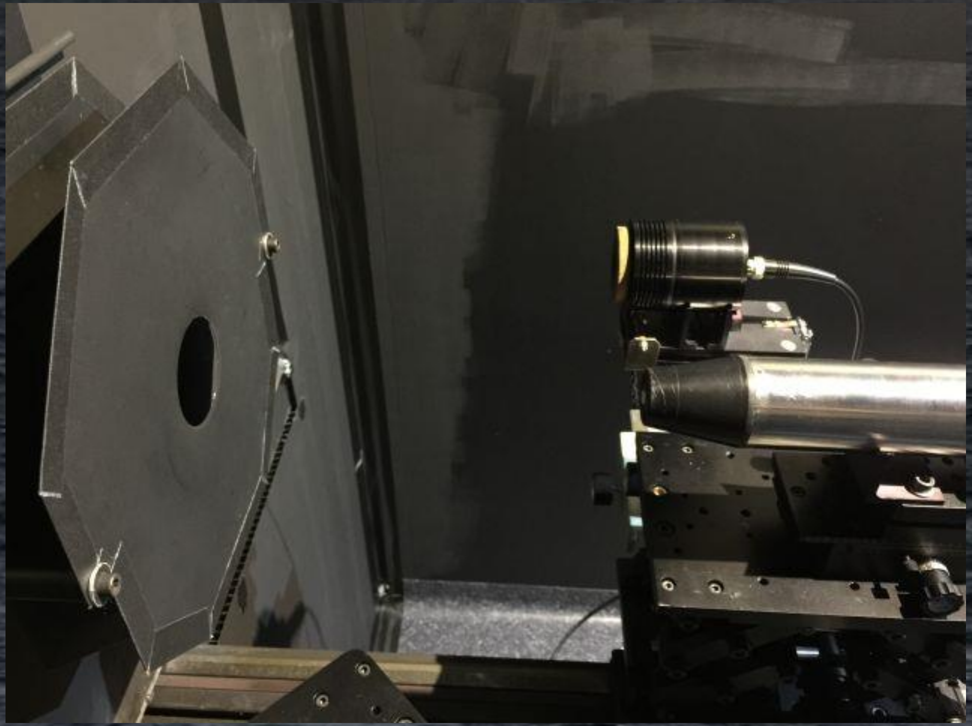

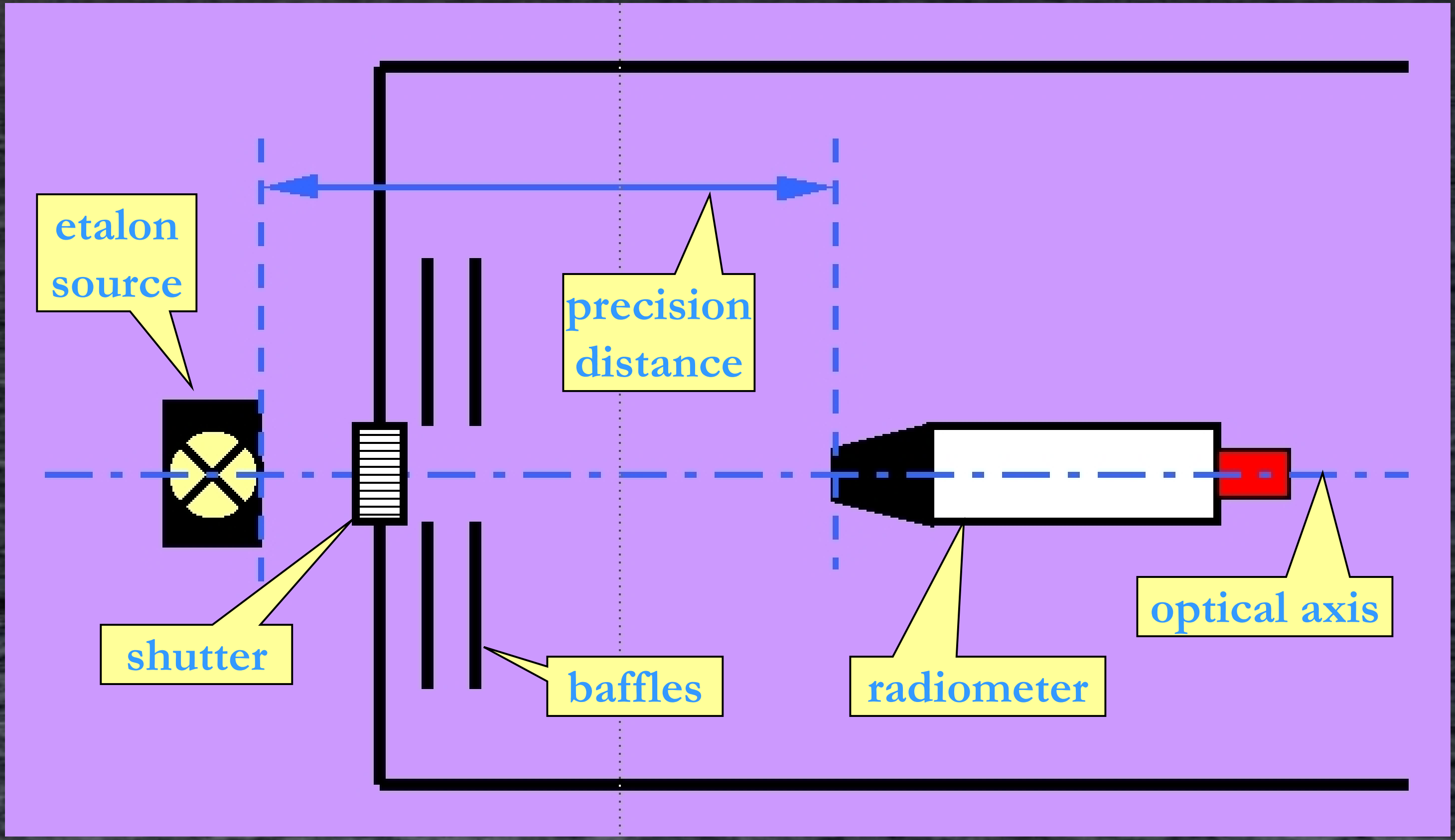

Radiometric calibration setup for radiance

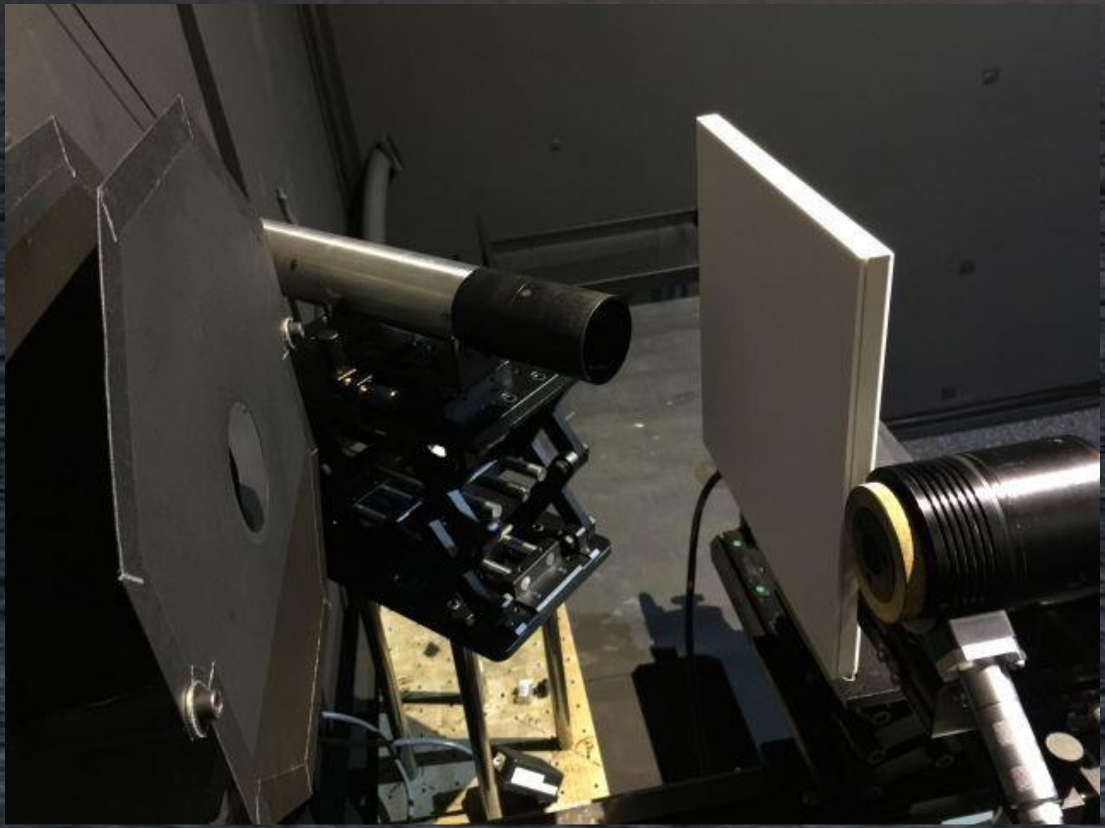

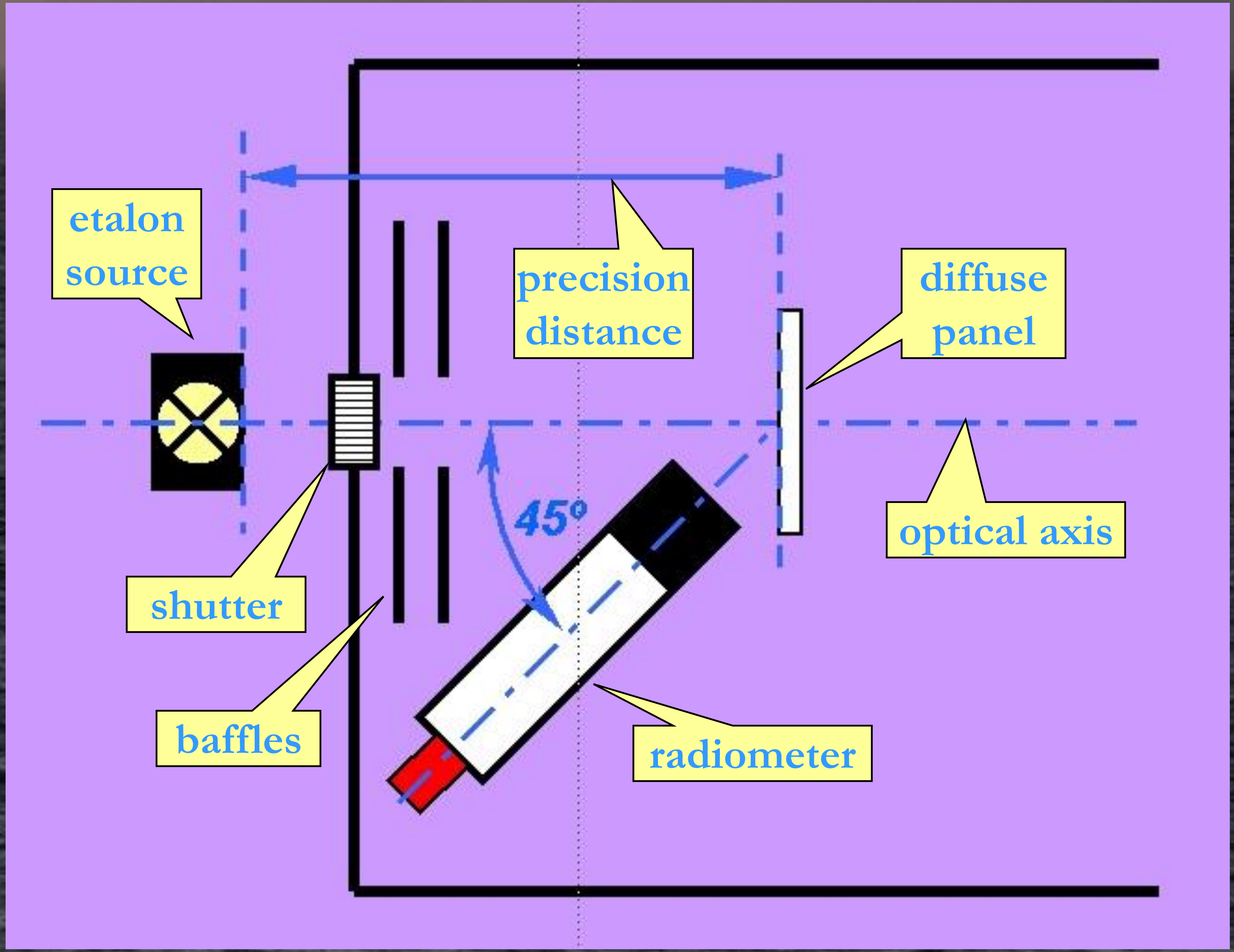

Radiometric responsivity

RAMSES

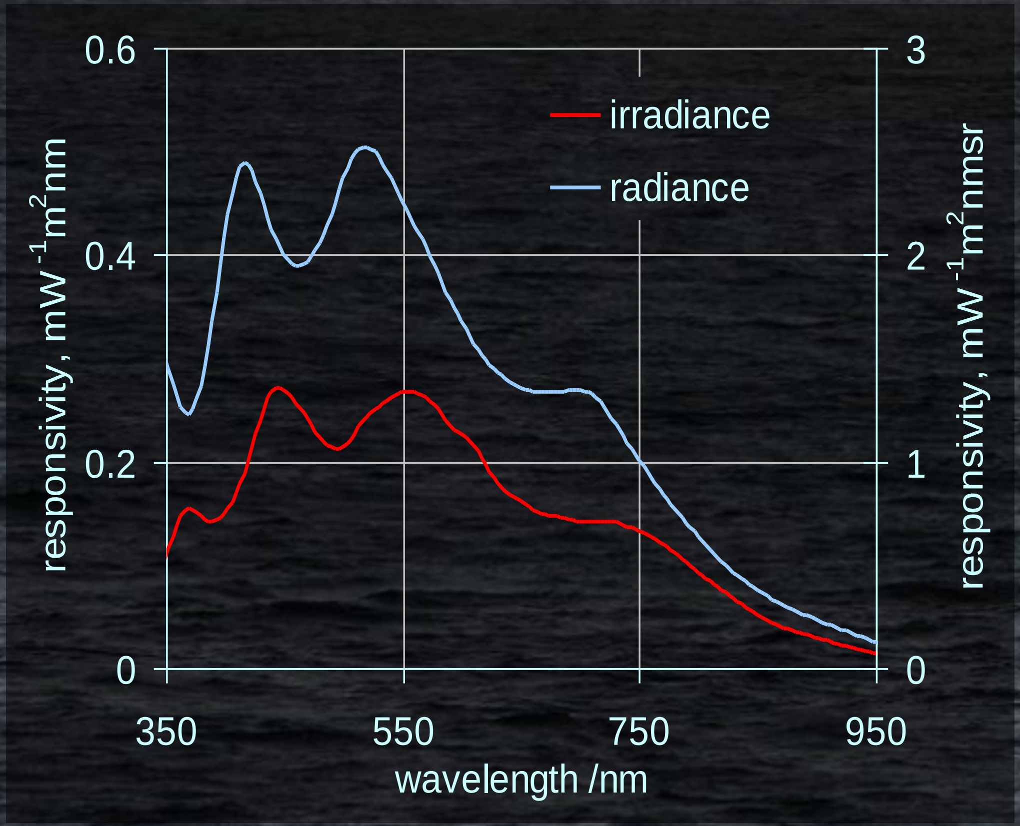

HyperOCR

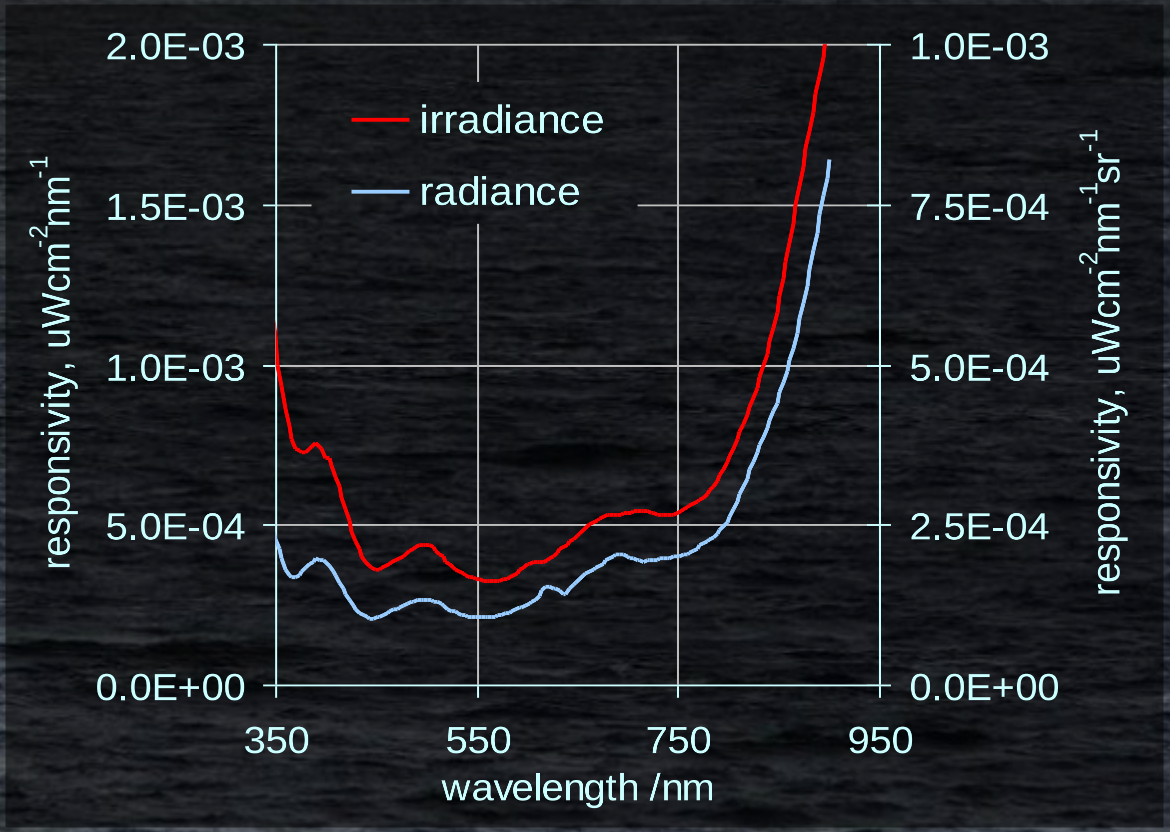

Applying calibration factors (RAMSES example)

For individual radiometer:

$$\text{CalibratedFieldSignal} = \frac{\text{RawFieldSignal*}}{\boxed{\text{CalFactor}}} = \frac{\text{RawFieldSignal*} \cdot \text{EtalonIrradiance}}{\text{RawCalSignal*}}$$

can be corrected

*Dark is subtracted

Uncertainty of R_{rs} due to the calibration uncertainty

Simplified measurement equations:

$$L_T = \frac{RawFieldSignal}{CalFactor} \dashrightarrow u(L_T)$$

$$L_i \dashrightarrow u(L_i)$$

$$E_d \dashrightarrow u(E_d)$$

$$R_{rs} = \frac{L_T - \rho L_i}{E_d} \dashrightarrow u(R_{rs})$$

Calibration uncertainty of R_{rs} in the correlated case

Simplified measurement equation for R_{rs} with correlated calibrations:

$$R_{rs} = \frac{L_T - \rho L_i}{E_d} = \frac{\frac{Sraw}{Scal}\pi \cdot \cancel{Lamp} \cdot Panel - \rho \frac{Sraw}{Scal}\pi \cdot \cancel{Lamp} \cdot Panel}{\frac{Sraw}{Scal}\cancel{Lamp}}$$

$\Rightarrow u(R_{rs})$

Uncertainty will be reduced due to the correlation between L_T, L_i and E_d.

Uncertainty of R_{rs}

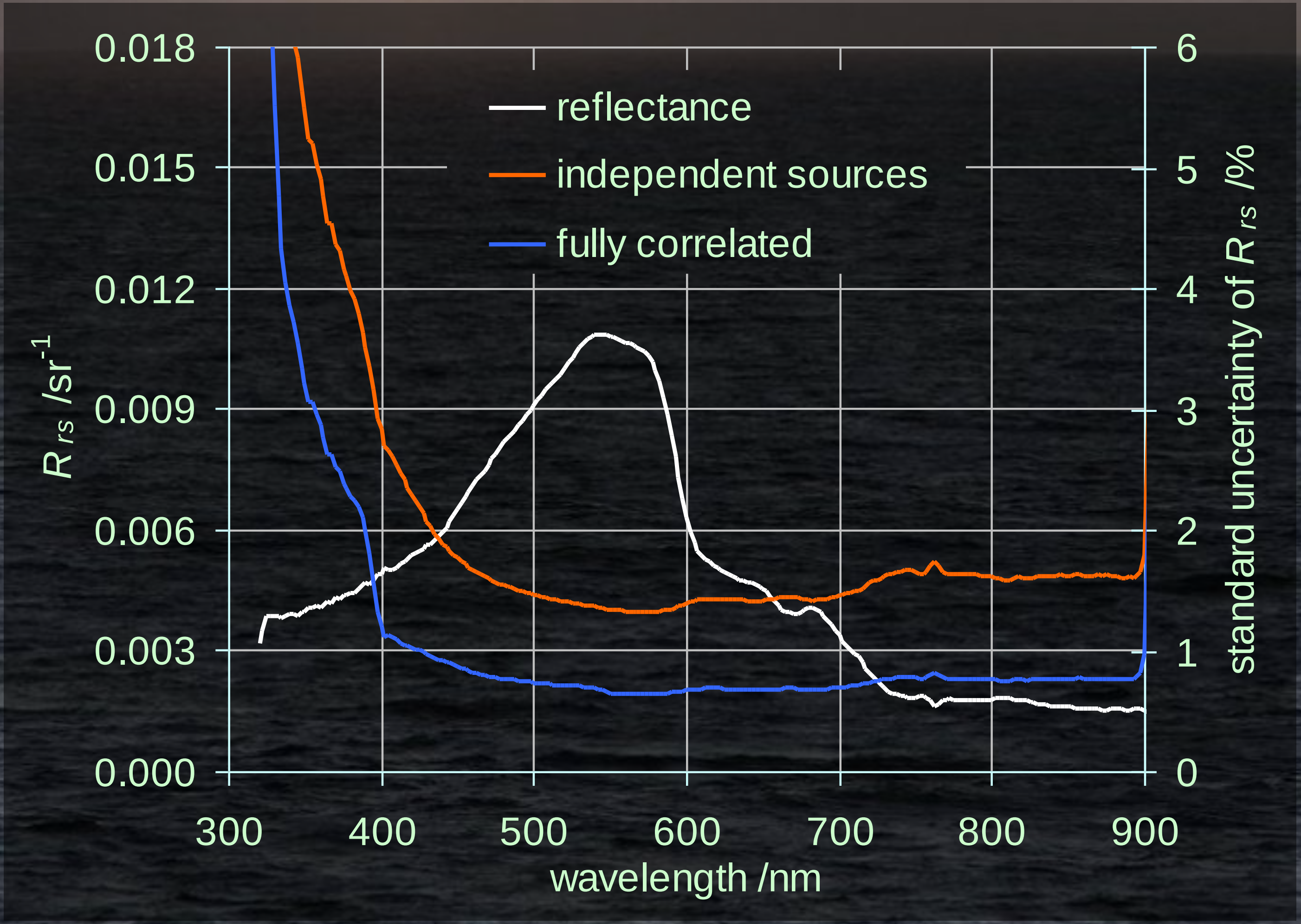

Temporal drift

example RAMSES radiometer

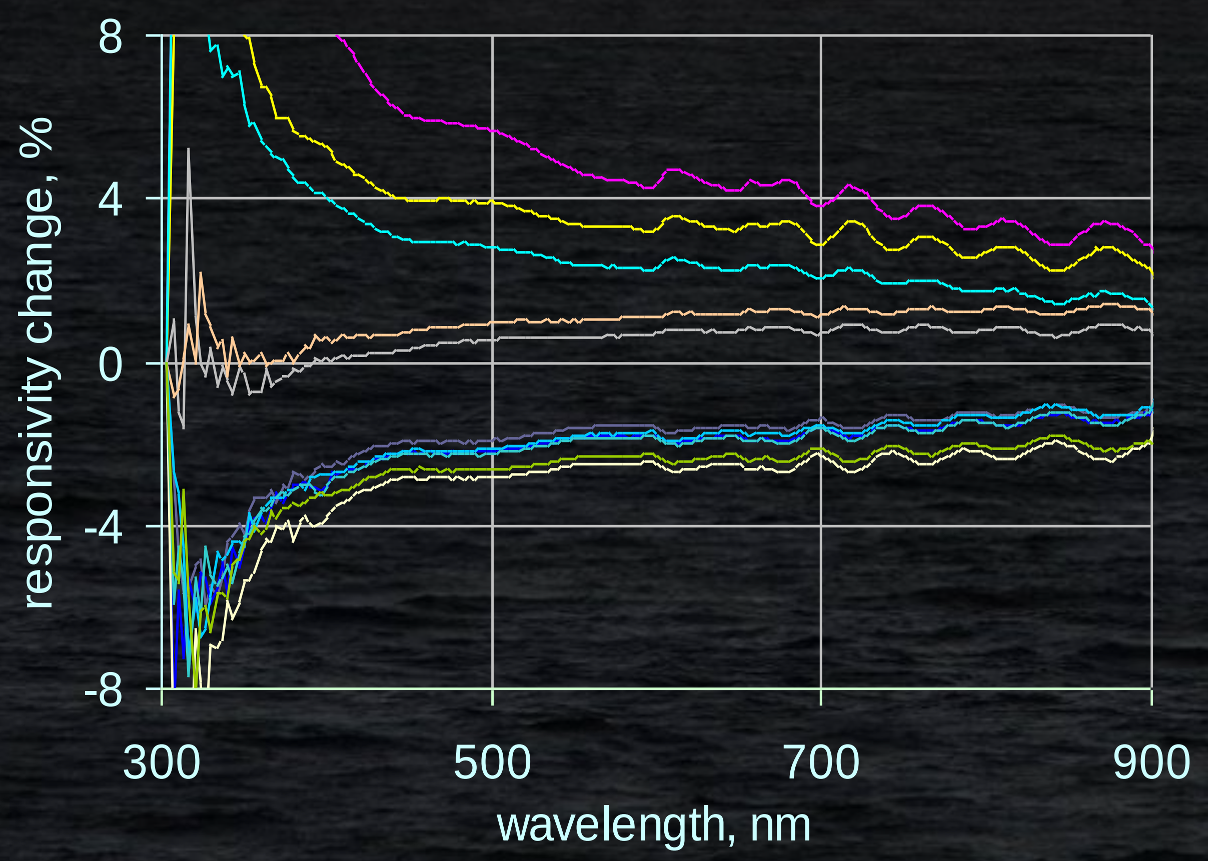

selected RAMSES & HyperOCR

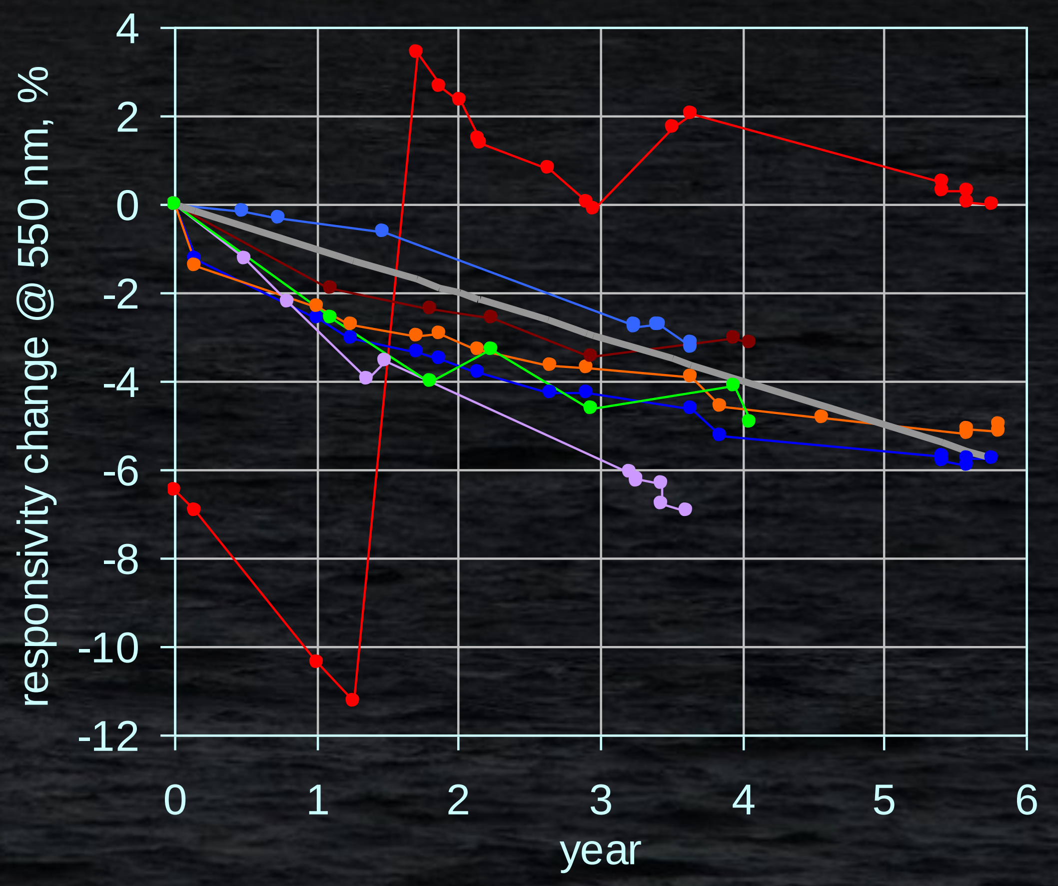

Radiometric non-linearity

Ideal case: output signal* of the radiometer is proportional to the excitation.
Reality: deviation from proportionality, usually at higher signal levels.

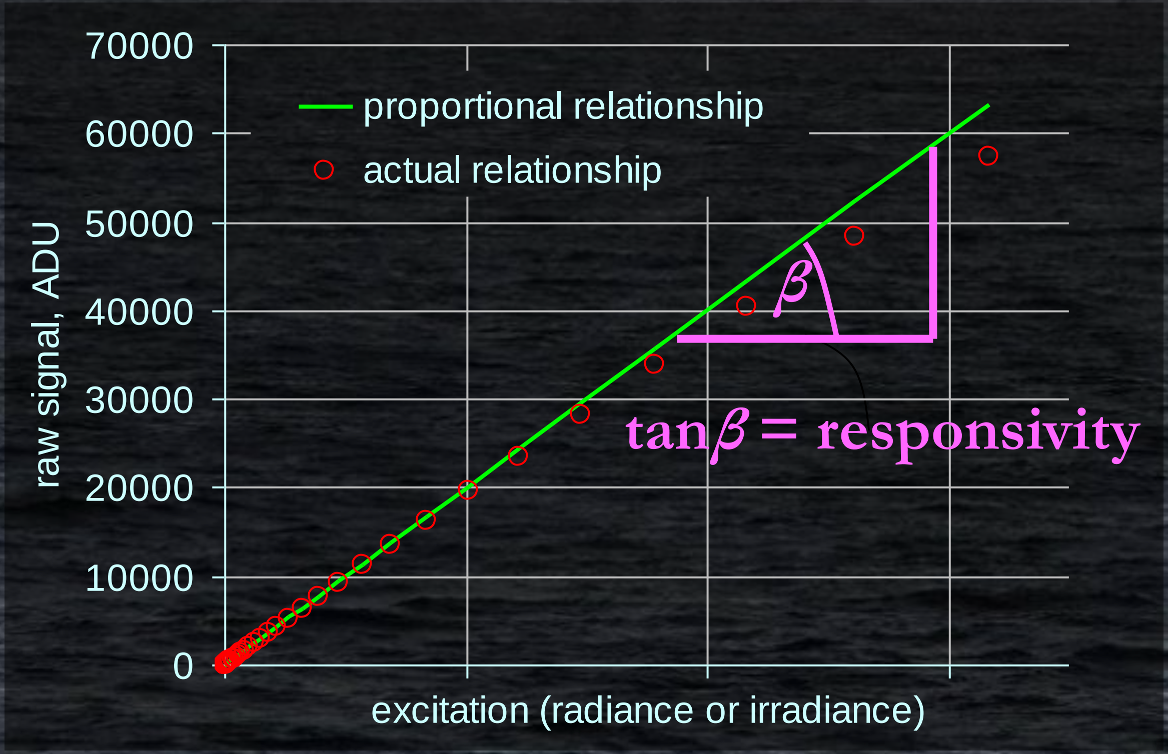

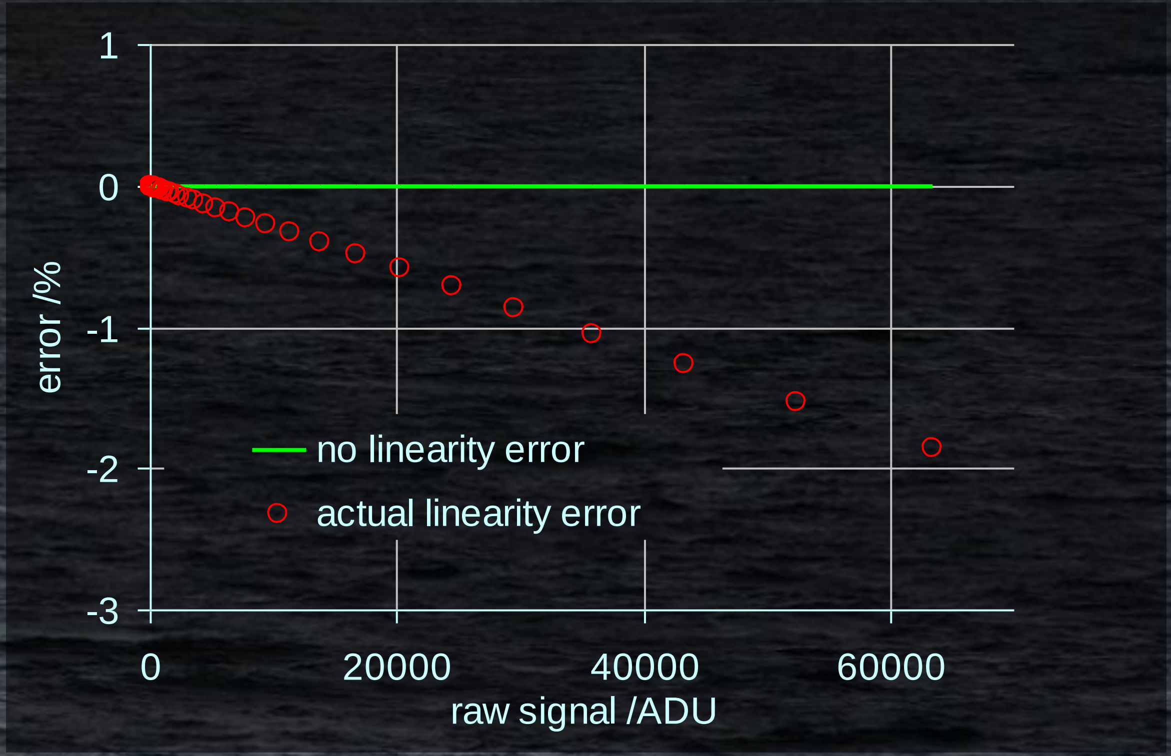

*Dark is subtracted

Radiometric non-linearity examples

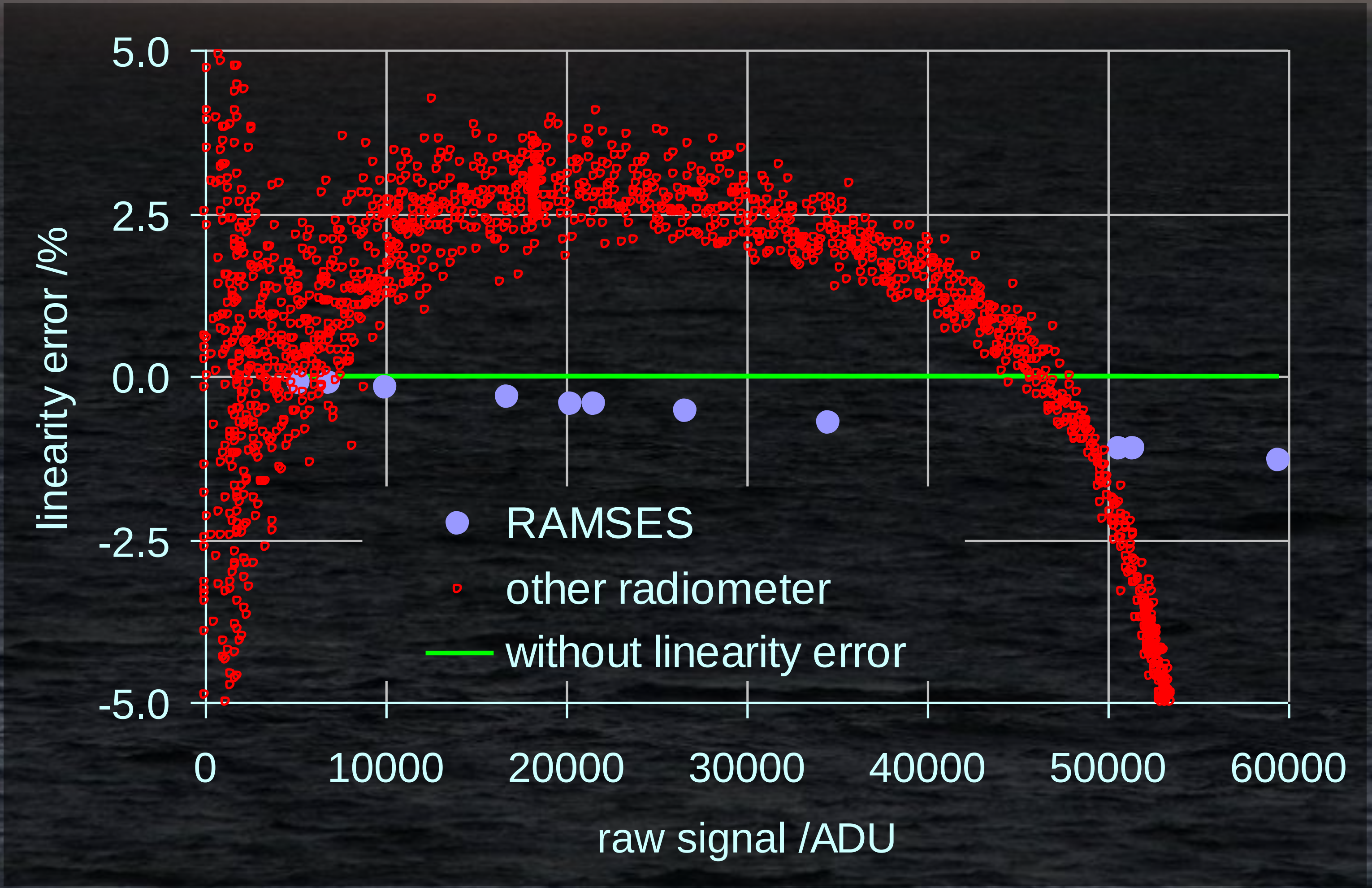

Measuring the radiometric non-linearity

For characterization of the radiometric non-linearity we need a signal source with precisely controlled variable intensity:

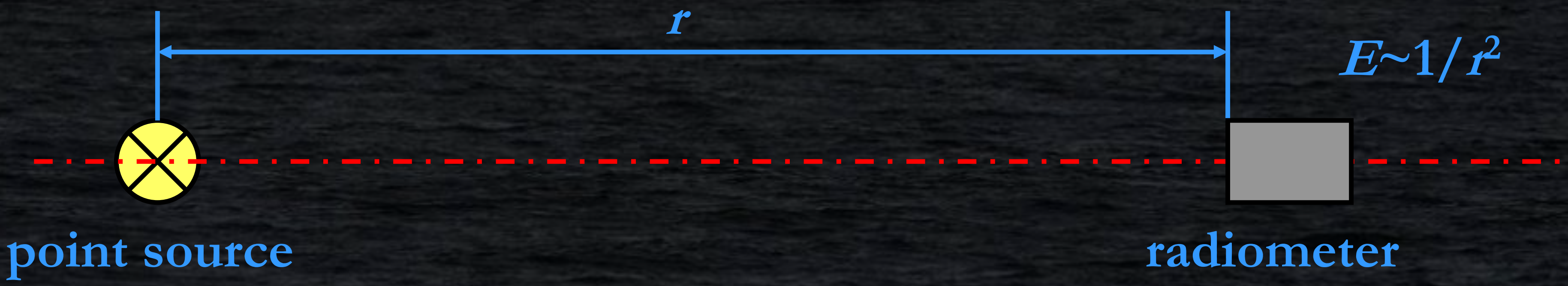

the varying distance method

Measuring the radiometric non-linearity

For characterization of the radiometric non-linearity we need a signal source with precisely controlled variable intensity:

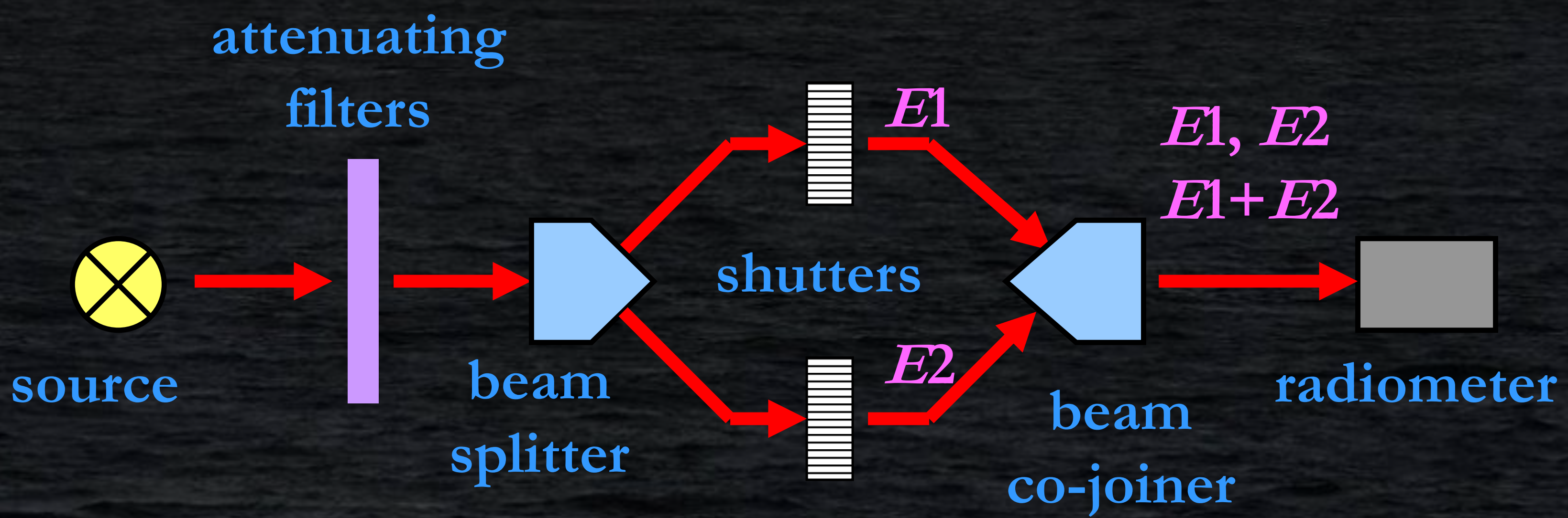

the beam addition method

Radiometric non-linearity

Output raw signal* of the radiometer is proportional to the integration time.
We can replace the varying excitation with varying output signal level
by using different integration times.
The integration time ratios need to be precise.

*Dark is subtracted

Radiometric non-linearity

new graph

Empirical relationship, proposed by V.Vabson during the FRM4SOC Phase 1 project:

$$\frac{\Delta S}{S_{true}} = \frac{S - S_{true}}{S_{true}} = \alpha \cdot S_{true}$$

Valid for RAMSES and HyperOCR according to experimental results.

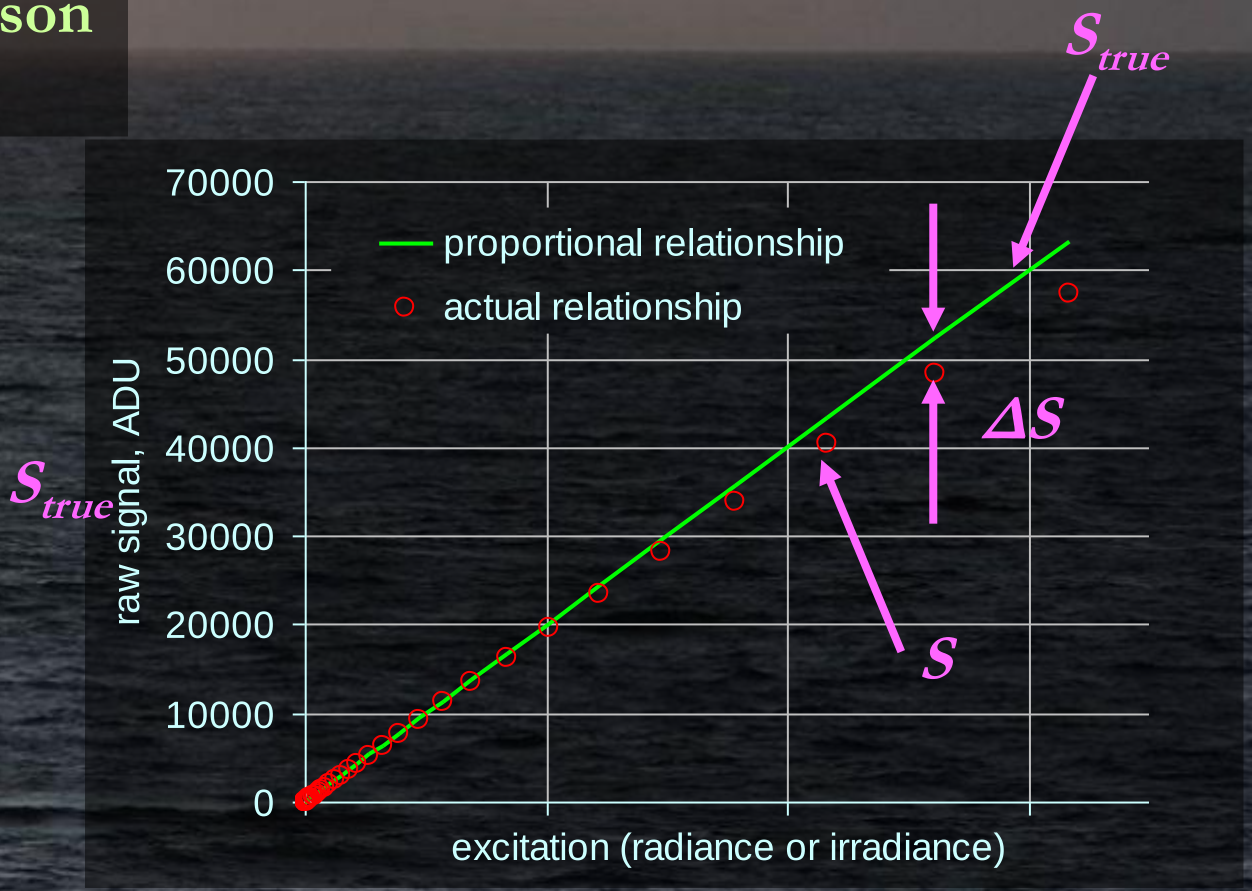

Radiometric non-linearity

The nonlinearity can be easily demonstrated when measuring a stable source with different integration times.

The non-linearity error for RAMSES and HyperOCR dependes on the wavelength.

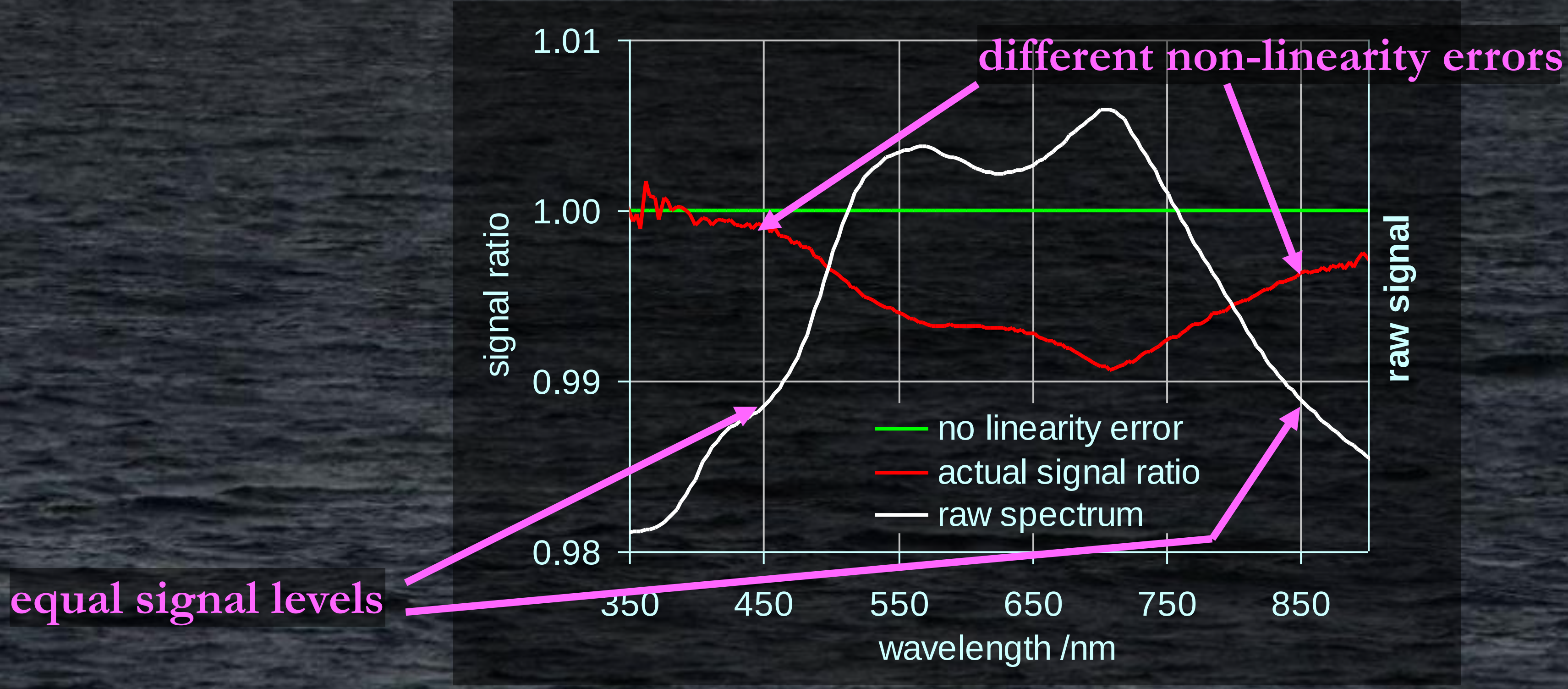

Derivation of the non-linearity coefficient

Calibration source is measured with two integration times *t1* and *t2*:

$$\begin{cases} \dfrac{S(t1) - S_{true}}{S_{true}} = \alpha \cdot S_{true} \\ \dfrac{S(t2) - S_{true}}{S_{true}} = \alpha \cdot S_{true} \end{cases}$$

Will be solved for S_{true} and α,
both depend on the wavelength.

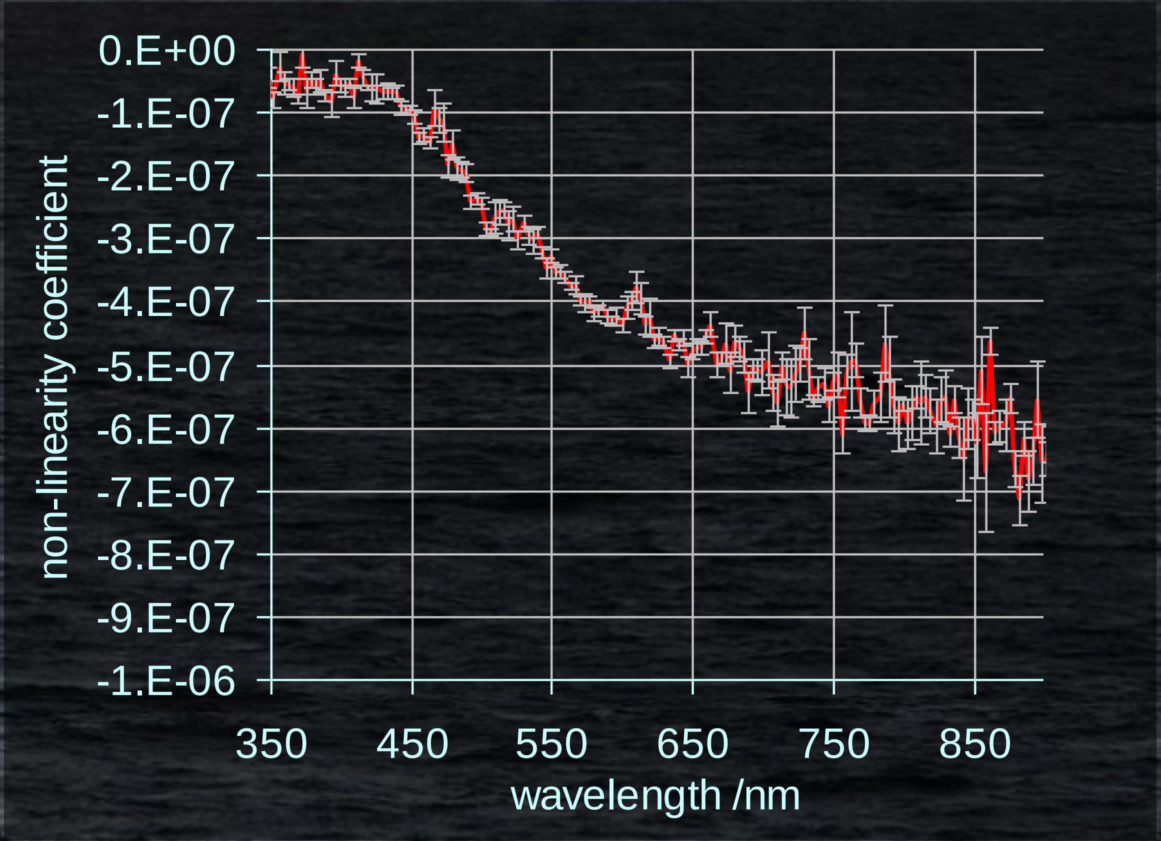

The CP_*_RADCAL_* file

The CP_RADCAL* file contains $S(t1)$, $S(t2)$, lamp, panel etc. data, necessary for derivation of the cal factors and α with uncertainties.
Calculation details can be found in HyperCP documentation.

pixel number

wavelength

cal factor

expanded uncertainty

$S(t1)$

$S(t2)$

```
[CALDATA]
0      304.22   4         0.00     12        0.000000  64      0.00  32      0.00
1      307.55   0.299505  6.36     0.015587  0.022274  85.14   0.69  83.21   1.12
2      310.87   0.382907  4.82     0.015494  0.022285  116.91  0.63  116.68  1.14
...
255    1143.49  0.000000  141.27   0.016136  0.023577  -4.09   0.72  -3.99   1.33
[END_OF_CALDATA]
```

Comparison of the non-linearity measurement methods

The integration time method was compared to the more traditional beam addition method.
The integration time method was modified by using monochromatic source.
Non-linearity coefficient was determined at different sensor temperatures.

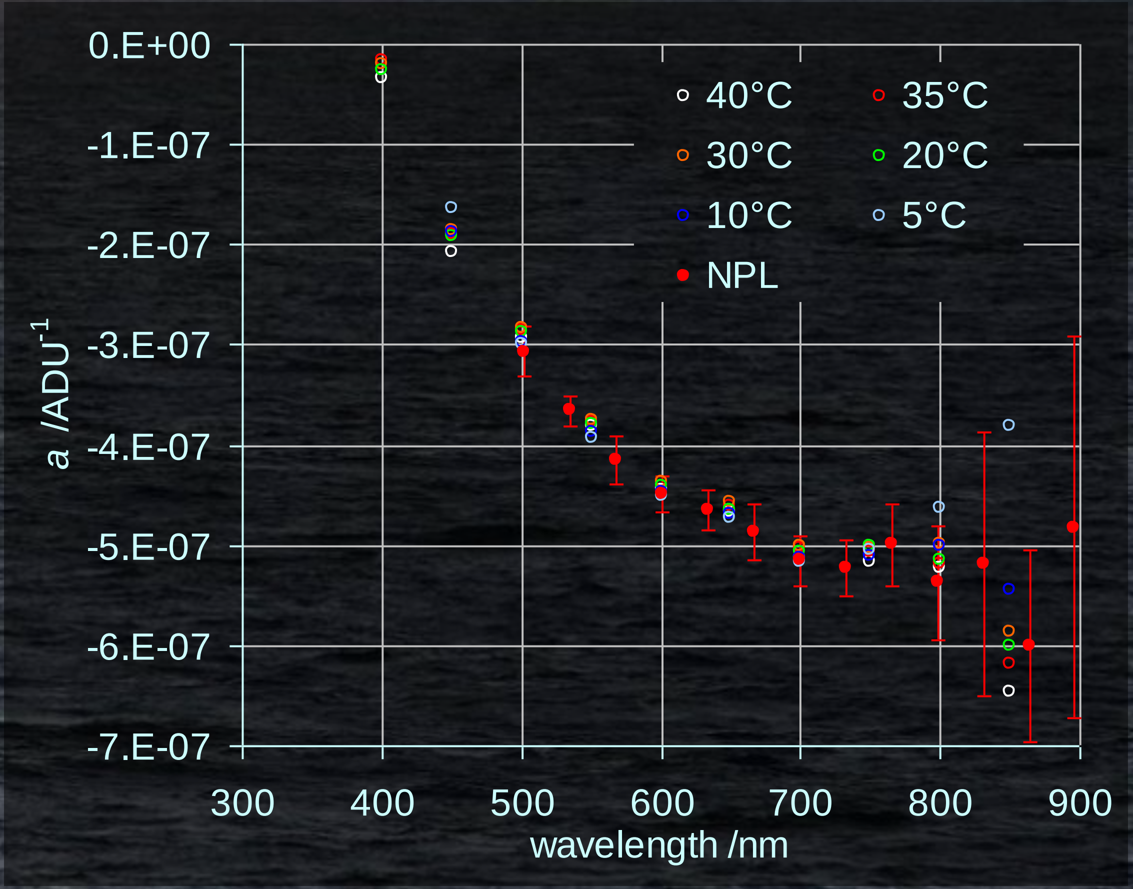

Radiometric non-linearity results

Individual characterization preferred because easy to perform during calibration.

Correction not recommended below 450 nm because of the noisy α.

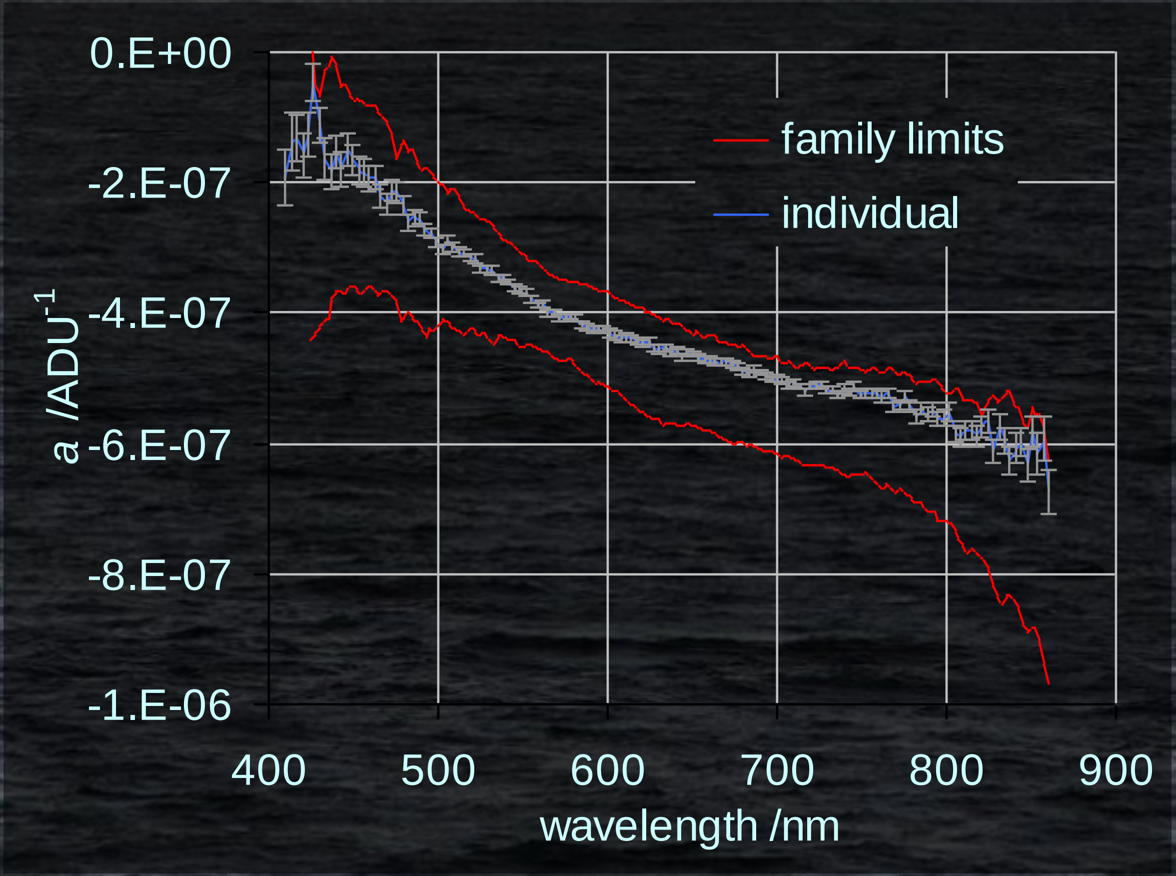

Non-linearity correctionon of the field spectra

Each individual raw spectrum* can be corrected for radiometric non-linearity:

$$S_{lincorr} = \frac{-1 + \sqrt{1 + 4\alpha S_{meas}}}{2\alpha}$$

example case

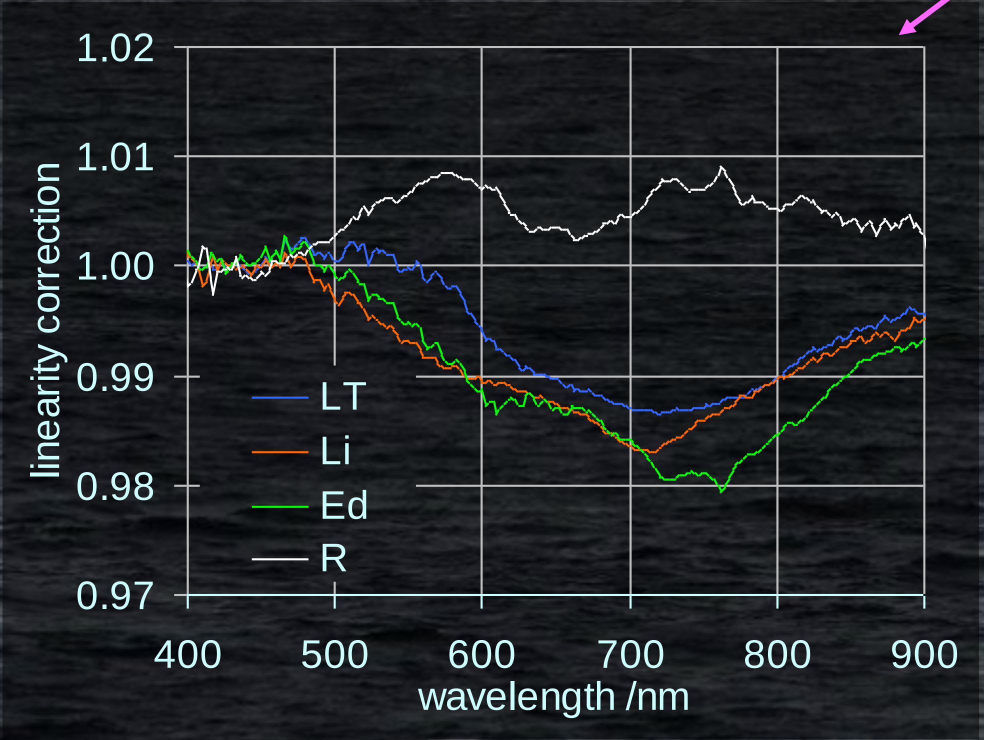

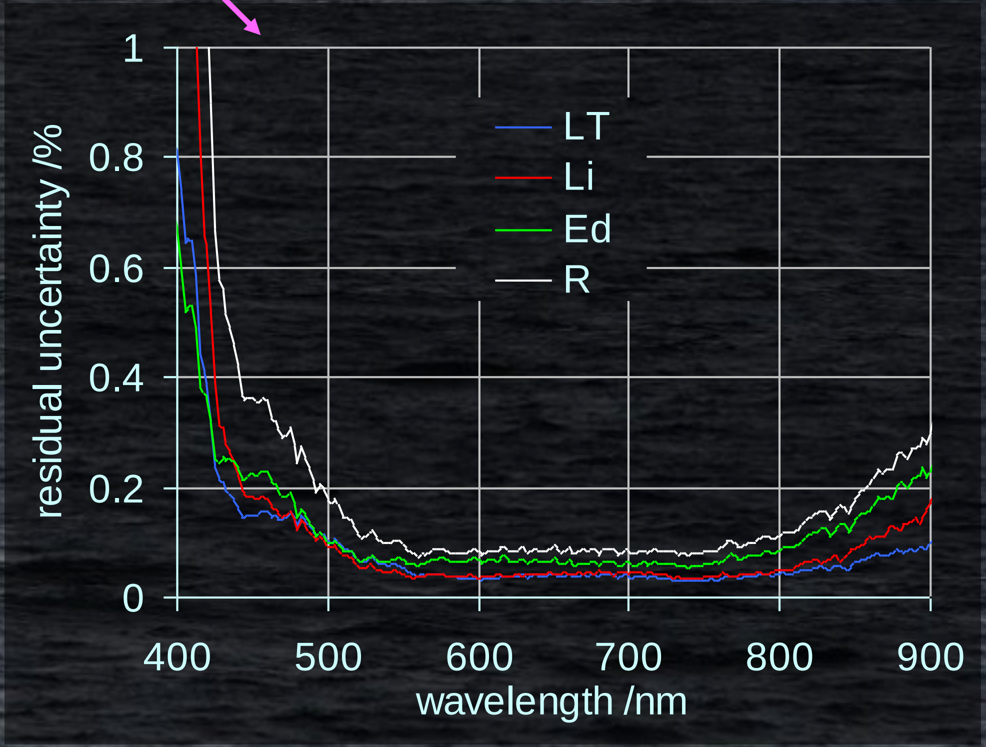

*Dark is subtracted

Dark signal

Due to the constraints in optoelctronics and signal processing,
the radiometer shows output signal even when the optical signal is blocked.
The optical signal can be blocked with the internal (HyperOCR)
or external (RAMSES) shutter.
Dark signal depends on the temperature and the integration time.
Dark signal shall be subtracted from the target signal
before any further processing.
Dark signal origins from the light sensor and from the front-end electronics.
Dark signal shall be measured as close as possible to the target signal
and with the equal integration time.
Dark signal is often handled by the acquisition or data conversion software.
Using of the stored or modelled dark signals is not recommended.
Dark signal can be used to derive the radiometer's internal temperature.

Dark signal examples

Dark spectra at 20 °C

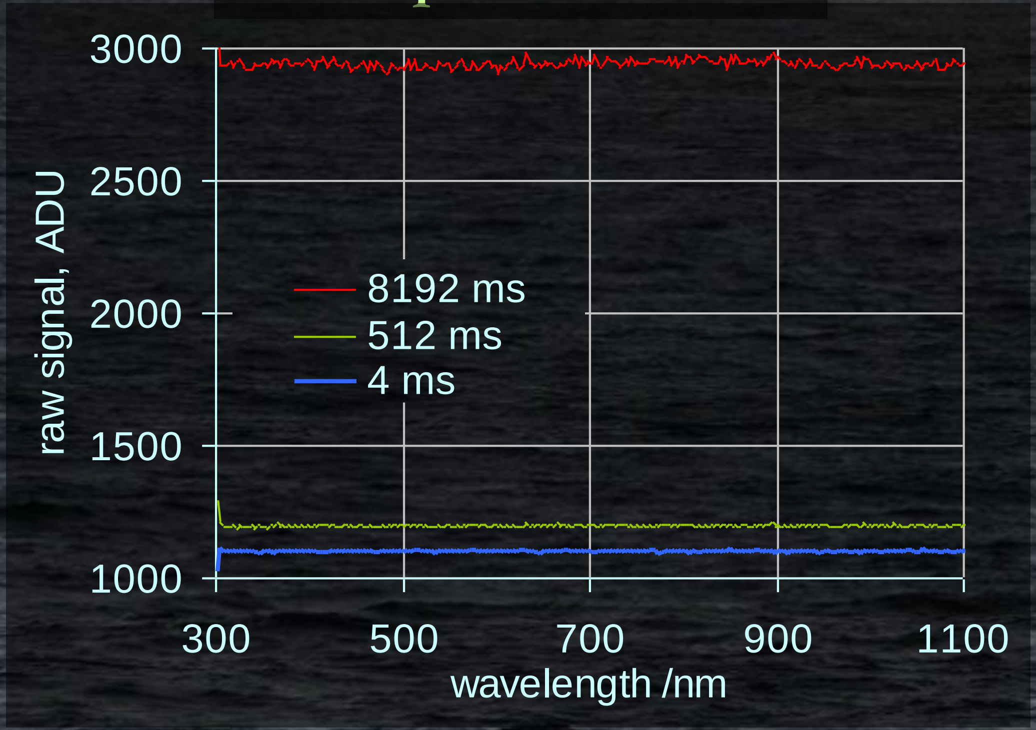

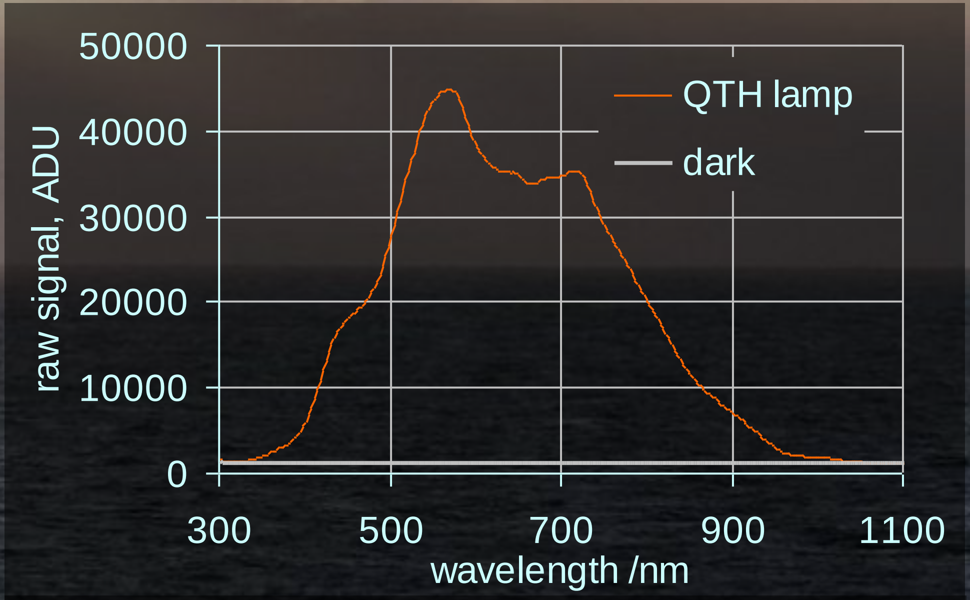

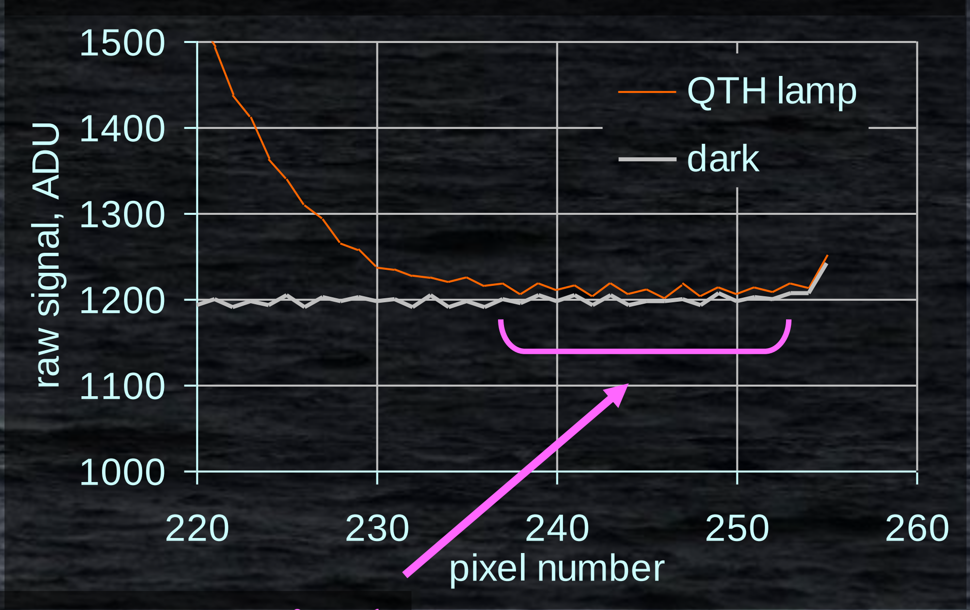

RAMSES opaque pixels

Dark signal vs. temperature

Photodetector dominates the dark signal at longer integration times.
Temperature dependence of the photodiode is typically exponential.

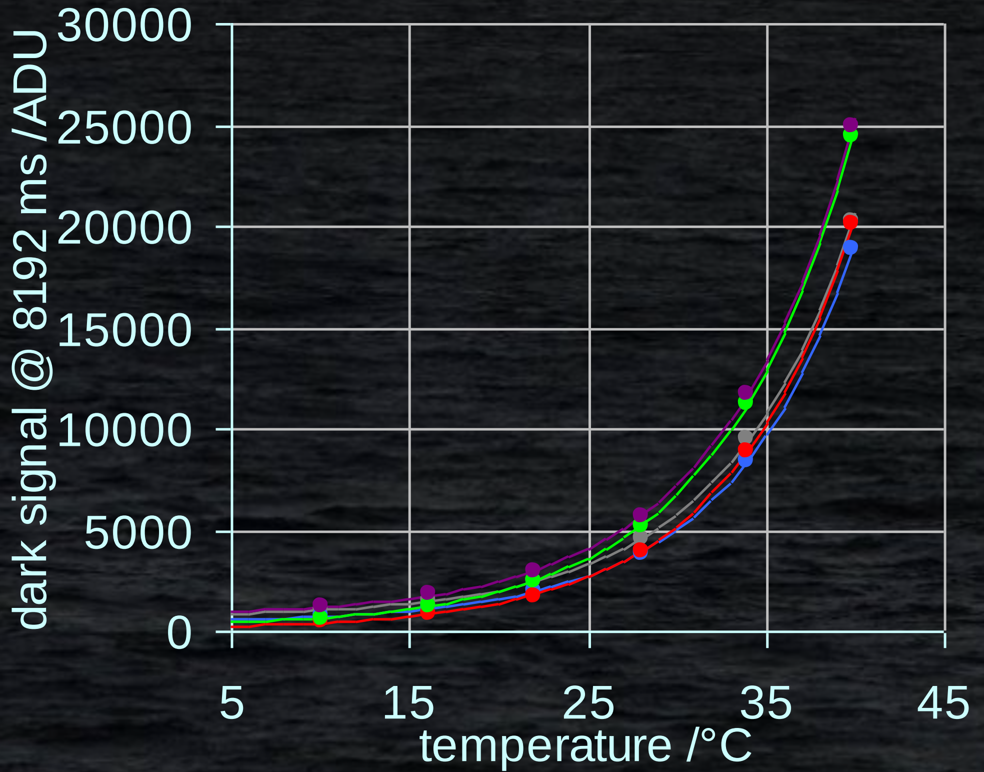

At short integration times, behaviour of the front-end electronics becomes evident.
Front-end electronics: amplifiers, ADC, voltage references etc.

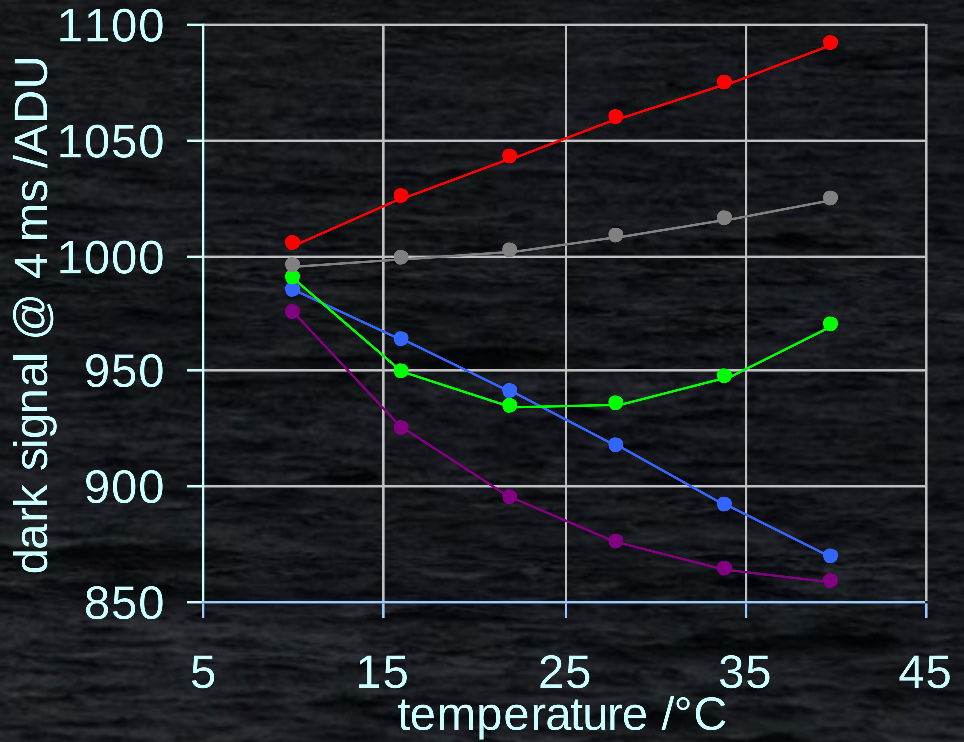

Dark signal: detection of misbehaviour

Dark signal can be sometimes used to detect hardware problems.
No special equipment needed.
Immunity to the electromagnetic interferences can be examined.

perfectly random dark signal

dominating periodic component means noisy electronics or noisy environment

Uncertainty of R_{rs} due to the dark signal

During characterization we establish possible uncertainty of the applied dark level.
HyperOCR: thermal drifts between the target and dark acquisitions;
RAMSES differences between the modelled and real darks at higher temperatures and longer integration times (up to 50 ADU) + leak into the opaque pixels.
The uncertainty depends on the temperature, integration time and signal level.

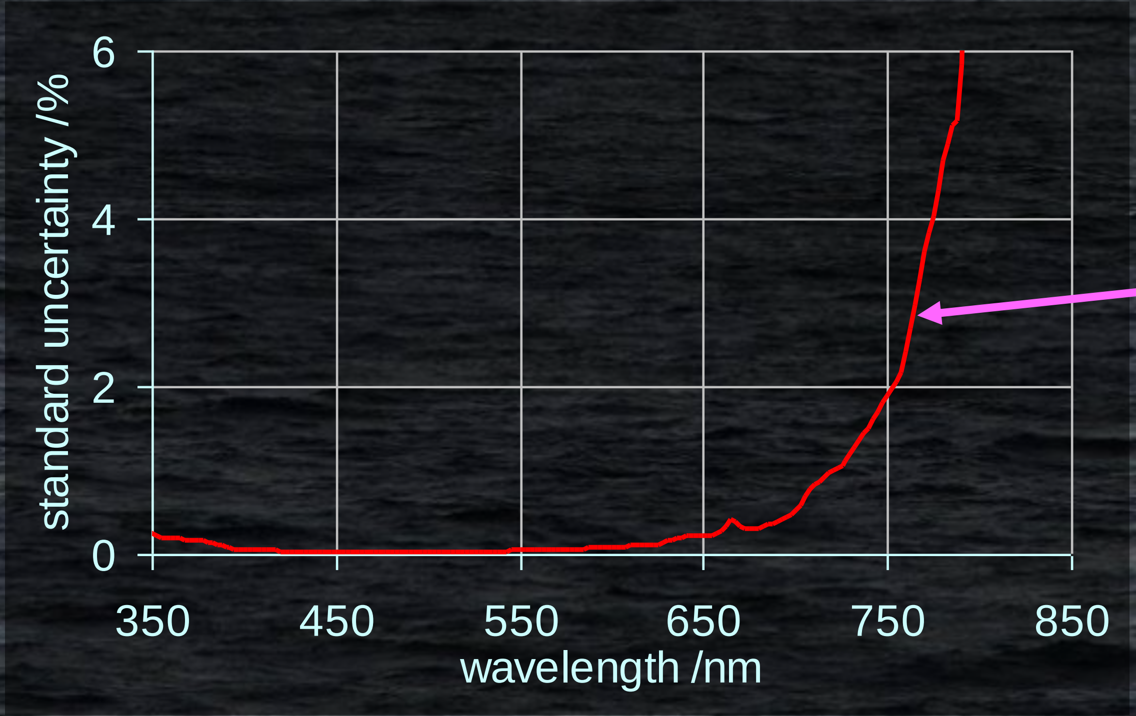

high uncertainty due to the low raw signal levels of the natural targets

Signal-to-noise ratio (*SNR*)

Noise is random change of the output signal when measuring constant input.
Origin: fundamental processes in the underlying opto-electronical componets.
Noise magnitude depends on the signal level and temperature.

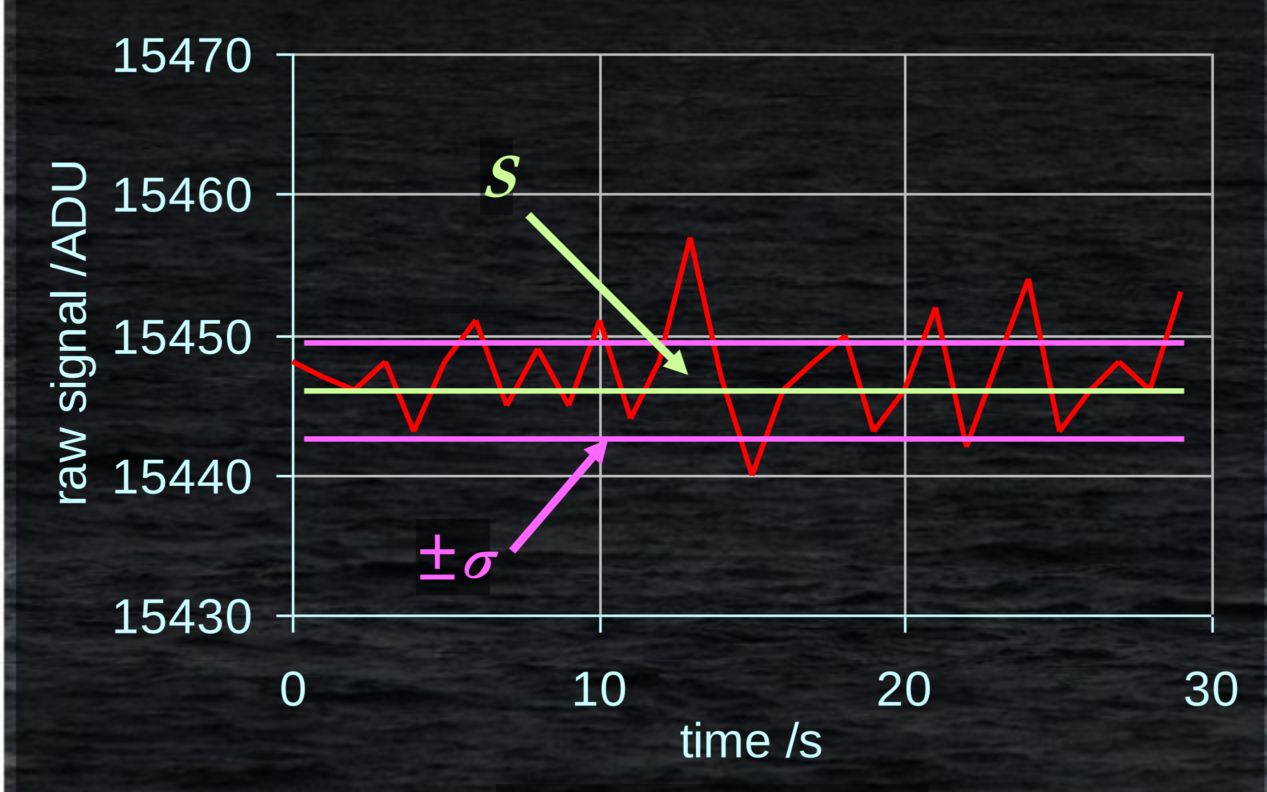

time domain

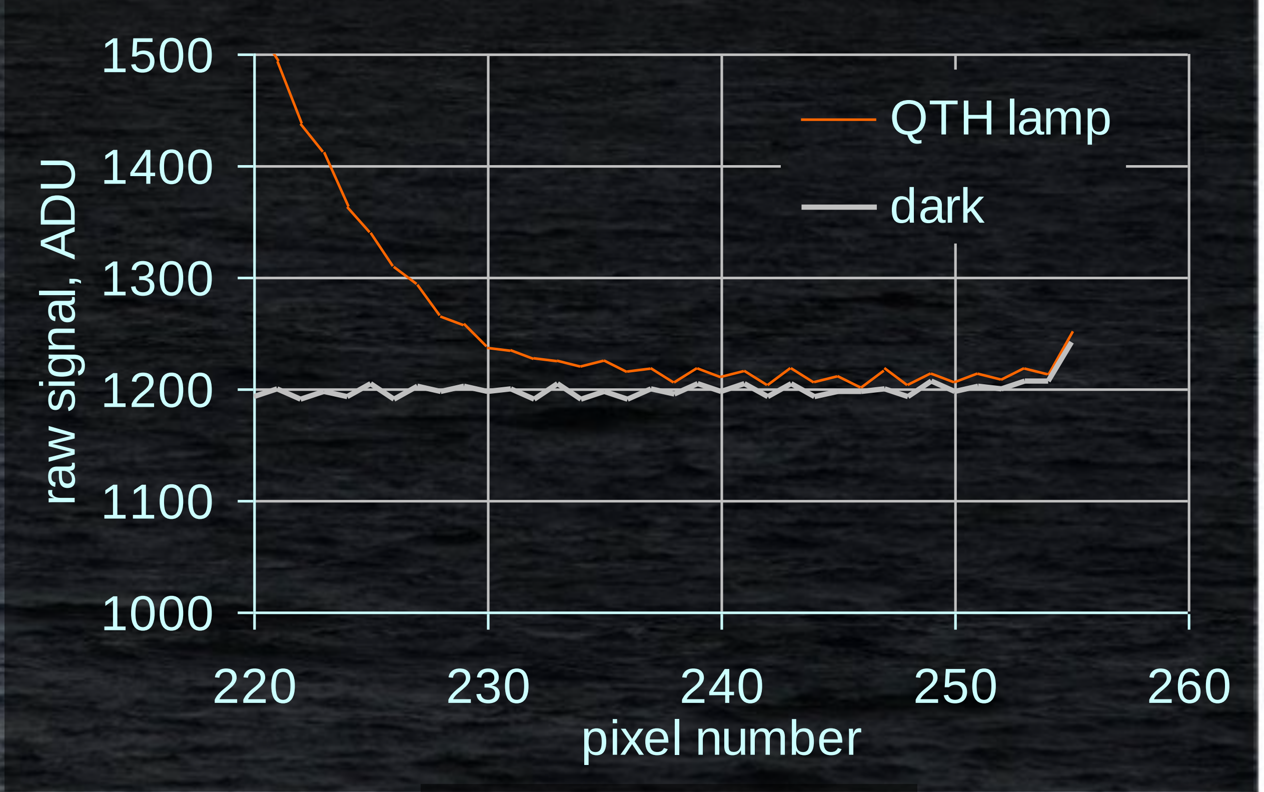

spectral domain

Signal-to-noise ratio (*SNR*)

raw signals

$$SNR = \frac{S_{light} - S_{dark}}{\sqrt{\sigma_{light}^2 + \sigma_{dark}^2}}$$

standard deviations

Be aware of temporal drifts when using standard deviation of the mean:

$$\sigma \to \frac{\sigma}{\sqrt{nf}}$$

nf: effective degrees of freedom, typically smaller than the number of averaged values.

Drift of the time series shall not exceed 10% of the standard deviation. Otherwise, take autocorrelation into account.

Signal-to-noise ratio (*SNR*)

***SNR*'s correspond to the 30-fold averaging.**

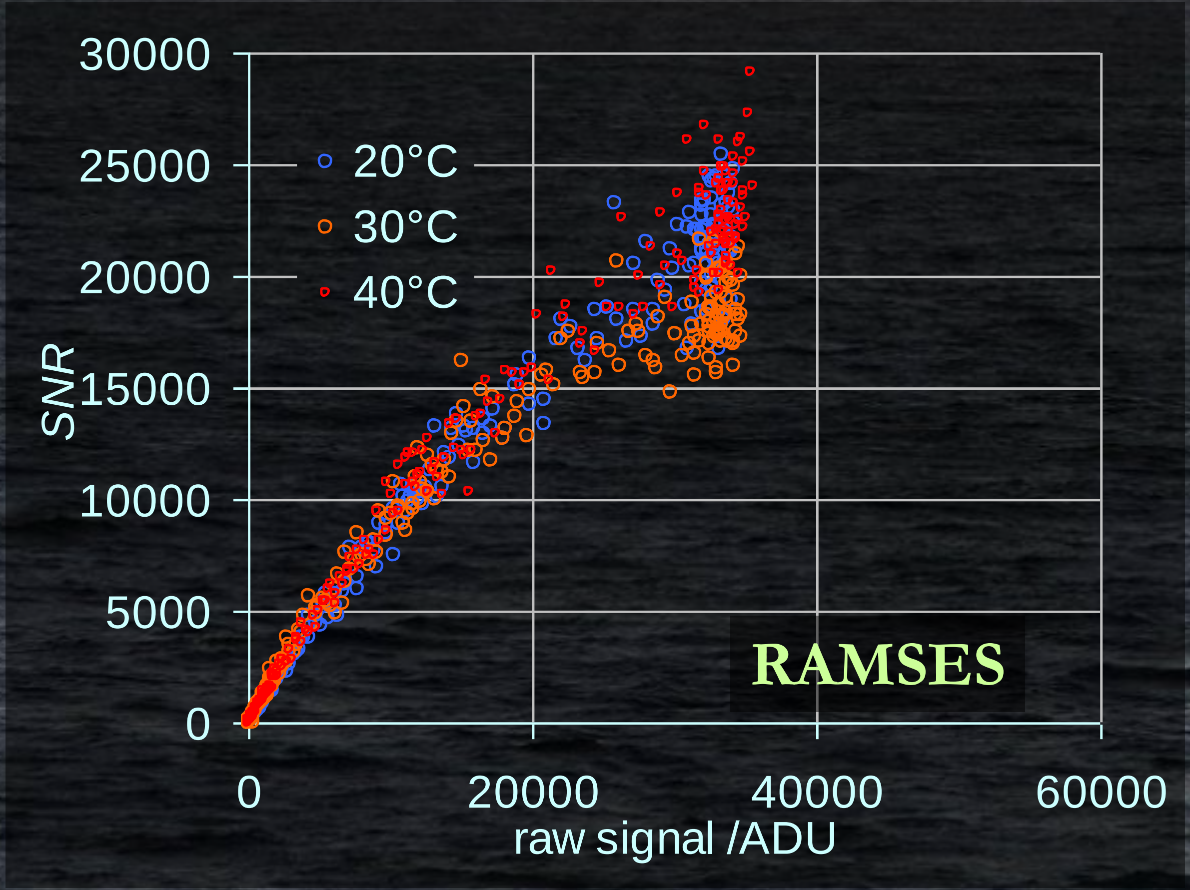

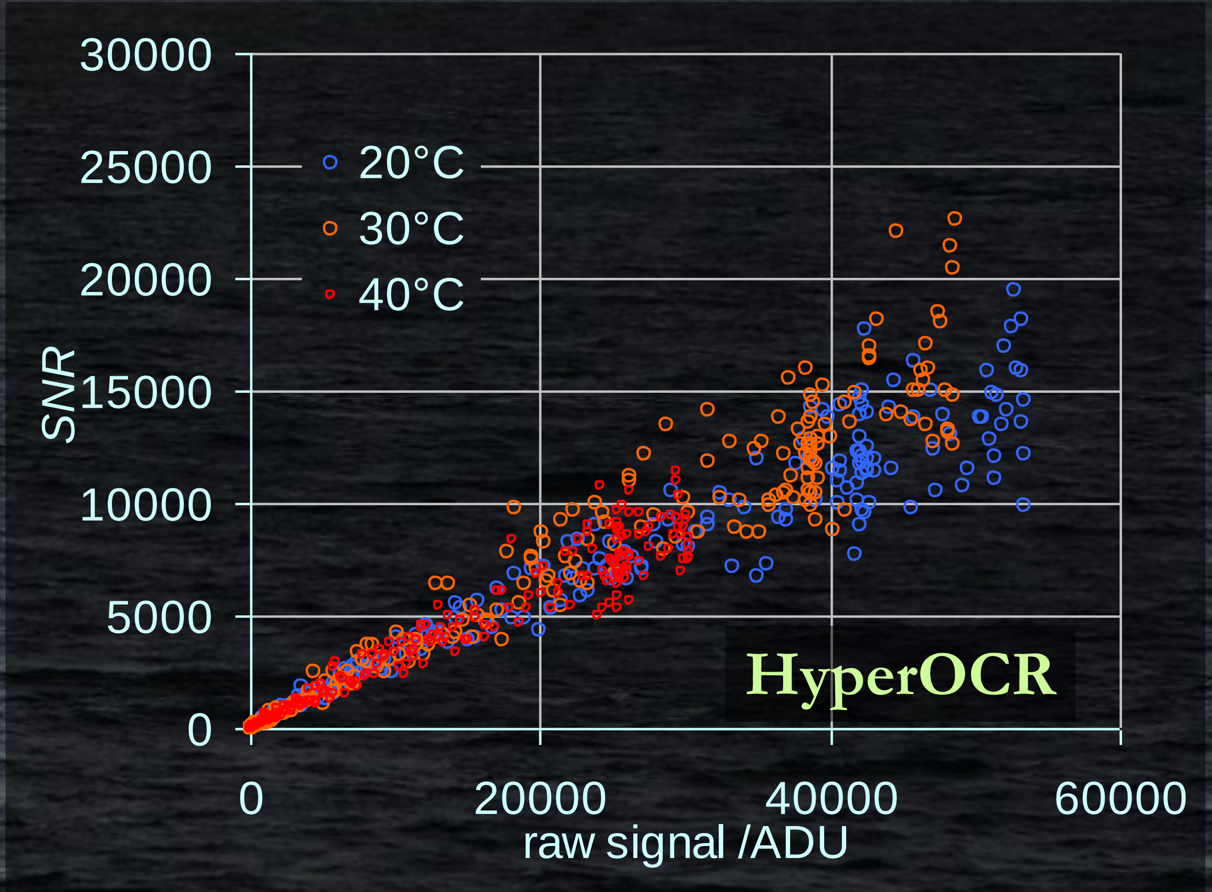

Uncertainty due to *SNR*

SNR of individual field signals*

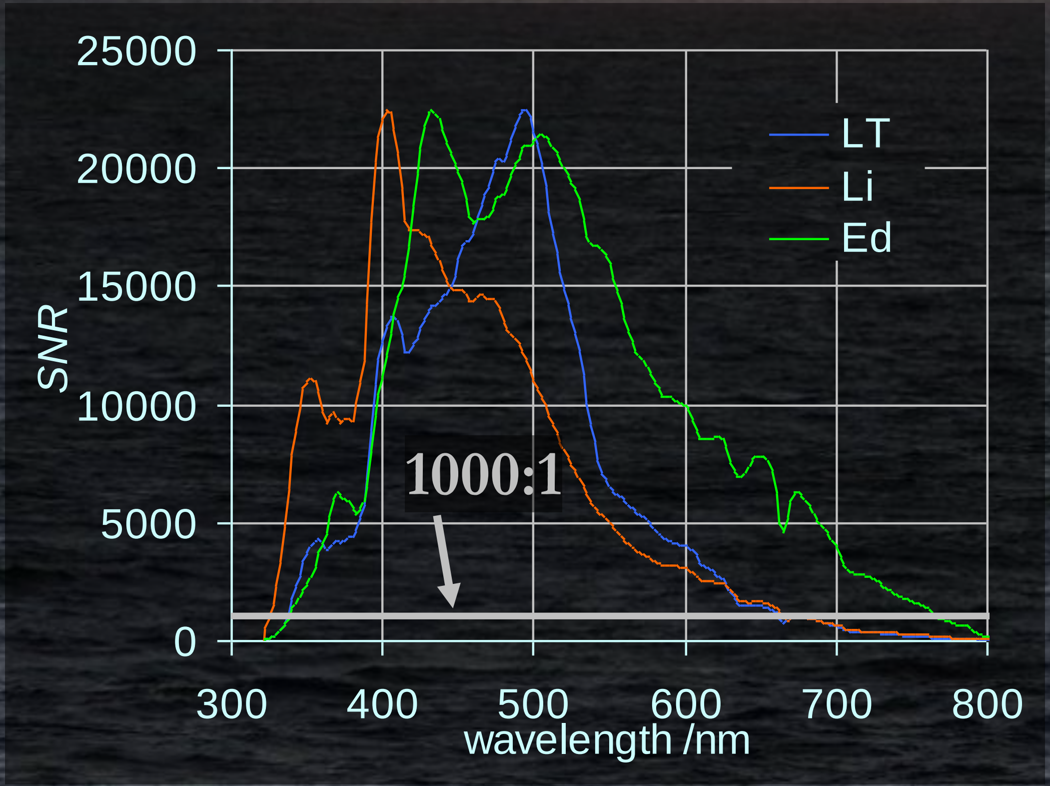

Standard uncertainties due to the *SNR**

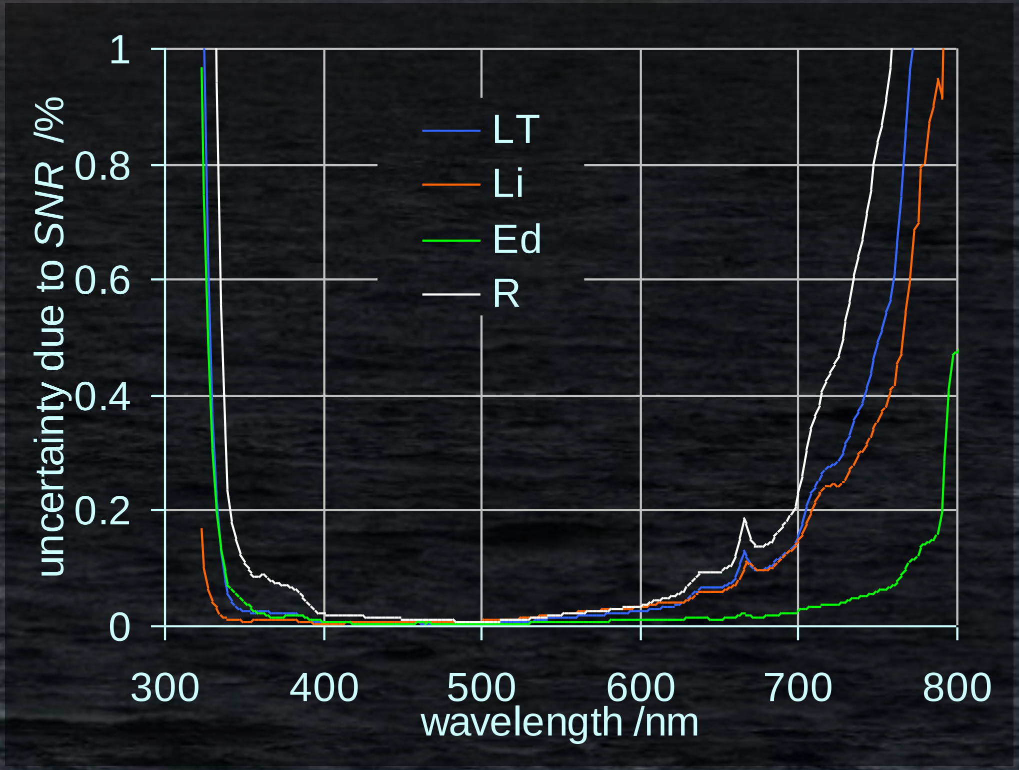

*assuming averaging of 30 spectra

Wavelength scale

Use a spectral line source (discharge lamps, gas laser) to establish relationship between the wavelength and the pixel number.

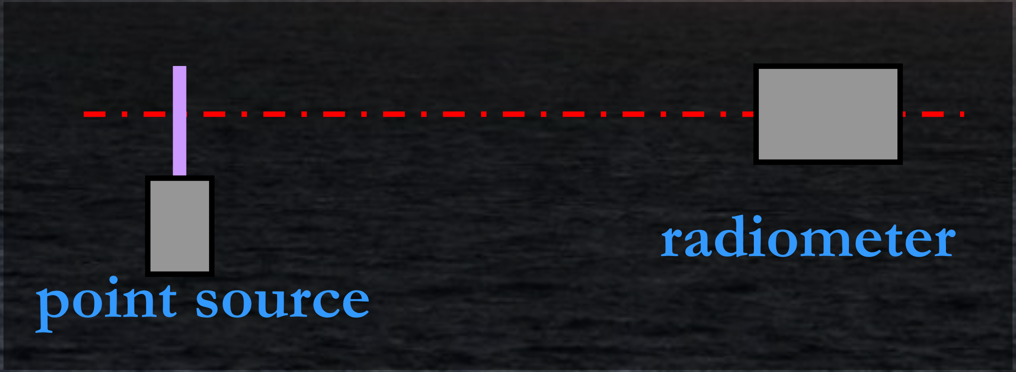

Pen-Ray lamp (Kr, Ar, Hg, ...)

low pressure Hg lamp

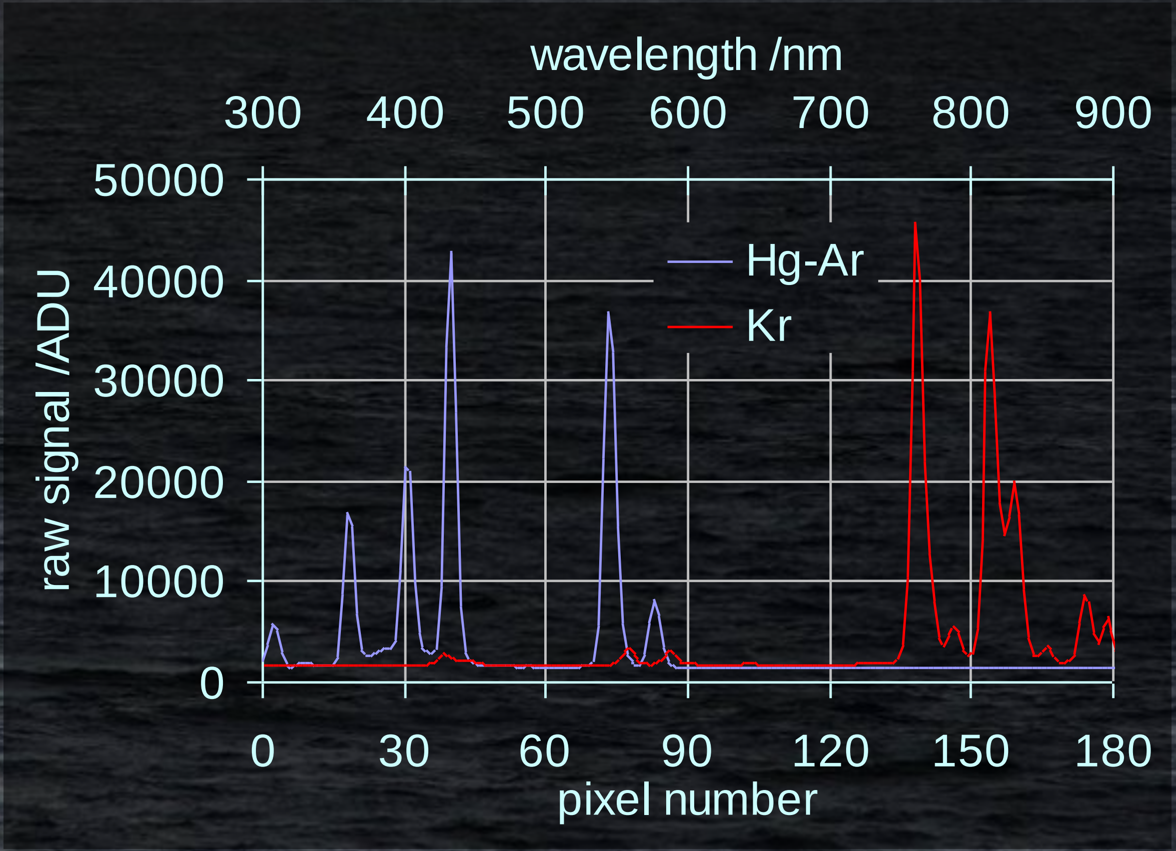

Wavelength scale

Strong lines are detected first, based on the tabulated spectral data.
The peaks are detected with sub-pixel resolution.

A low-order polynomial is used for approximation

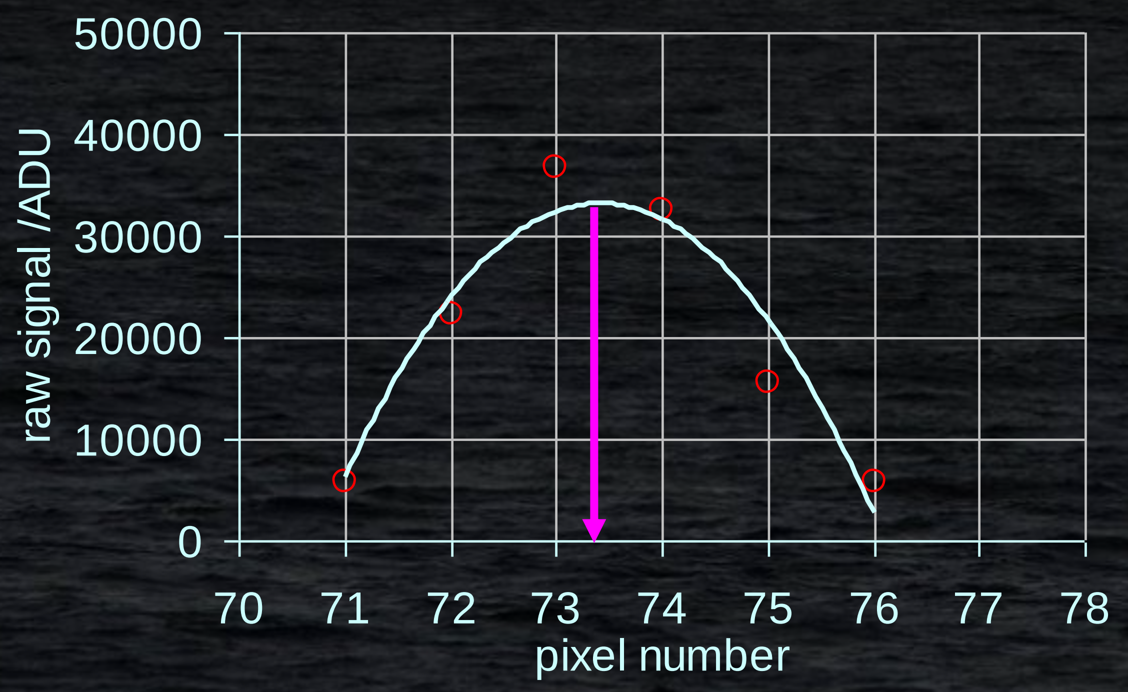

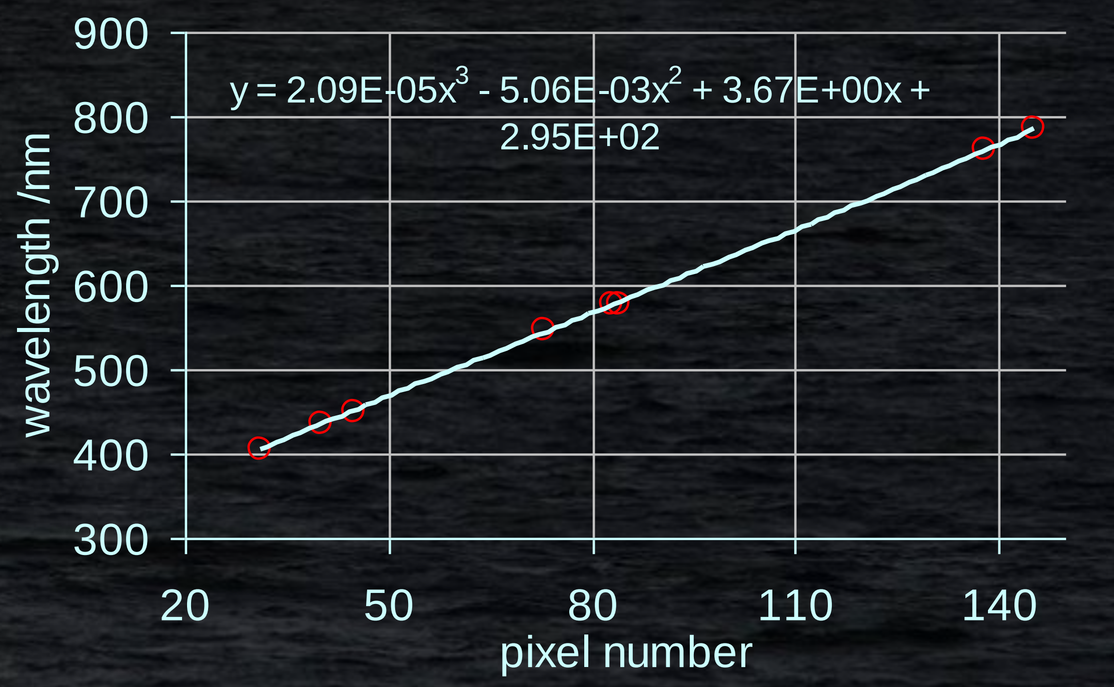

Uncertainty due to the wavelength scale

The wavelength scale of RAMSES and HyperOCR was determined in the +(5..40) °C temperature range, uncertainties stay within ±0.3 nm.

Uncertainty of radiometric quantities depend on the slope of the spectra.

Example uncertainty due to the wavelength

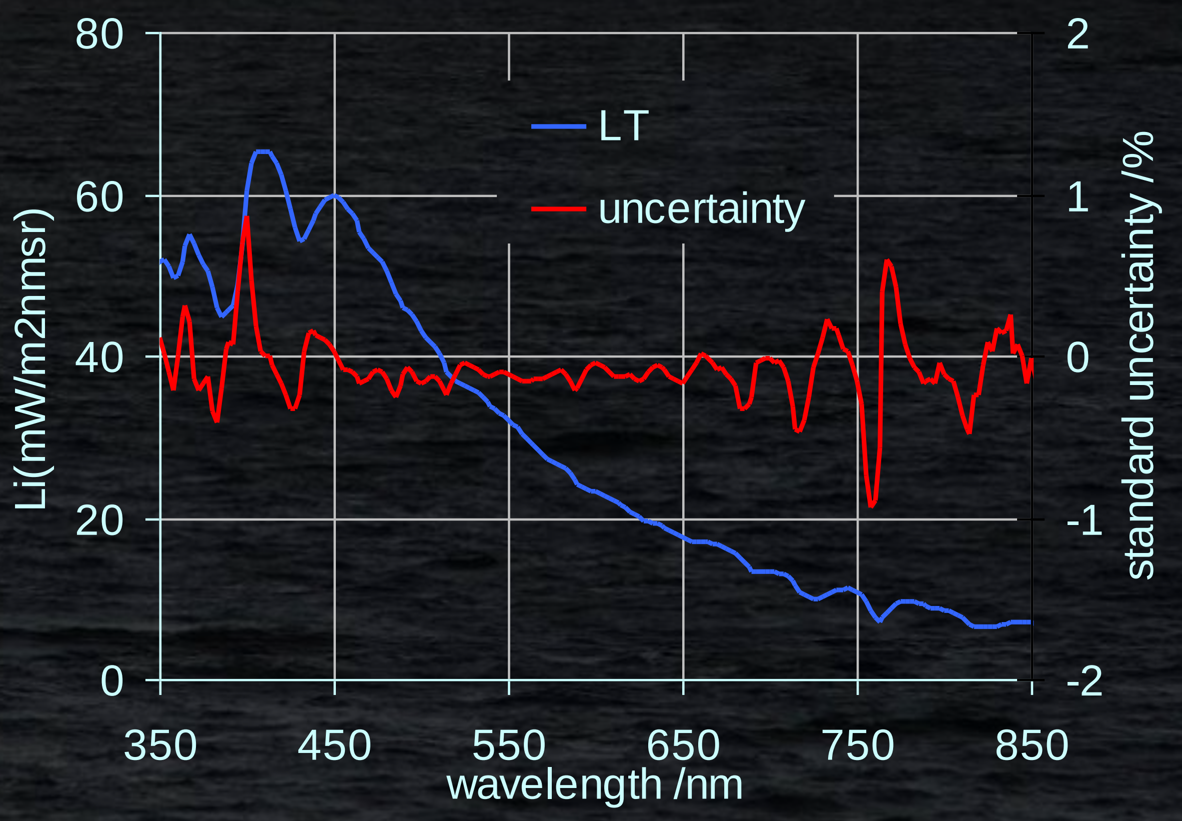

SAMIP pixel 32 issue

The Inclination/Pressure module inside the RAMSES SAMIP devices occasionally interferes with the data communication.

Detection and correction algorithm available.

Pixel 31 has bogus signal

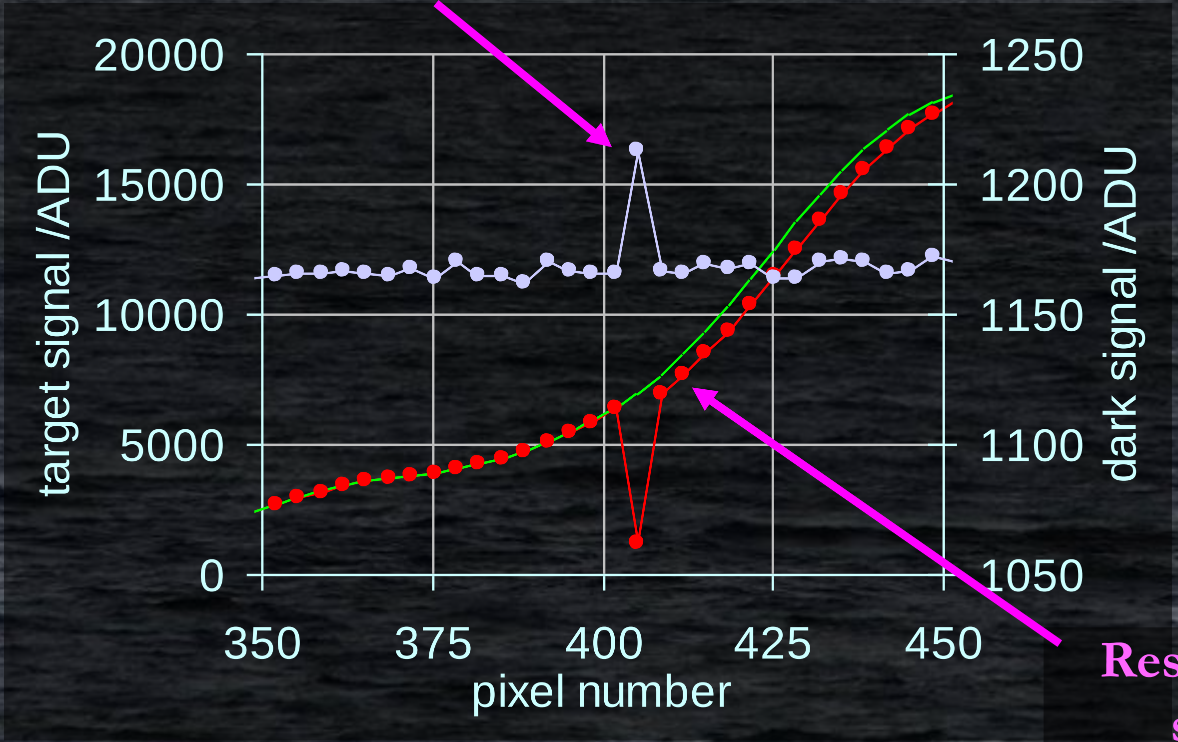

Rest of the pixel values are shifted by 1 position.

Spectral stray light

Ideal case: each pixel records signal at the pixel's wavelength.
Reality: certain amount of the pixel's signal is caused by other wavelengths.

Monochromator

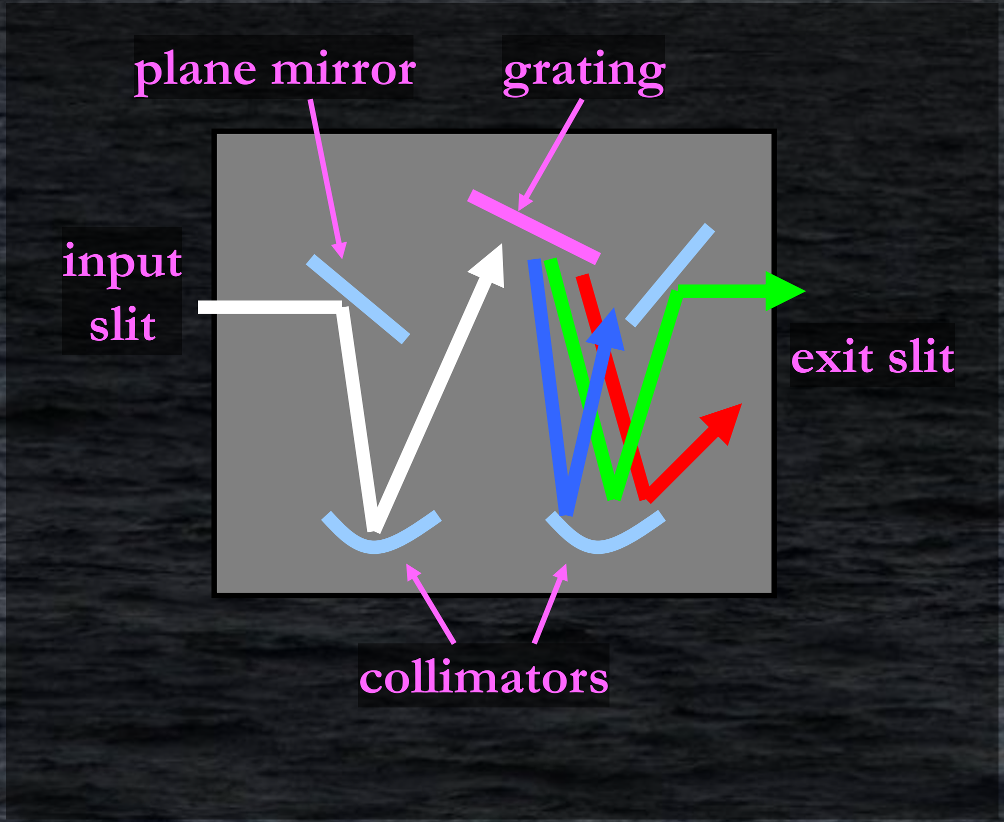

Zeiss MMS1 module

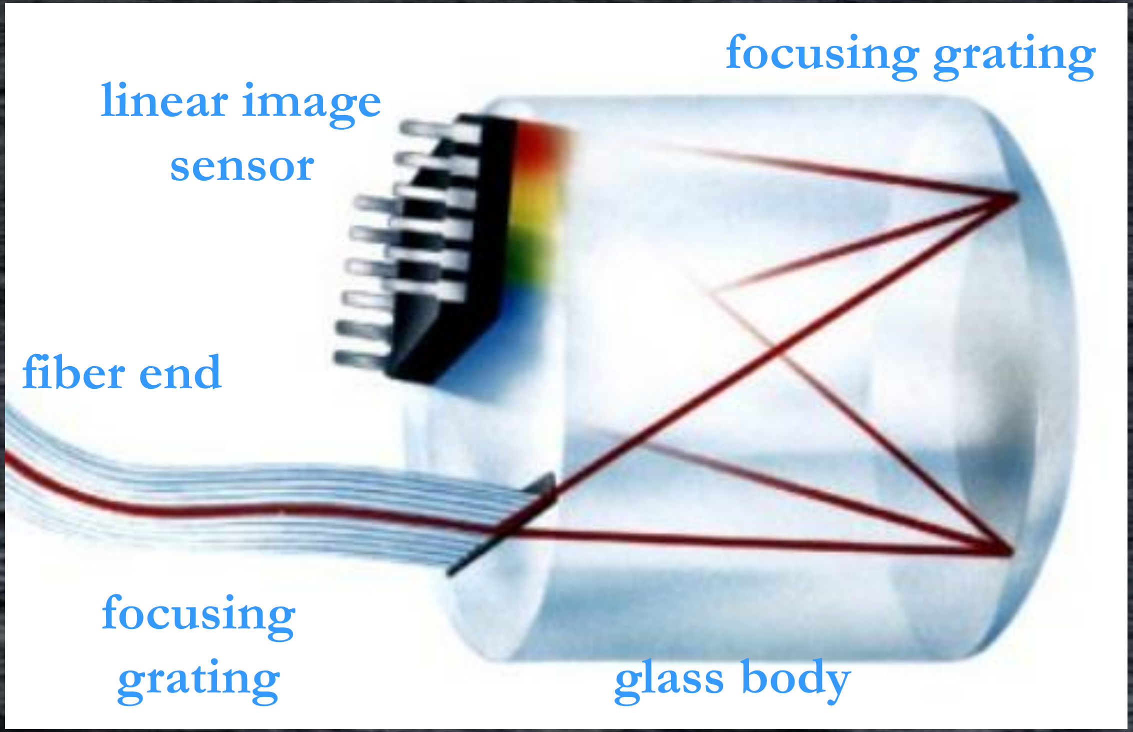

Spectral stray light

For stray-light characterization, we use tunable monochromatic source to directly measure the line spread function (LSF) for each pixel.
Tunable laser can be used instead of monochromator.

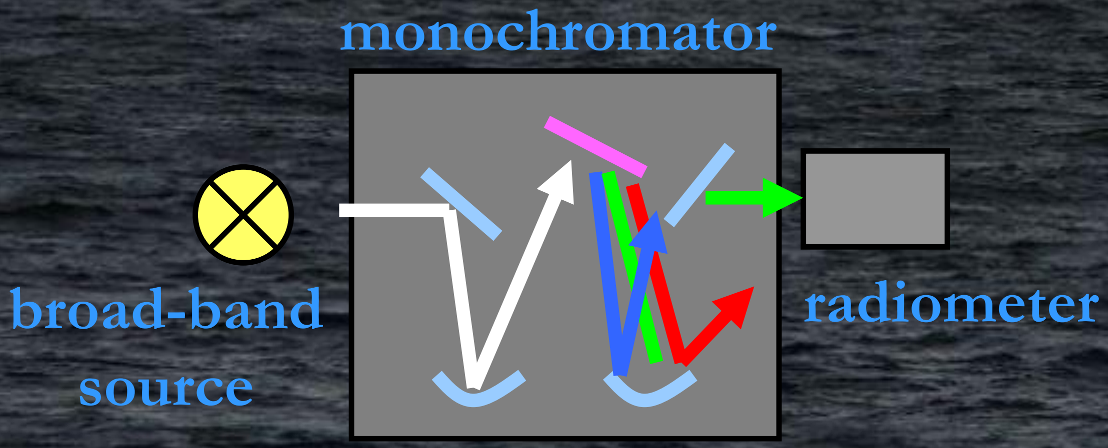

example LSFs

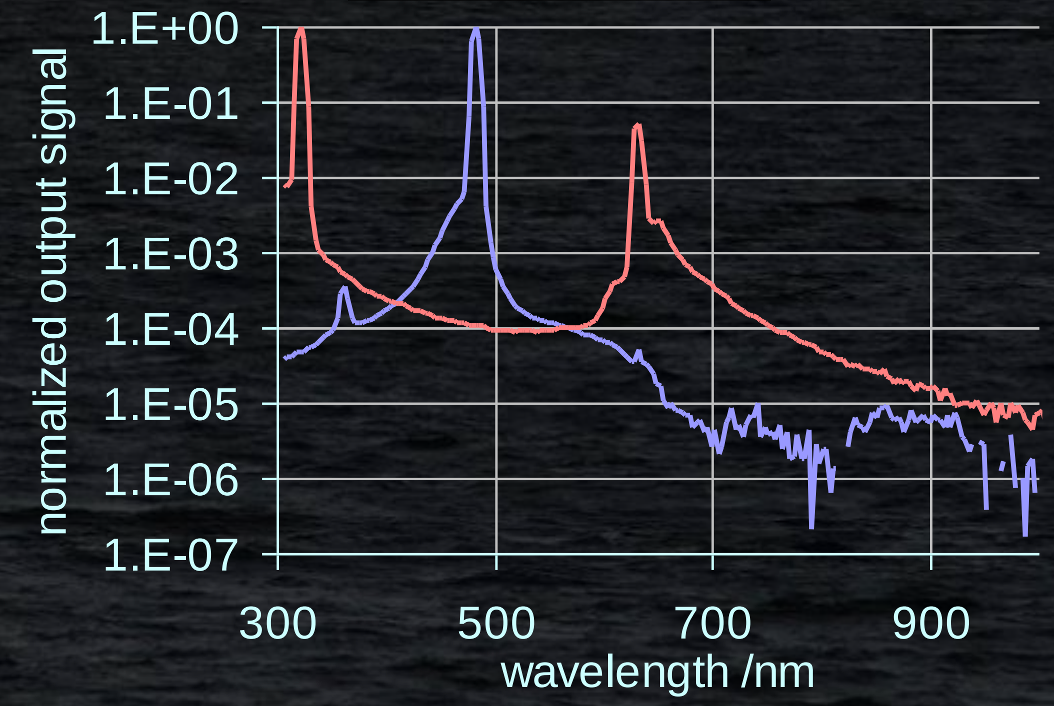

Spectral stray light

Line spread functions (LSF) are combined into stray light matrix (SLM).

LSFs in columns

$$\begin{bmatrix} z_{n0} & z_{n1} & \cdots & 1 \\ \cdots & \cdots & \cdots & \cdots \\ z_{10} & 1 & \cdots & z_{1n} \\ 1 & z_{01} & \cdots & z_{0n} \end{bmatrix}$$

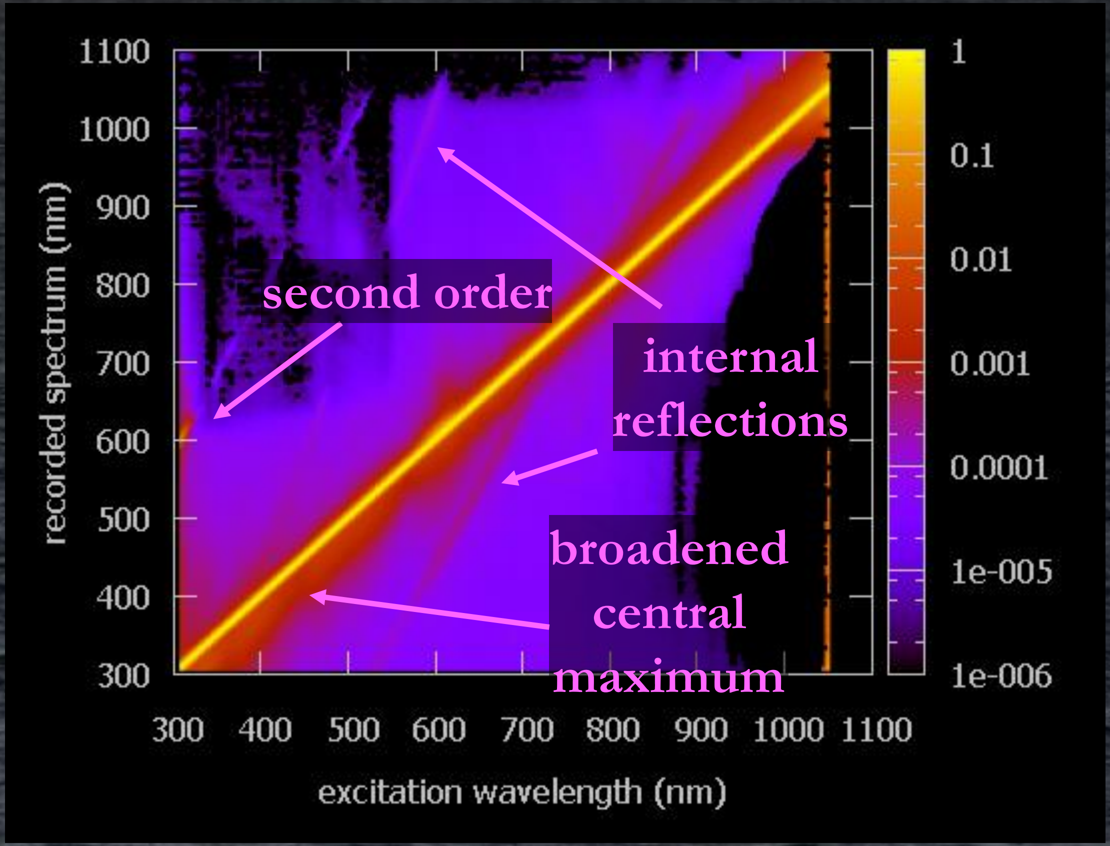

Spectral stray light

Spectral stray light re-distributes unwanted radiant flux between the sensor pixels.
Accordingly, output signal is re-distributed to the wrong pixels.
This process is mathematically called "convolution".
In matrix formalism: multiply raw spectrum* by the *SLM*.

true signal (unknown)

$$S_{meas}(\lambda) = SLM * S_{true} = \int SLM(\lambda - \Delta) S_{true}(\Lambda) d\Lambda$$

distorted signal (measured output)

*Dark is subtracted

Stray light correction

Stray light matrix (SLM) can be used to correct individual raw spectra.
The correction is mathematically called "de-convolution".
De-convolution is an iterative process: search for the input spectrum S_{true} to give the measured spectrum S_{meas} after the convolution with SLM.
Two methods implemented in HyperCP:
de-convolution [Slaper 1995]
matrix method [Zong 2006]

Correction scheme:

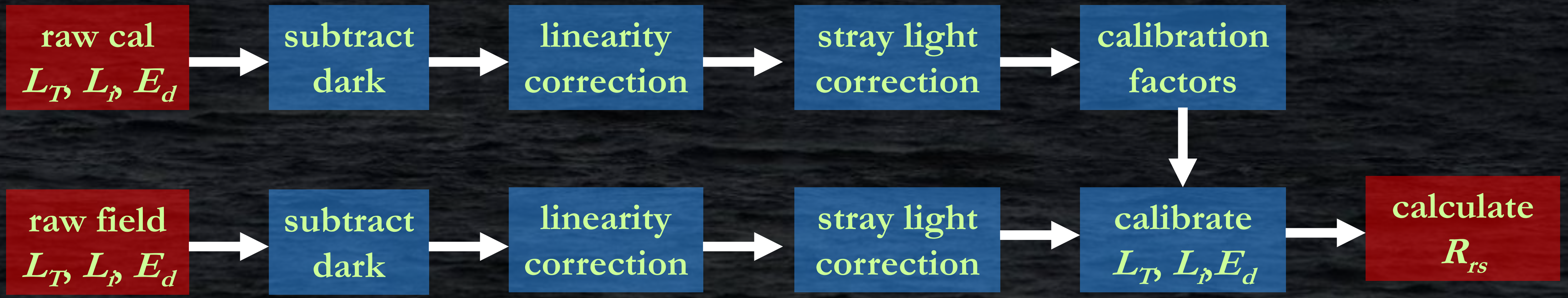

Uncertainty due to the spectral stray light

Example uncertainty:

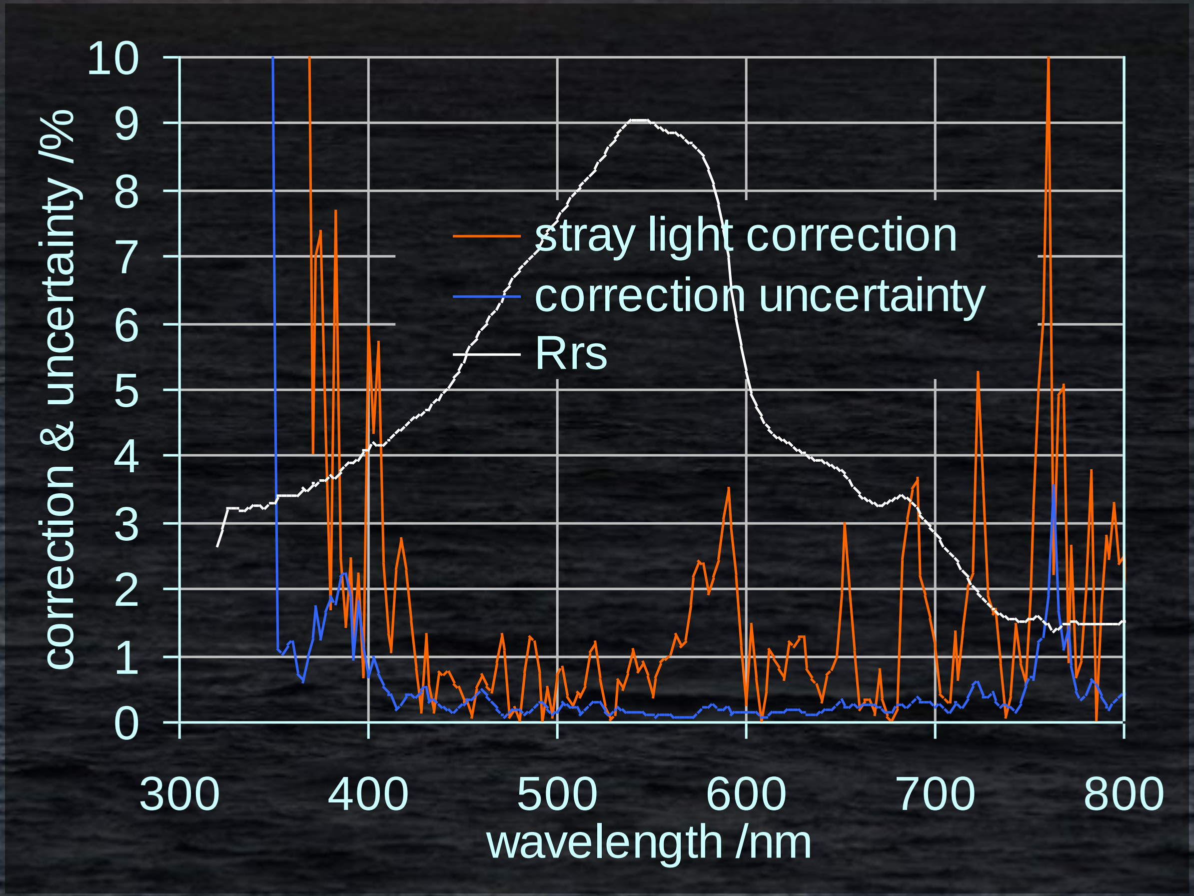

Thermal response

Expected temperature range during the field work is +(2..40) °C.
The instrumental parameters change with temperature.
Most significant are the changes in dark signal and responsivity.
Measure the dark close to the target signal and with the same integration time.
Responsivity change is caused by the detector, front-end electronics
and thermal expansions of the opto-mechanical subsystem.
Responsivity change depends on the wavelength.

Measurement setup for thermal characterization

Thermal characterization is a lengthy process: relaxation times of ~1 h are required.
This puts high demands on the temporal stability of the source and the alignment.

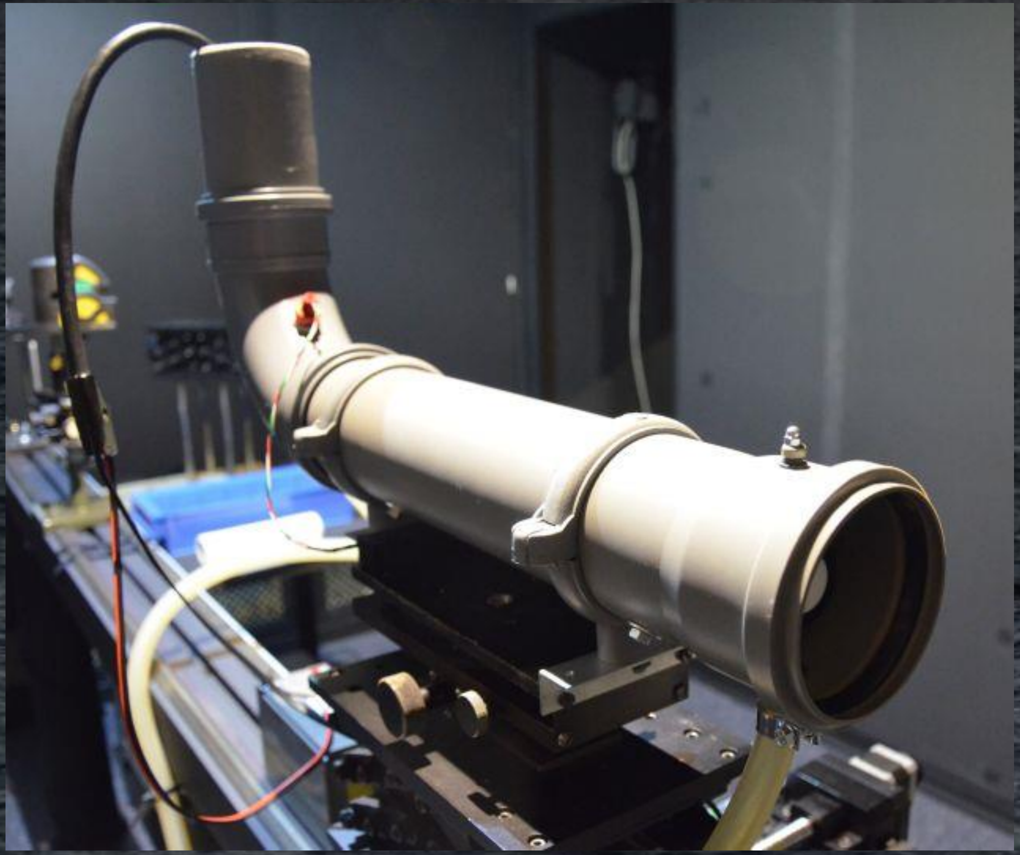

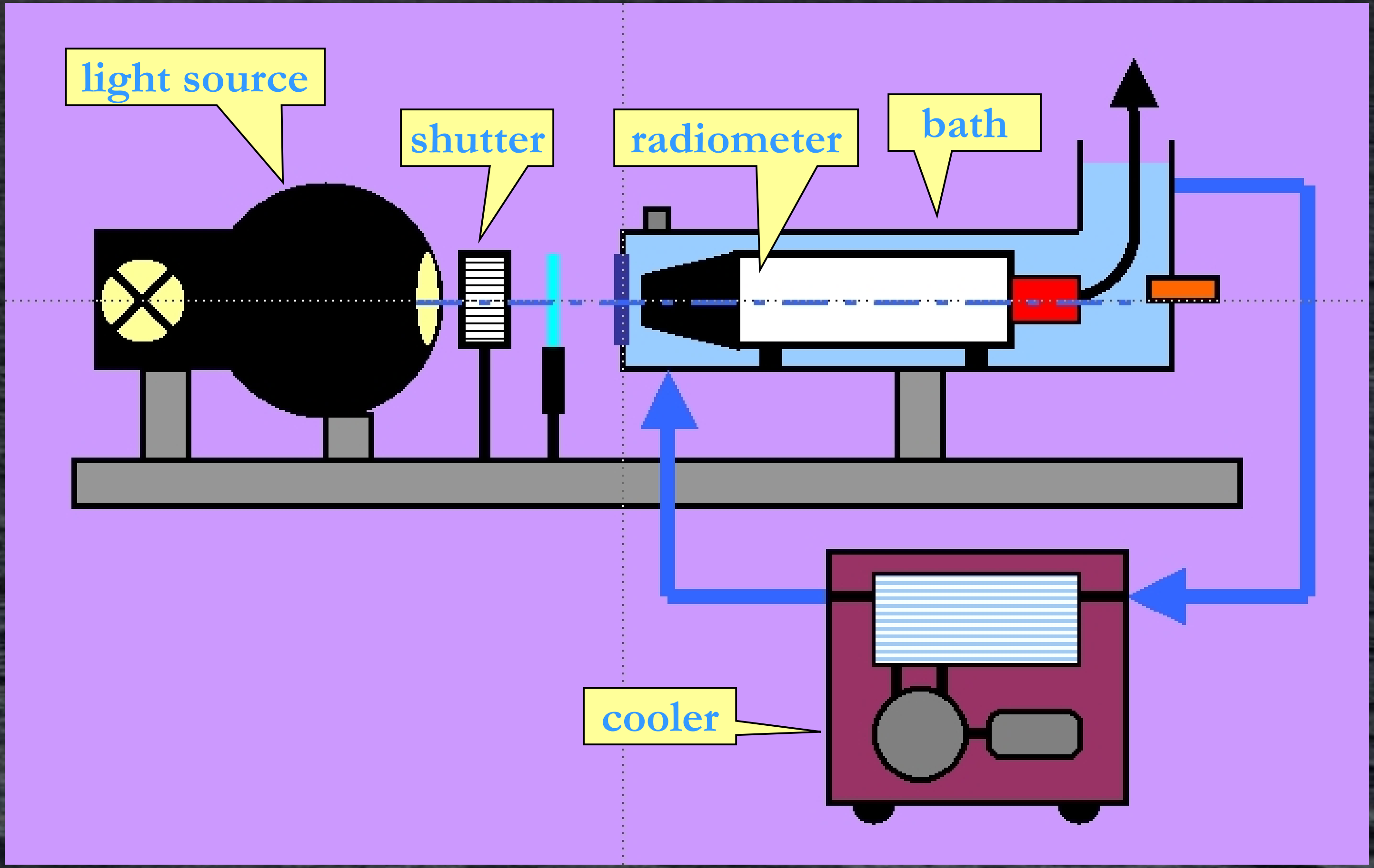

Thermal characterization method

Measure temporarily stable source at different radiometer temperatures to determine thermal coefficients of the radiometric responsivity.
Combine the experiment with characterization of the non-linearity, dark signal, wavelength scale, polarization sensitivity etc.
Thermal coefficients are evaluated separately for each pixel.
Measurement results are referenced to certain temperature, typically +20 °C.

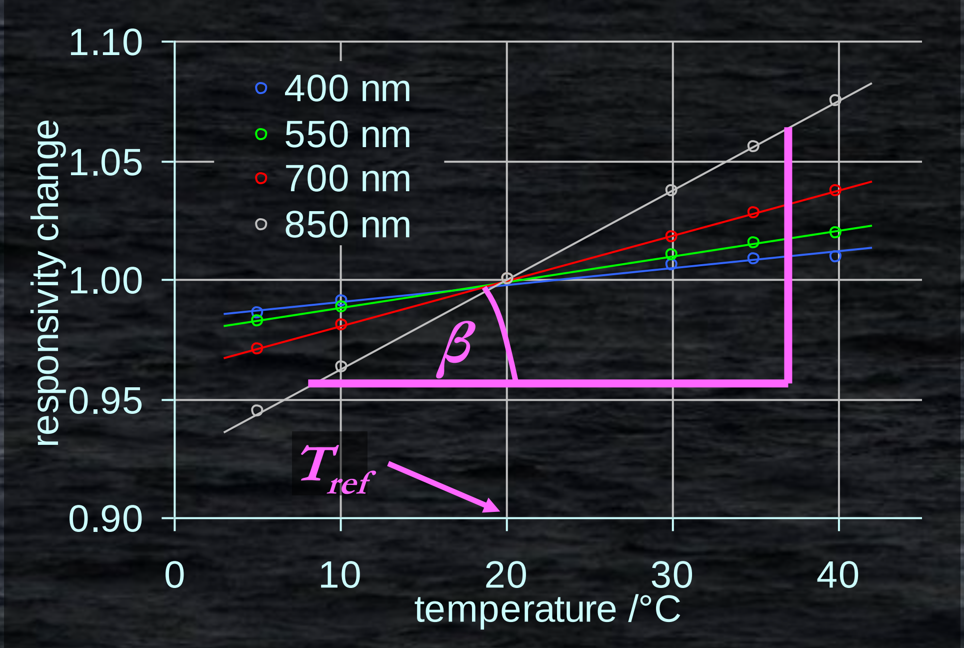

Thermal coefficient

$c_T(\lambda) = \tan\beta$

Correcting the field spectra:

$$S(\lambda, T_{ref}) = S(\lambda, T)\,[1 + (T - T_{ref})\,c_T(\lambda)]$$

raw or calibrated signal

Thermal response

Thermal characterization results are stored in the CP_*_THERMAL_* files and processed by HyperCP.

family average $c_T(\lambda)$ and expanded uncertainty

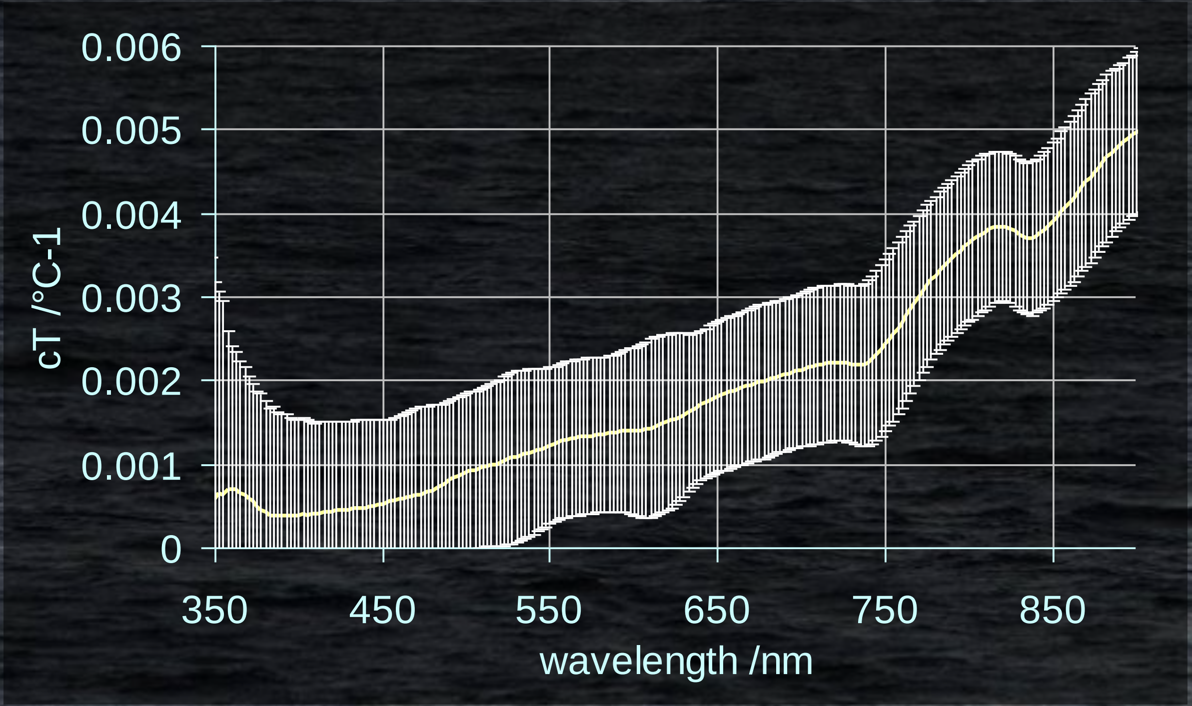

individual $c_T(\lambda)$ and expanded uncertainty

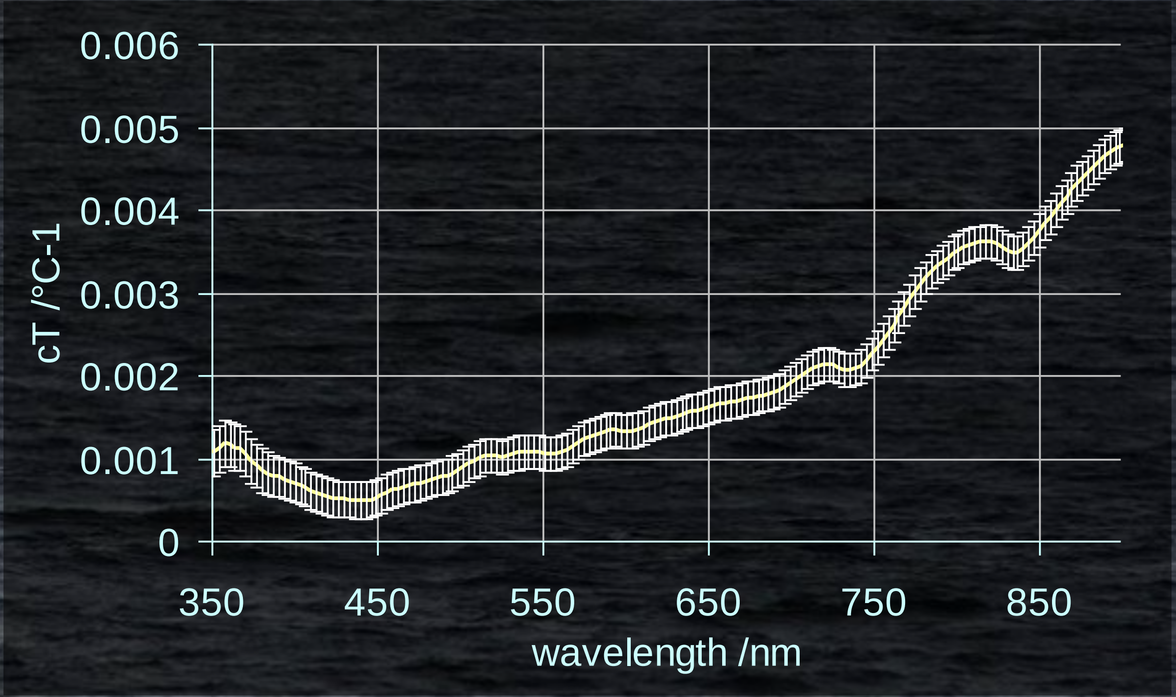

Thermal response

Validation of the thermal characterization method: TO vs. JRC vs. Sea-Bird.

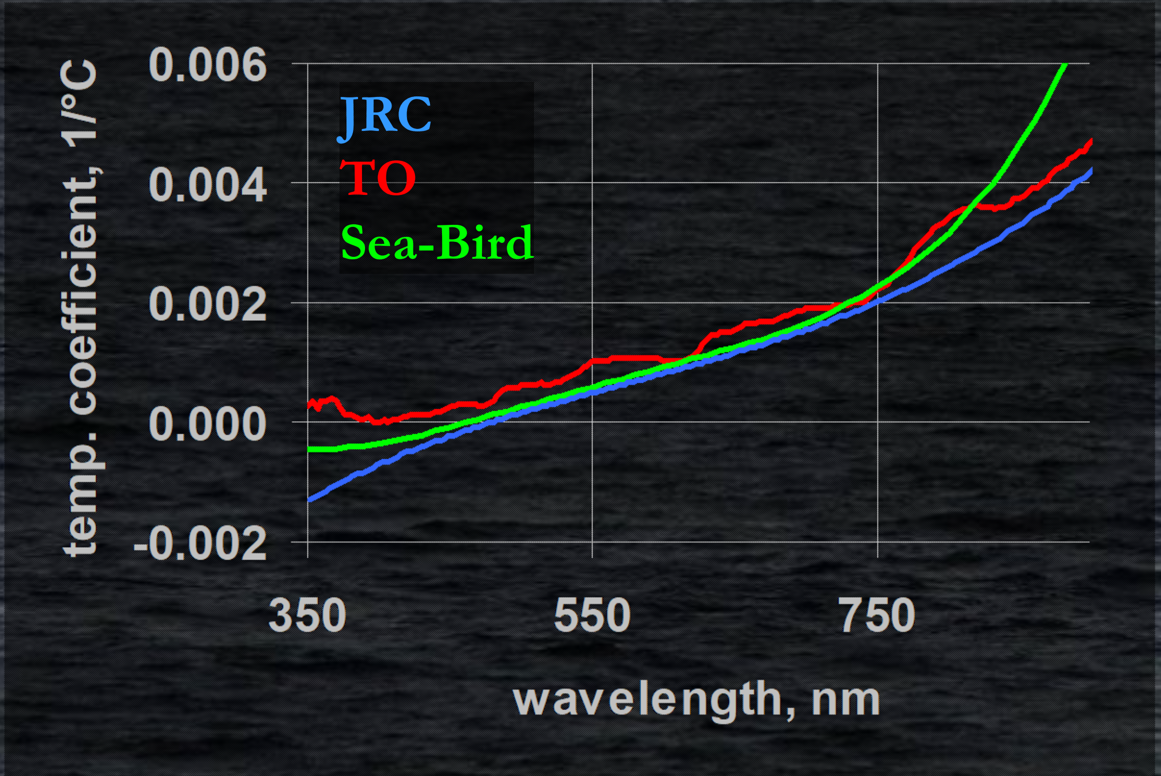

Fast temperature change: temperature sensor signal does not follow the responsivity.
Uncertainty will increase.
Dark signal is good temperature proxy.

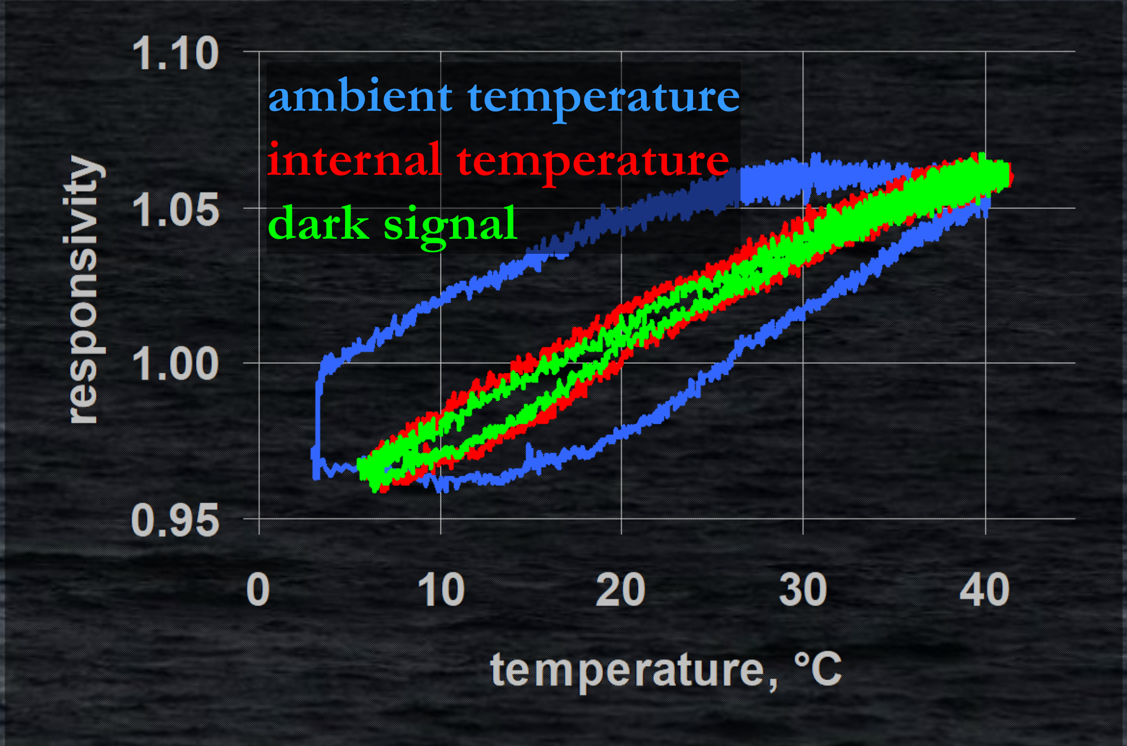

Thermal response: PTFE

Slow temperature change

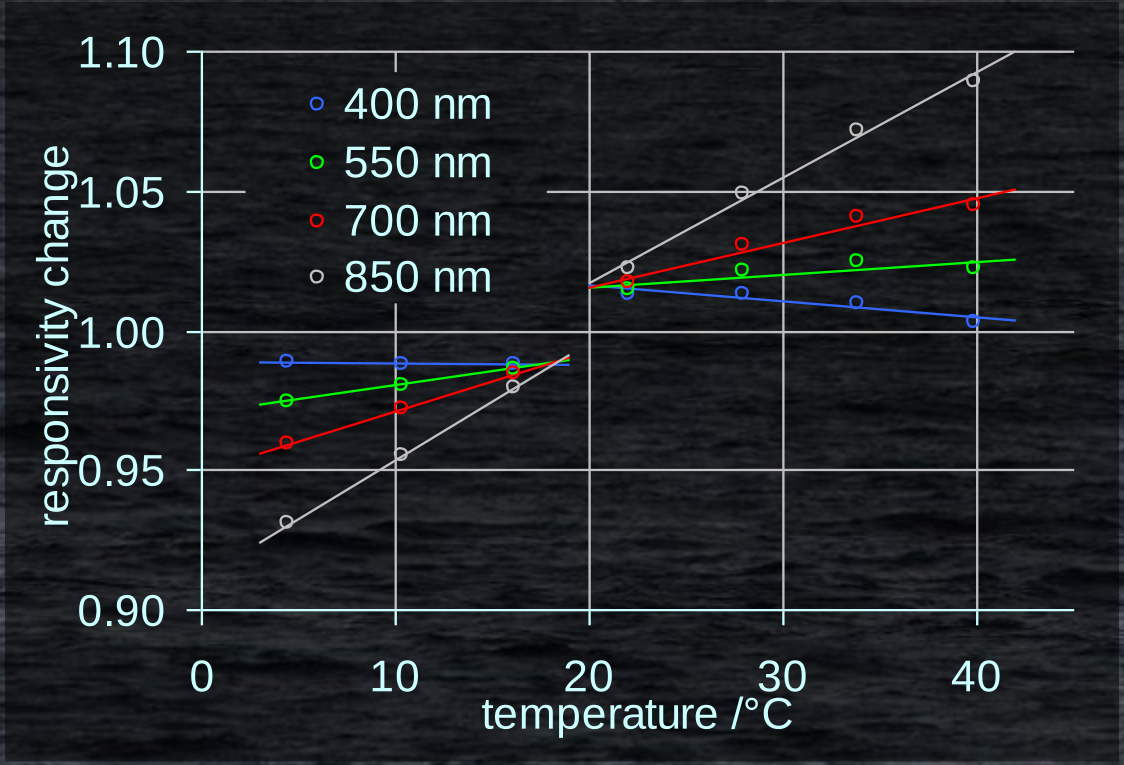

Fast temperature change

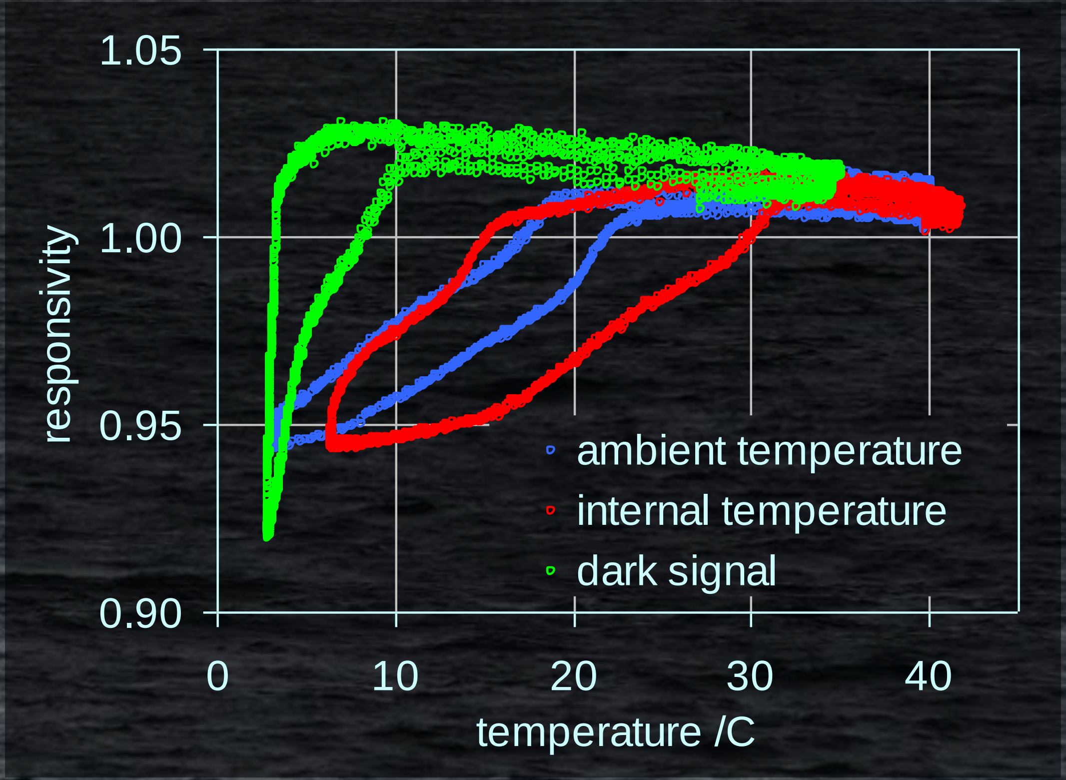

Uncertainty due to the thermal response

Error caused by 10 °C difference between the calibration and field temperatures.
L_T, L_i and E_d radiometers belong to the same family.

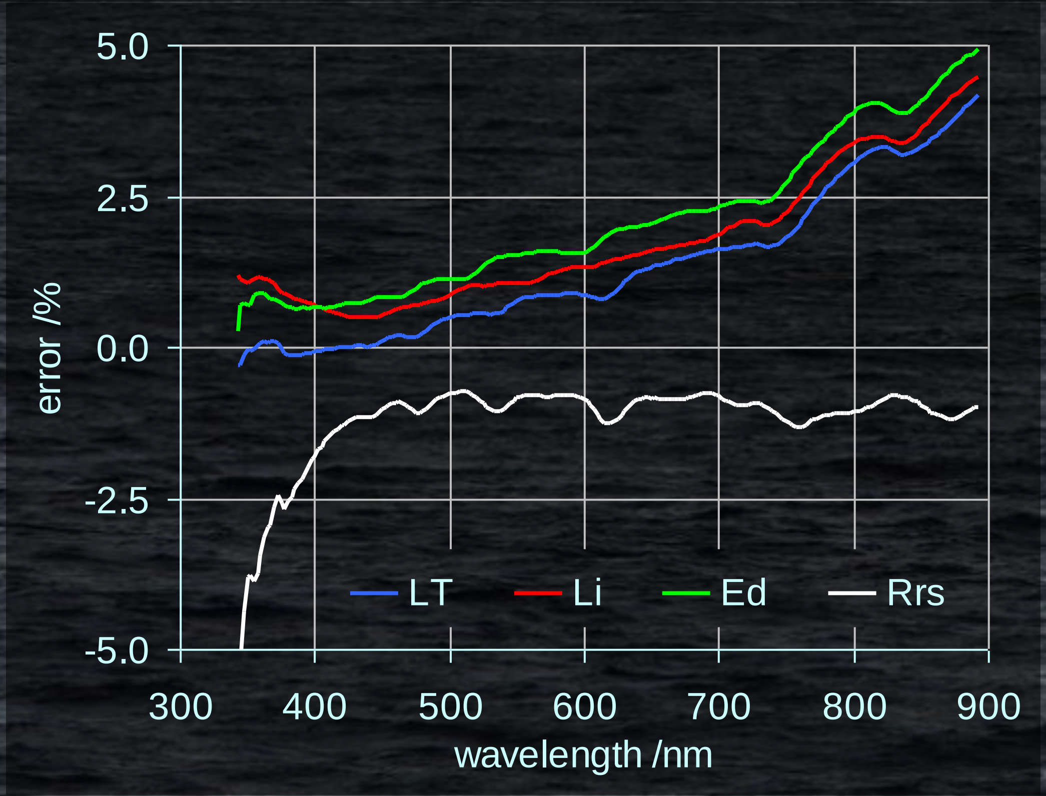

Residual uncertainty after temperature correction

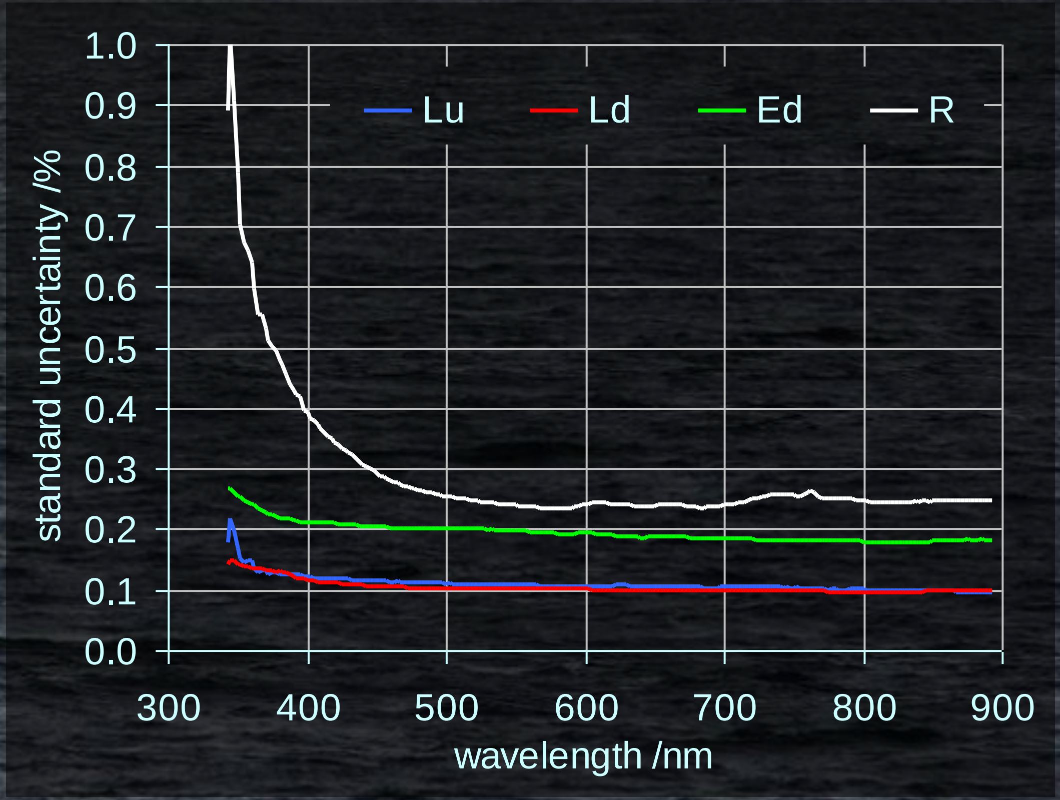

Angular response

Ideal case (radiance): narrow FOV with flat top and steep edges.
Ideal case (irradiance): angular response follows the cosine law.
Azimuthal symmetry of the response is assumed.

Reality (radiance): non-uniformity within the FOV, gentle slopes.
Reality (irradiance): deviation from the cosine law.
Angular response depends on the principal plane.

Angular response characterization setup

Measurement method: precise rotation of the radiometer within the collimated beam.

Zero azimuth is marked with a red dot on the radiometer's body.

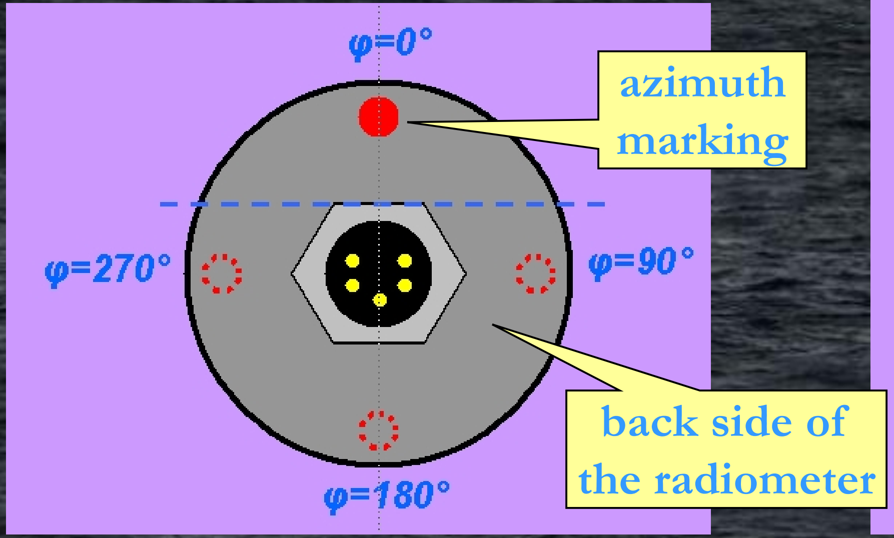

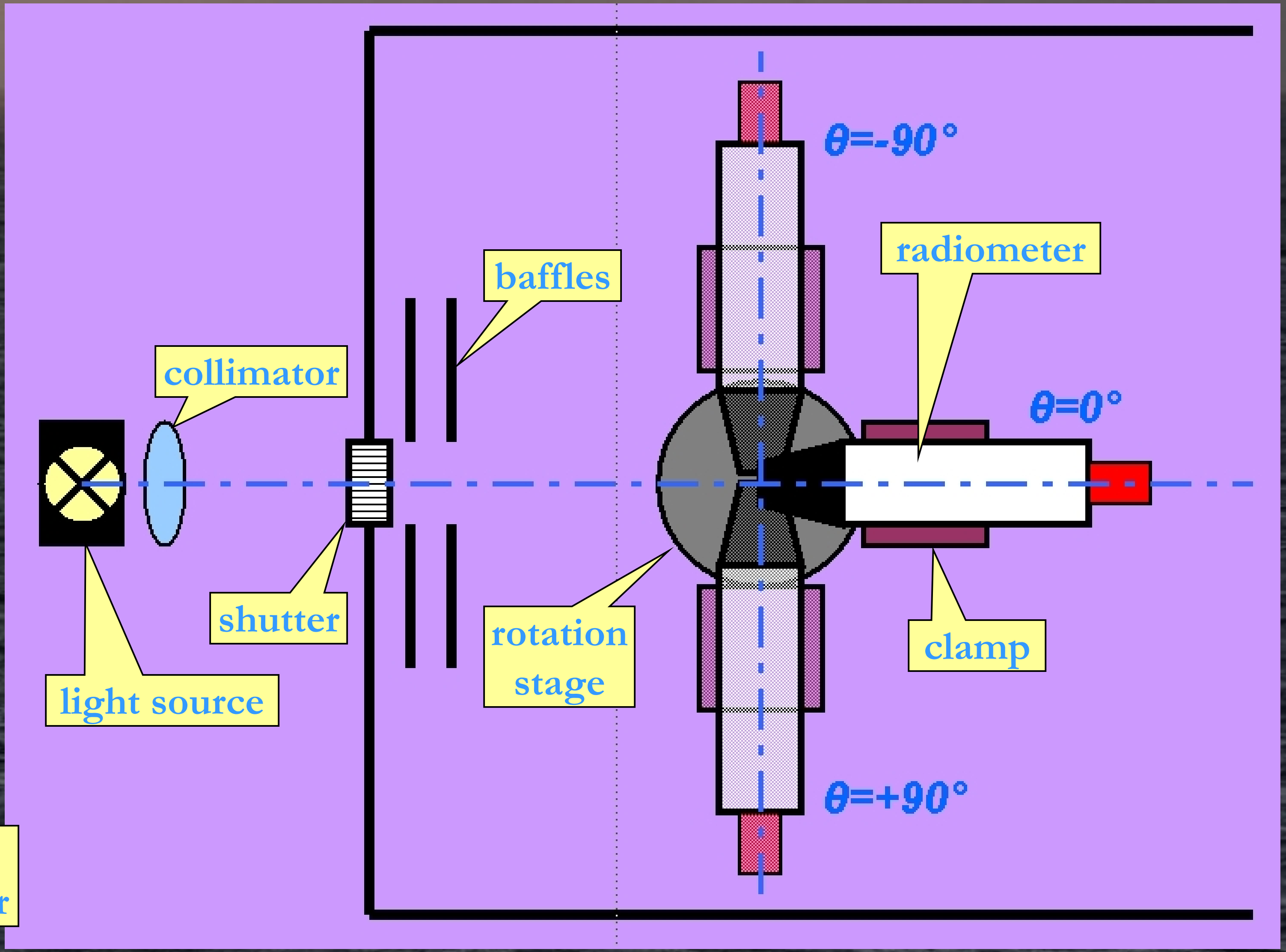

Angular response

Lamp and lens form a collimated beam.
Incident angle is changed by rotating the radiometer.
Characterization result: normalized responsivity vs. incident angle for each pixel.
Angular response is measured in two perpendicular principal planes.
Results stored in the CP_*ANGULAR_* files and processed by HyperCP.
The corrections and uncertaintiy evaluated in HyperCP.

Angular response examples: radiance sensors

FOV of the RAMSES and HyperOCR radiance sensors

FOV of a modified RAMSES sensor in two principal planes

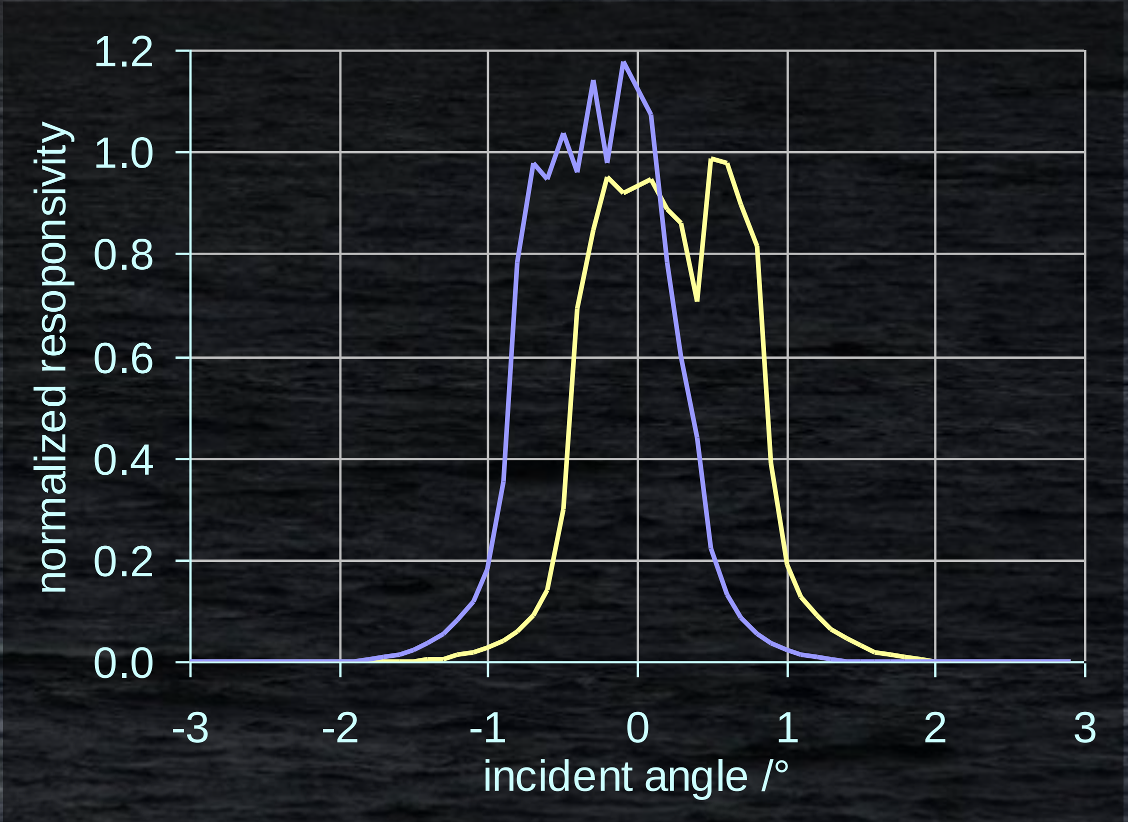

Angular response of the irradiance sensors

Ideal case: angular response of the irradiance sensor follows cosine law:

raw or calibrated signal

$$S(\theta,\lambda) = S(\theta = 0,\lambda)\cos(\theta)$$

Reality: angular response deviates from the cosine law by "cosine error":

$$CE(\theta,\lambda) = \frac{S(\theta,\lambda)/S(\theta = 0,\lambda) - \cos(\theta)}{\cos(\theta)} \cdot 100\%$$

The integral cosine error is defined as

$$ICE(\lambda) = \int_{0^\circ}^{85^\circ} CE(\theta,\lambda)\sin(2\theta)d\theta$$

Cosine error is amongst the key contributors to the uncertainty of E_d and R_{rs}.

Angular response examples: irradiance sensors

For uncertainty estimation we need direct-to-diffuse ratio of the downwelling irradiance.

Practical hint: uncertainty component for R_{rs} is close to the integral cosine error (which is close to the cosine error around 45° incident angle).

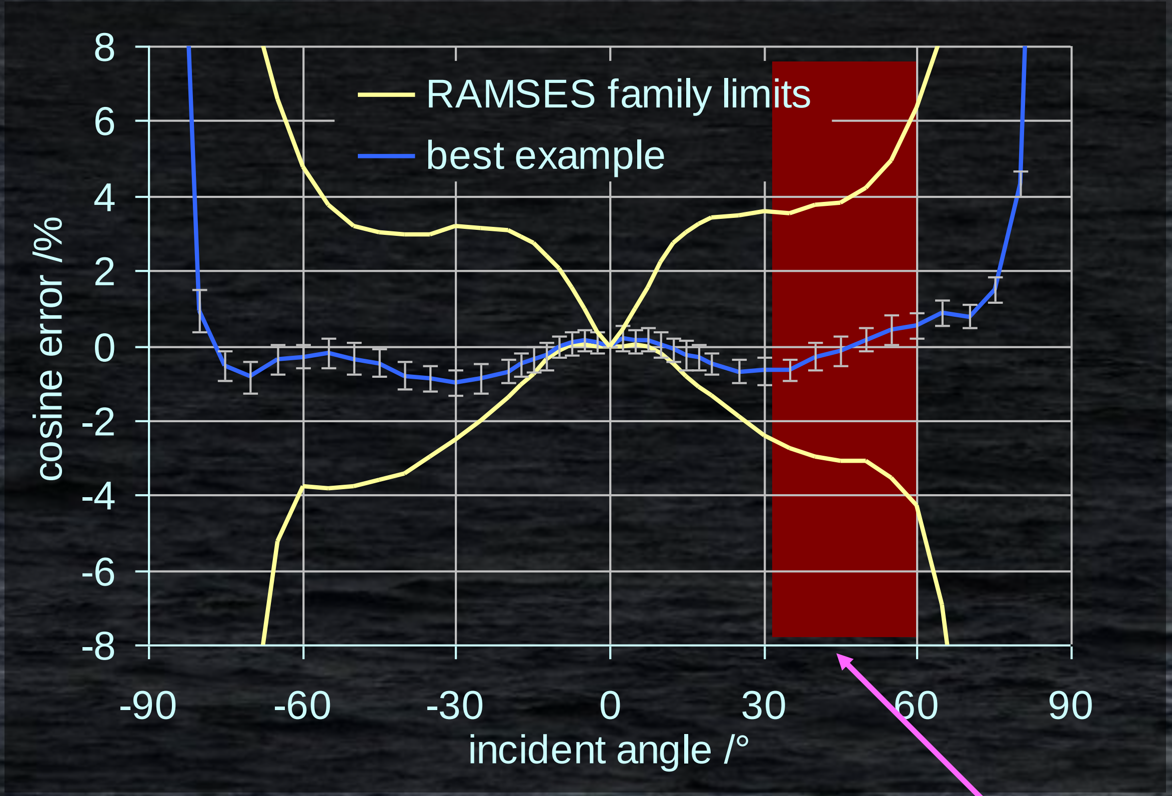

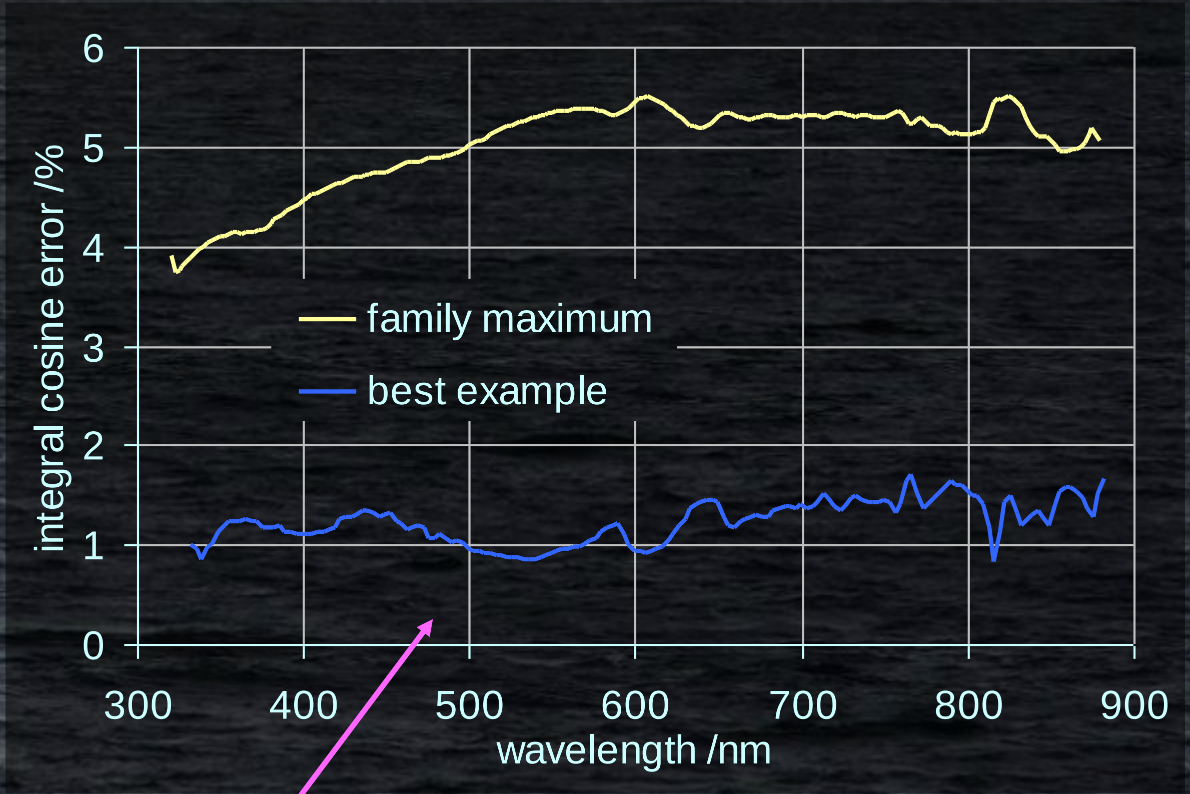

estimate for the uncertainty of E_d and R_{rs}

Polarization of light

Optical radiation is an electromagnetic wave.

Electromagnetic waves are transverse: the electric and magnetic vectors are perpendicular to the direction of wave propagation.

In the case of unpolarized light, all vector directions have equal probability.

Light detectors average the electric vector magnitude into electrical signal.

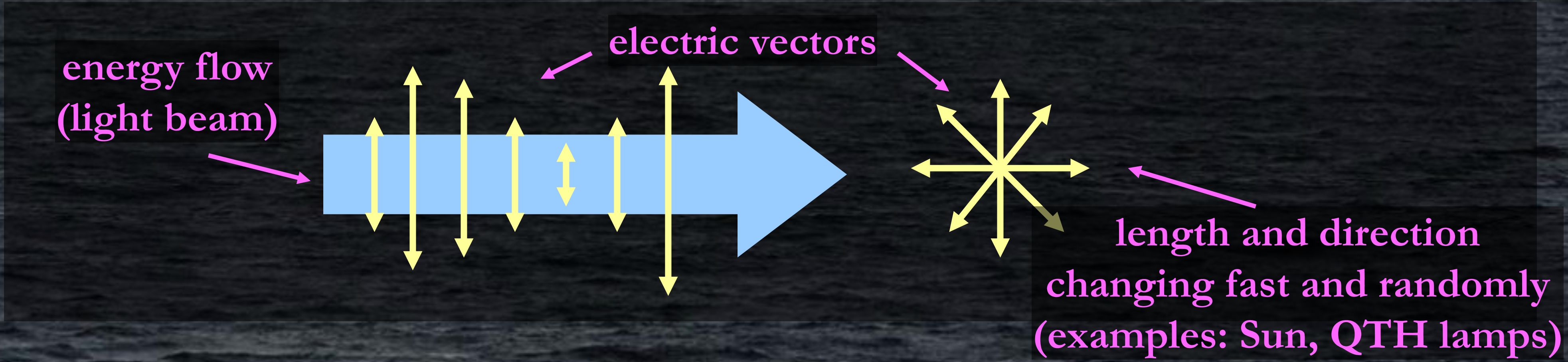

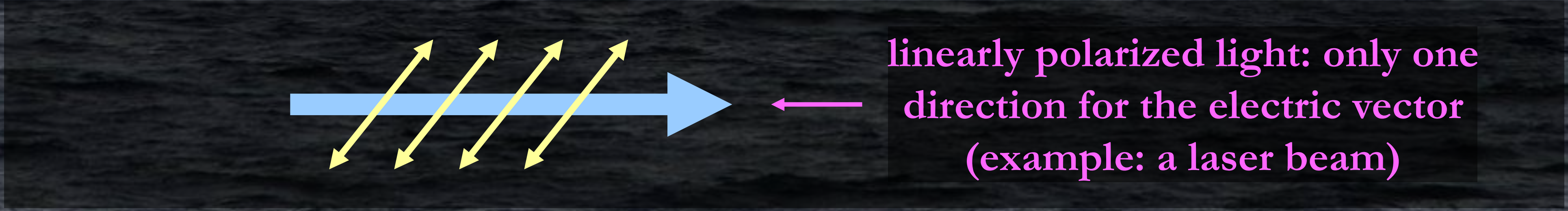

Polarization of light

Scattering and reflection change the radiation's degree of polarization.

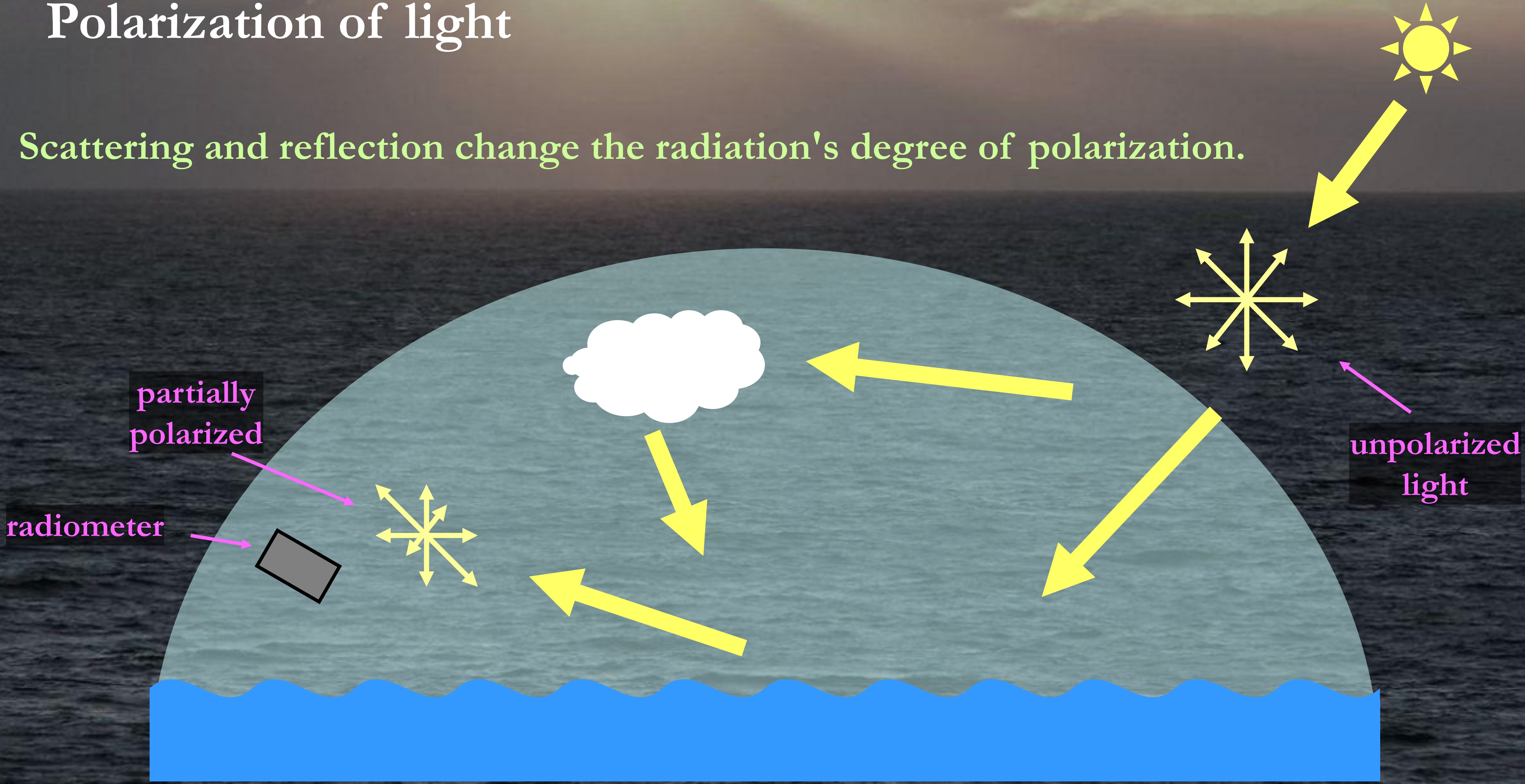

Polarization sensitivity

Polarized light interacts with the radiometer's polarization sensitivity.

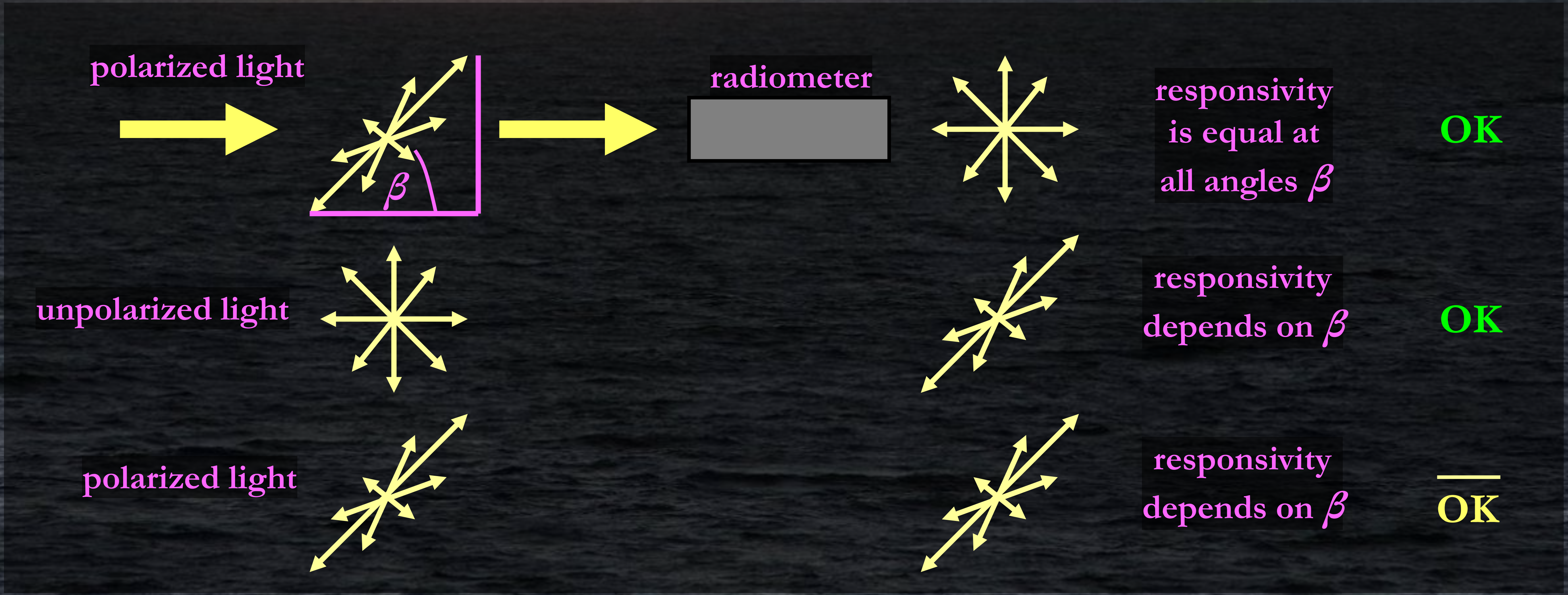

Polarization sensitivity

Polarization state of the radiation is described by Stokes vector.

Interaction with the polarized light is described by the Mueller matrix.

[Kostkowski: Reliable spectroradiometry]

Characterization of radiometers: determine responsivity at different angles β.

[Talone 2016]

Diffuser of the irradiance sensors de-polarizes the input radiation.

Characterization of the radiance sensors is needed.

Measurement of the polarization sensitivity

Output radiation of the sphere is unpolarized.
Polaroid creates linearly polarized beam.
Polaroid is rotated around the optical axis and the radiometer's output signal recorded.
Angle of the maximum responsivity is referenced to the "red dot".

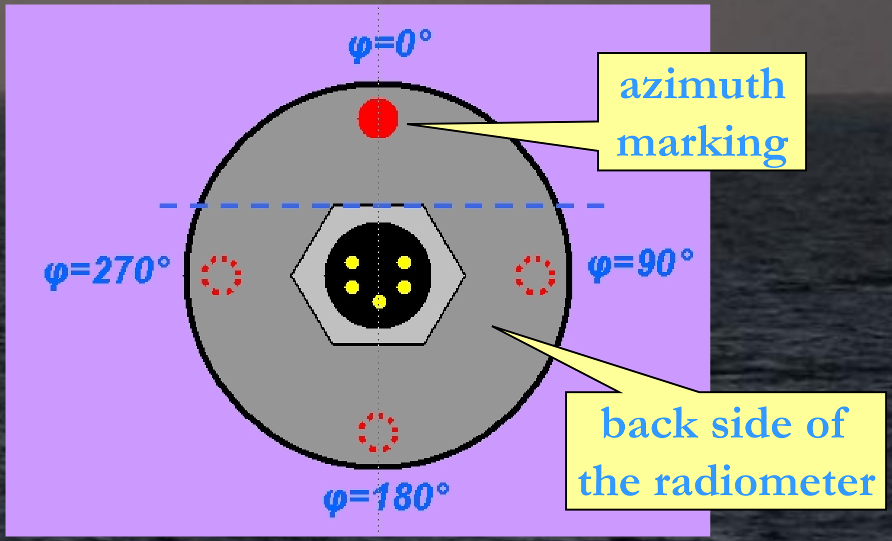

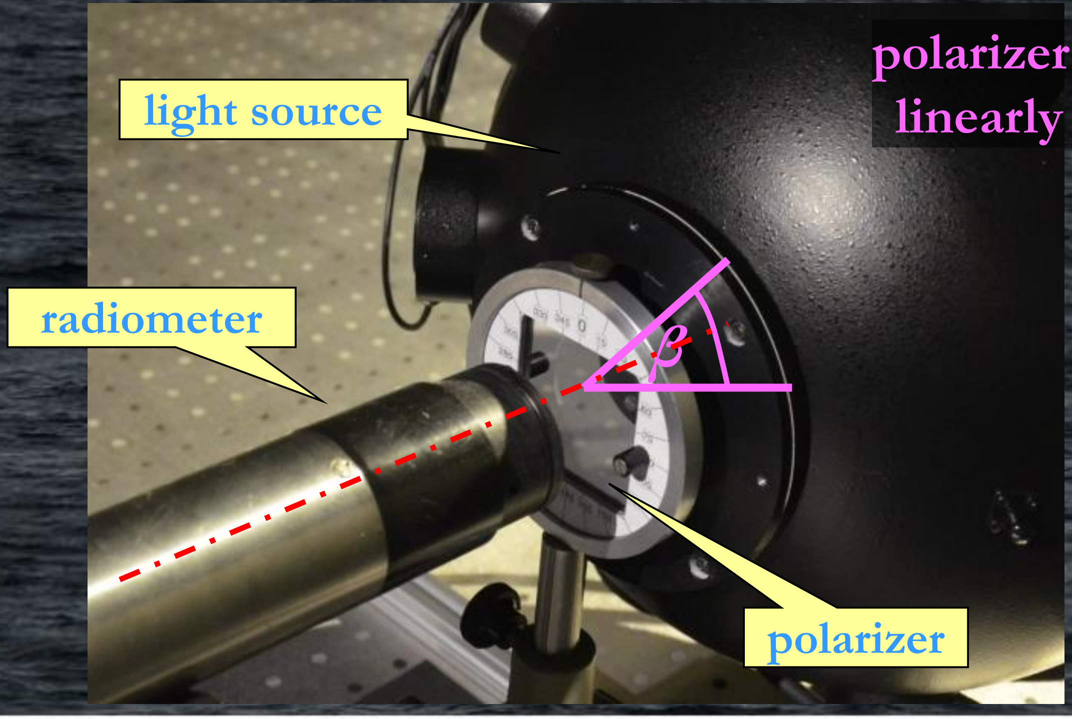

polarizer provides nearly linearly polarized light

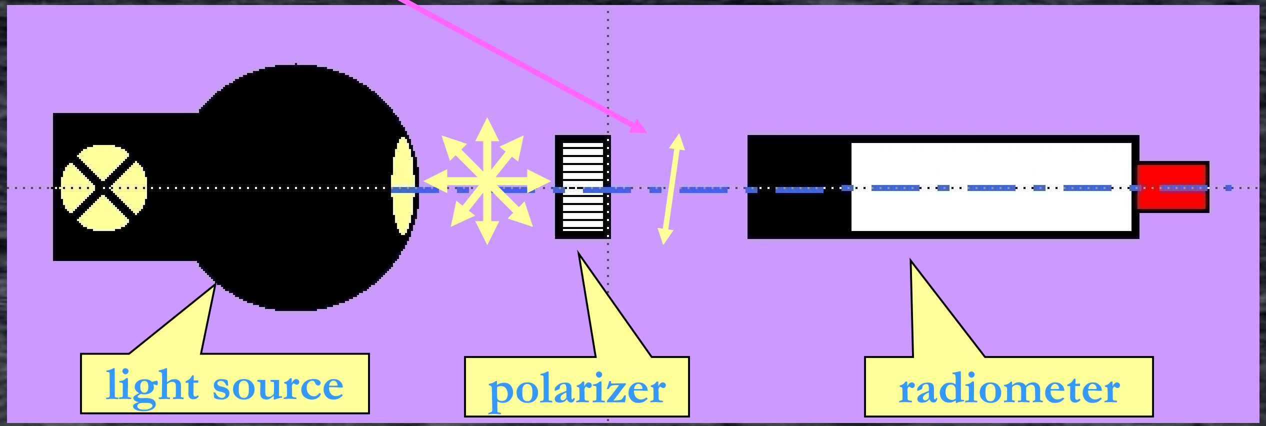

Polarization sensitivity

Because the detector acts on the magnitude of the electric vector, responsivity shows two maxima and minima per full rotation of the polarization plane.
Polarization sensitivity dependes on the wavelength.
Amplitude and phase angle of the signal change are reported in CP_*_POLAR_* files.

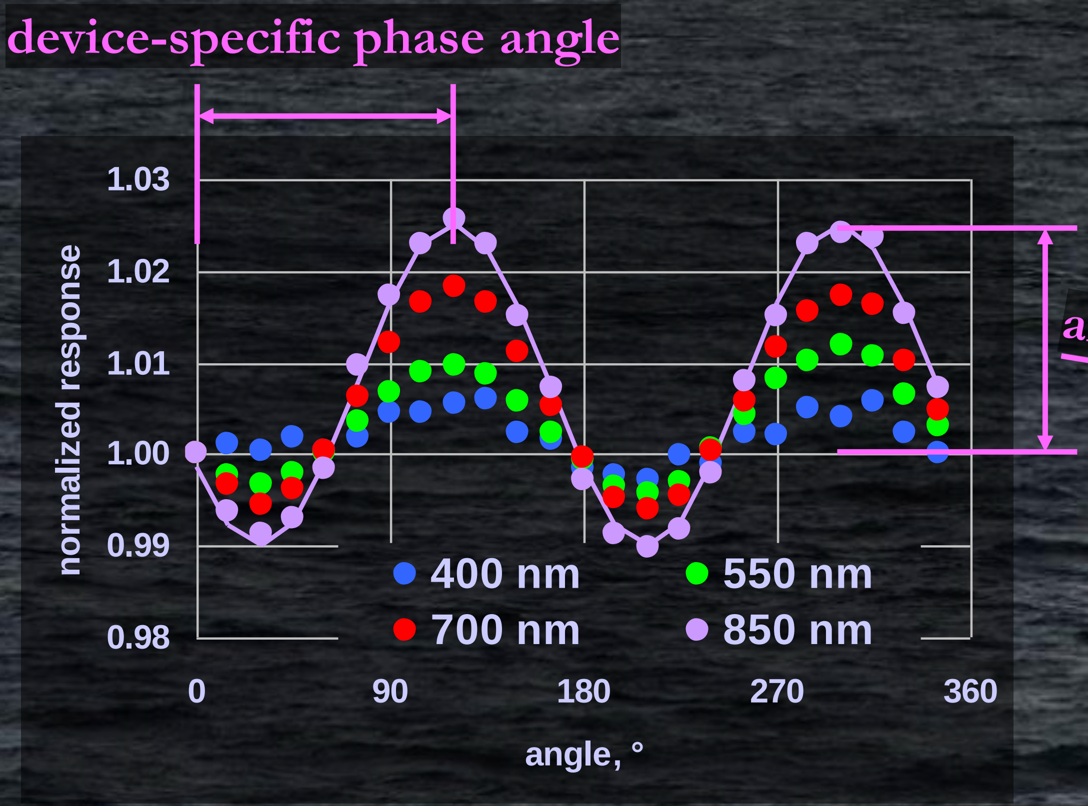

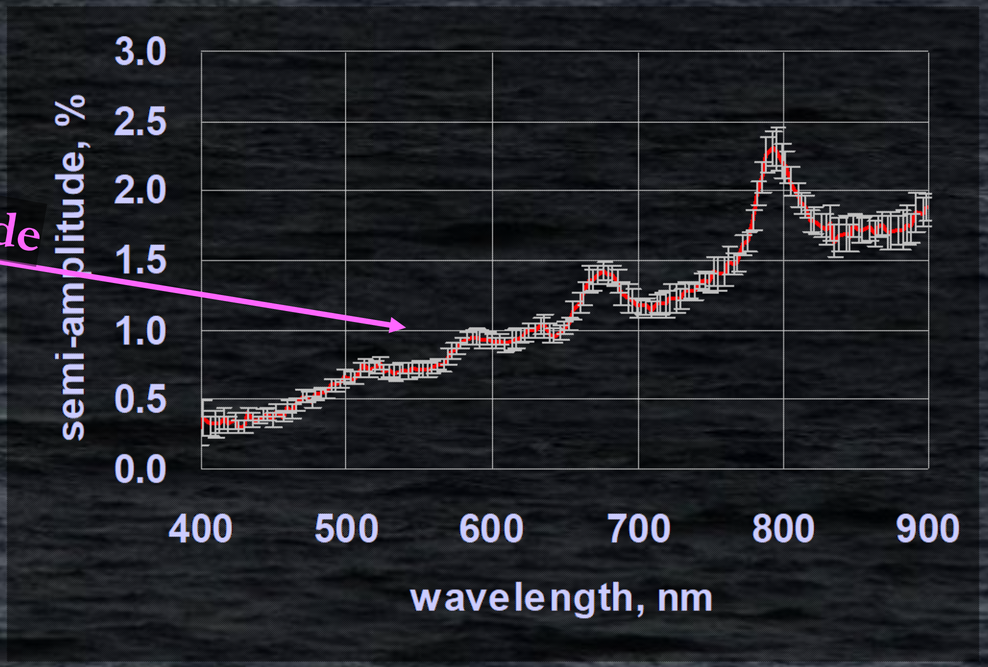

Uncertainty due to the polarization sensitivity

Degree of linear polarization (DOLP) of the OC signals interacts with the polarization sensitivity of the radiance sensors.

Example DOLP taken from [Mobley 2015, D'Alimonte 2016, Voss 2010]

Uncertainty of R_{rs} corresponds to the "worst case" scenario.

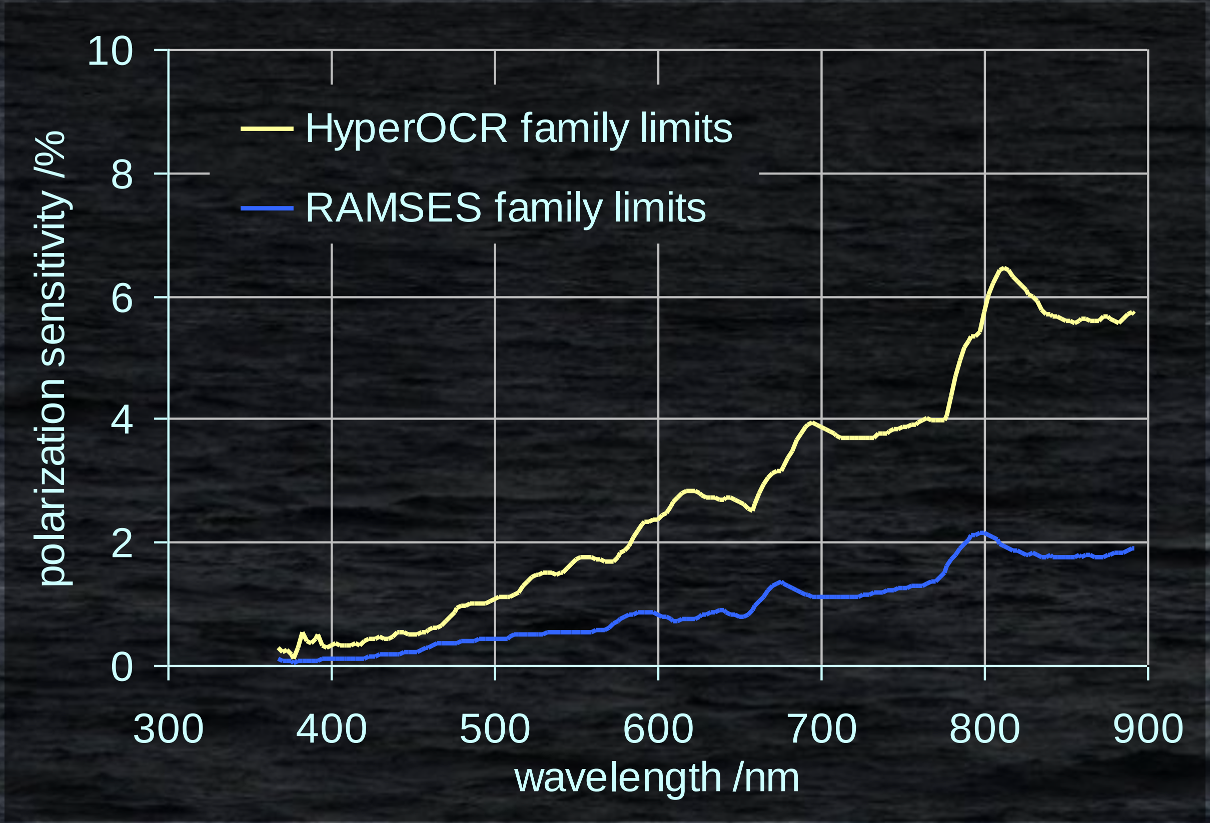

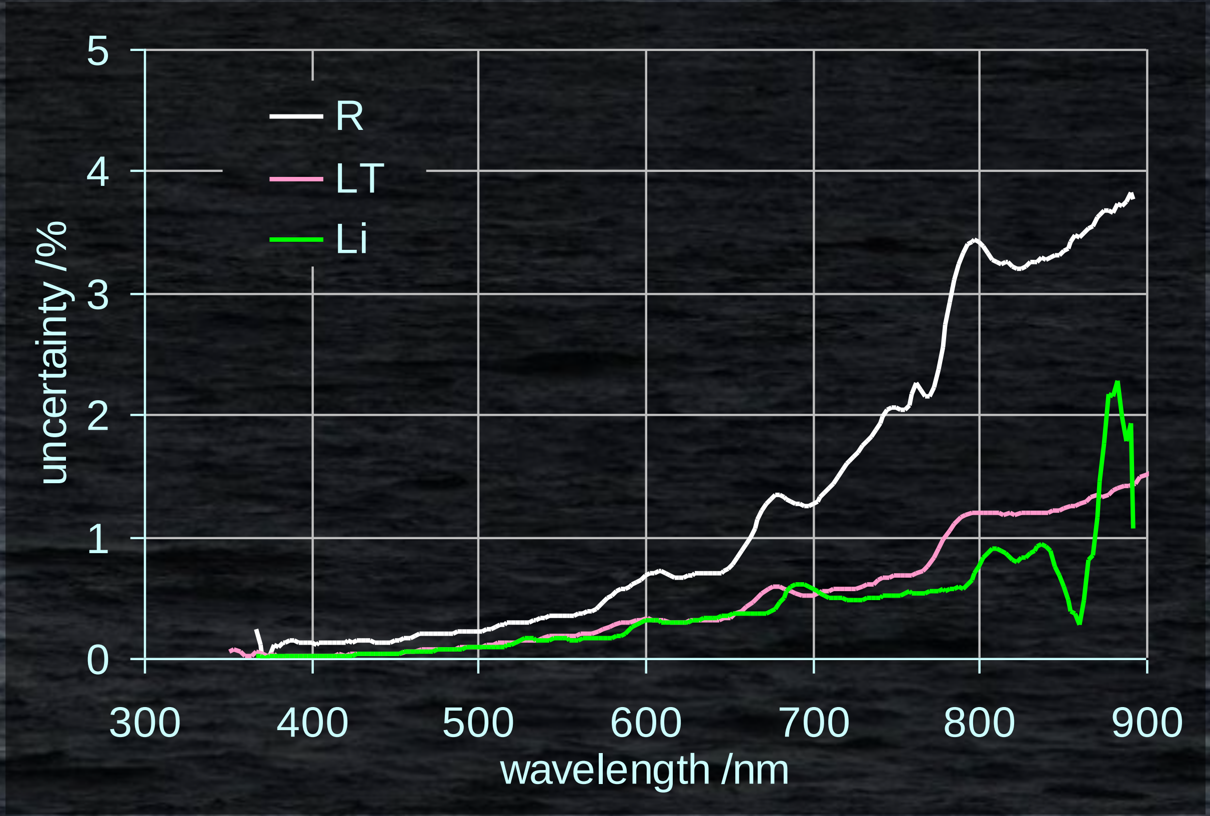

Other parameters, not implemented during FRM4SOC:

Temporal response

Ideal case: output signal of the radiometer corresponds to the temporal integral of the input flux during the integration time.

Reality: the output signal "remembers" previous flux or signal values.

Characterization method: test output signals at different integration times and illumination scenarios.

Remedy: drop a few spectra when changing the illumination level or integration time.

Other parameters, not implemented during FRM4SOC:

Accuracy of integration times

Characterization method: strobed light sources or reverse engineering.

Discrepancies at the 4 ms integration time discovered during the non-linearity characterization of RAMSES and HyperOCR.

The shortest integration time for HyperOCR is actually 5 ms.

The shortest integration time for RAMSES is actually 4.05 ms.

Remedy: avoid the 4 ms integration time.

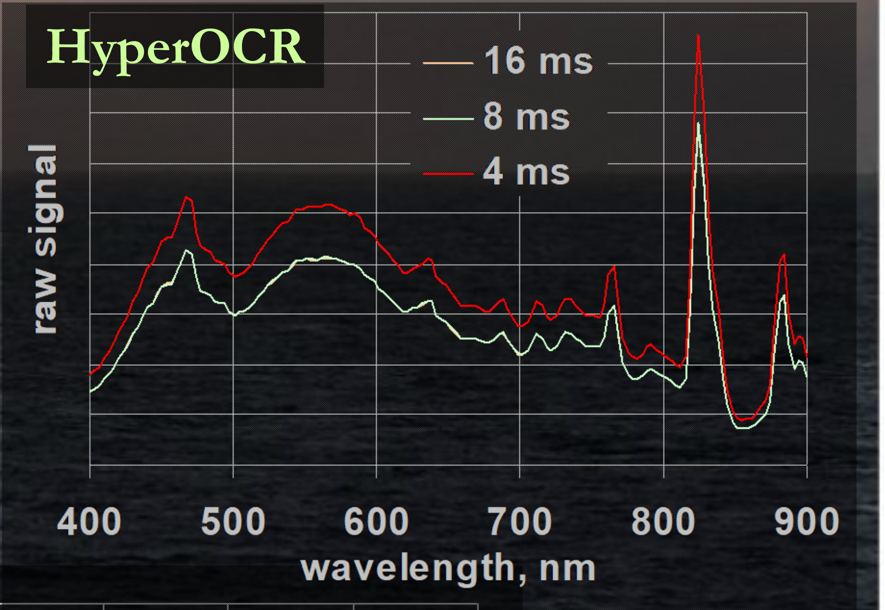

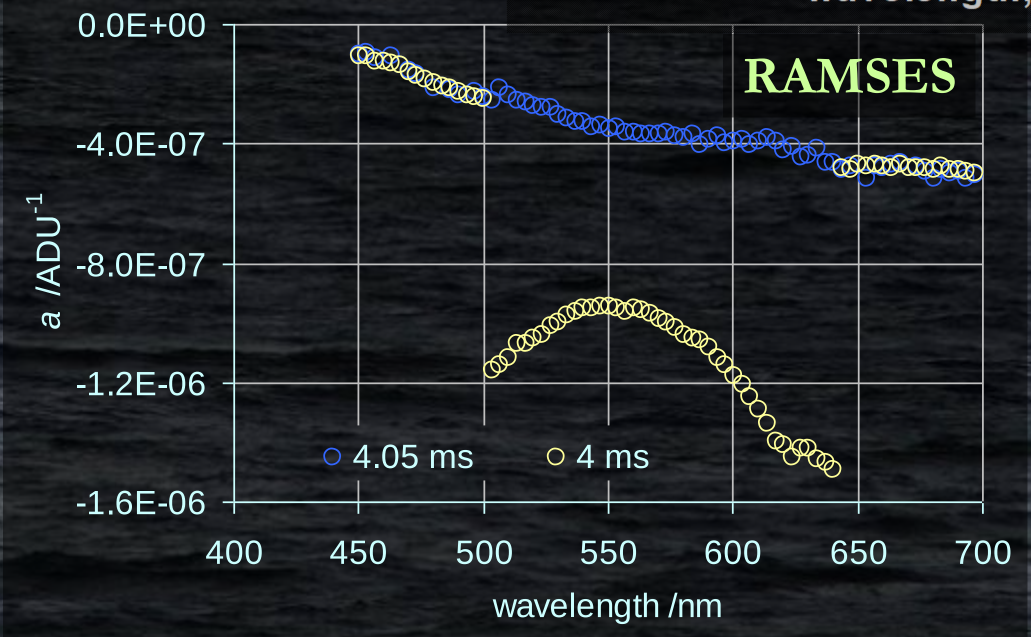

Other parameters, not implemented during FRM4SOC:

Immersion factors

Radiometric responsivity depends on the refraction index of the environment (1 for air, 1.34 for seawater). Reasons: changes in the acceptance solid angles and in the boundary reflection & transmission.

Characterization method: direct determination by using spezialized water tank [Zibordi 2004].

Angular response depends on environment as well: HyperOCR is produced in two versions for in- and above-water applications while RAMSES is optimized for above-water.

Remedy: use proper calibration coefficients or apply immersion factors.

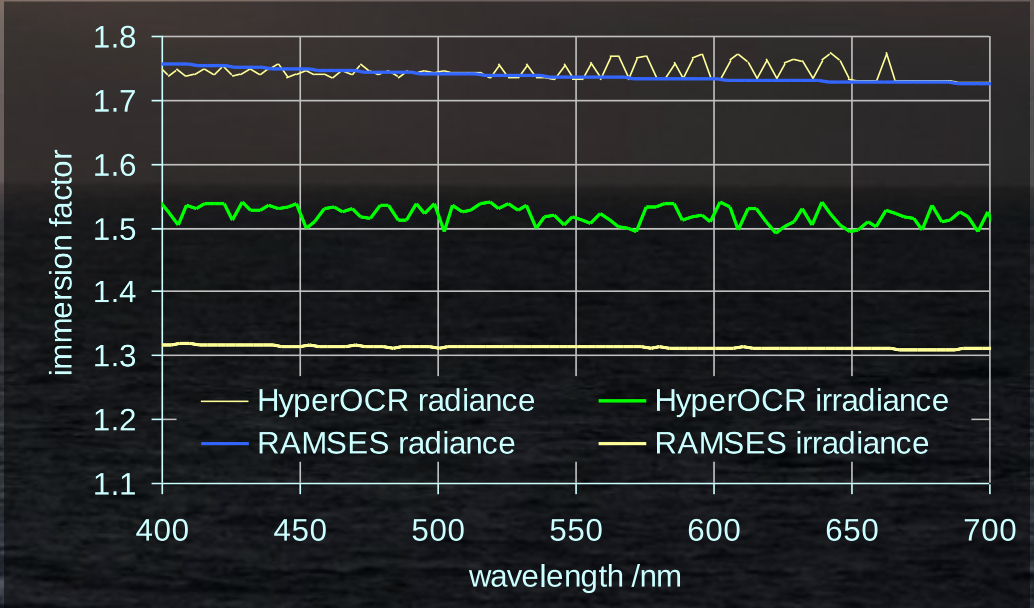

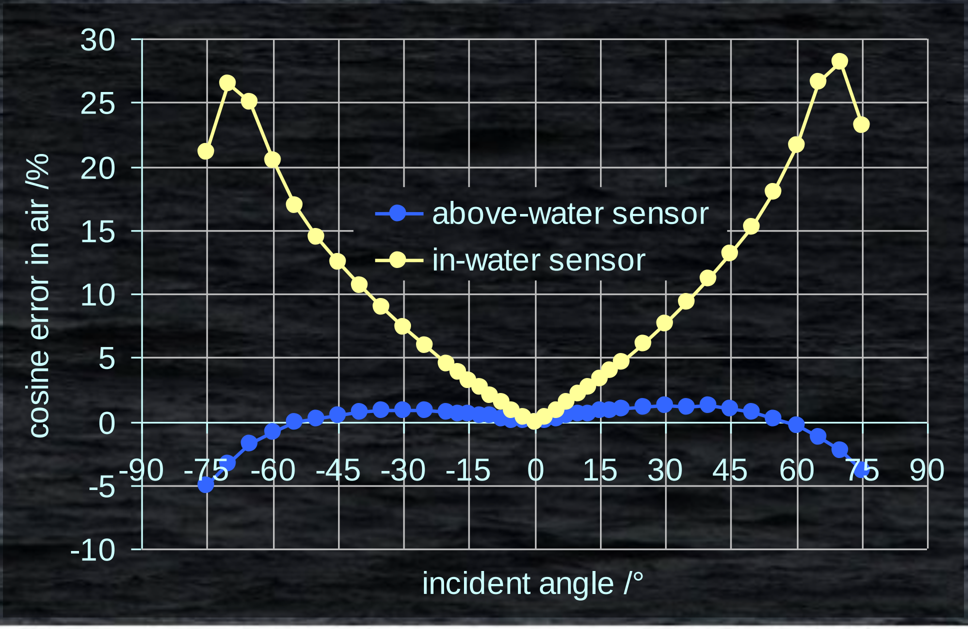

Other parameters, not implemented during FRM4SOC:

Pressure effects

Objectives: possible change of optical path inside the radiometer due to mechanical stress.

Proposed characterization method: barochamber with optical window.

Not needed for above-water applications.

[Das Boot (1981)]

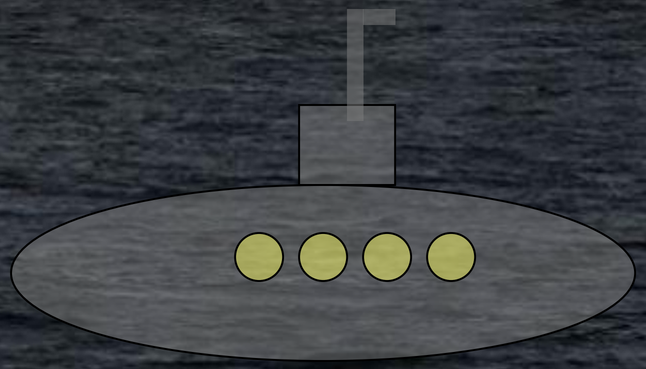

On the measurement precision

Unwanted drifts and SNR need to be suppressed below 0.1 % level during the characterization measurements in order to achieve reasonable uncertainties.

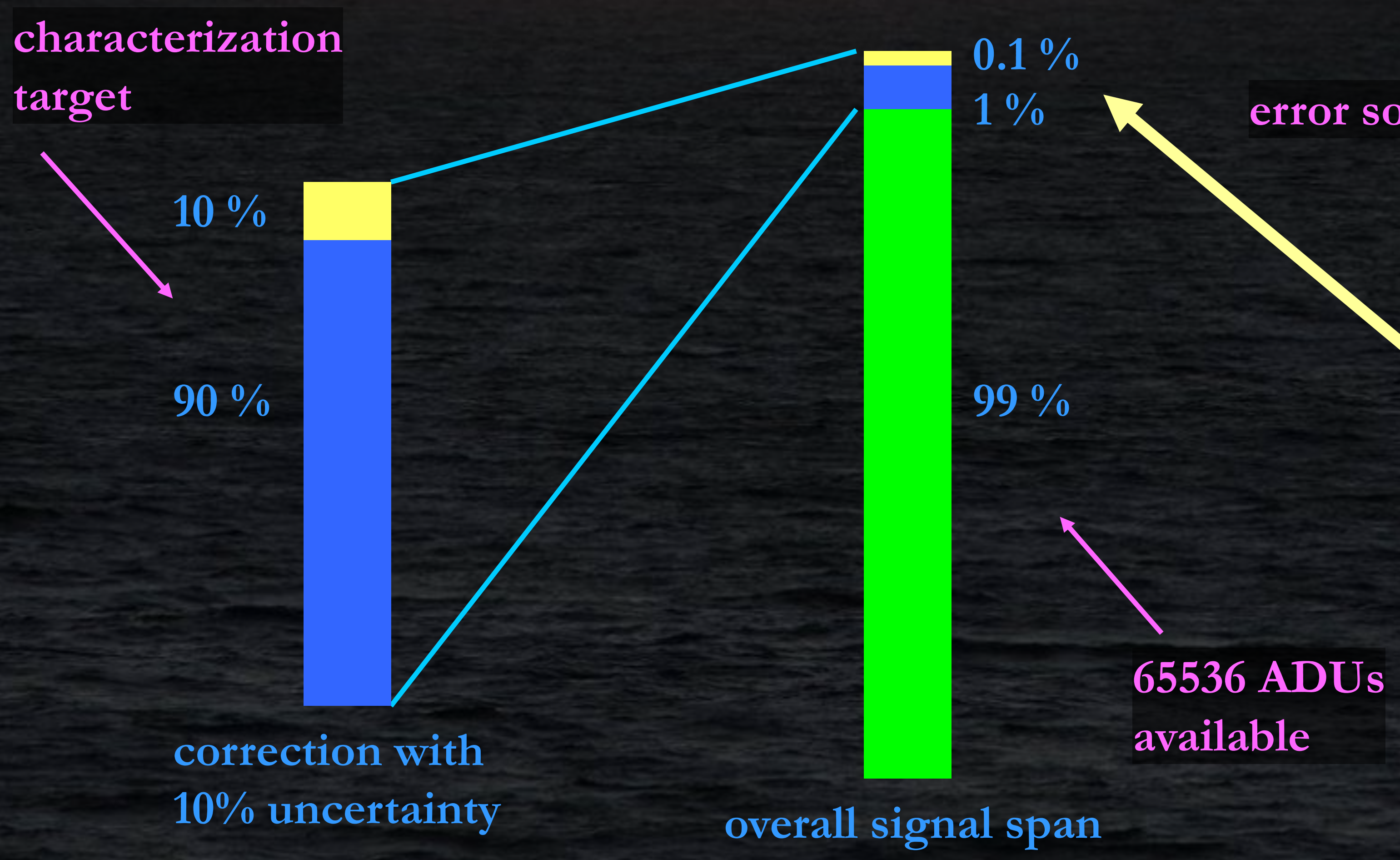

error sources, % of the useful signal

non-linearity: 2 %

thermal: 2 % / 10°C

dark drift: 1.5% / °C

polarization: 1 %

source drift: 0.1 %

SNR: 0.1 %

Uncertainty of R_{rs}

contributions if not corrected

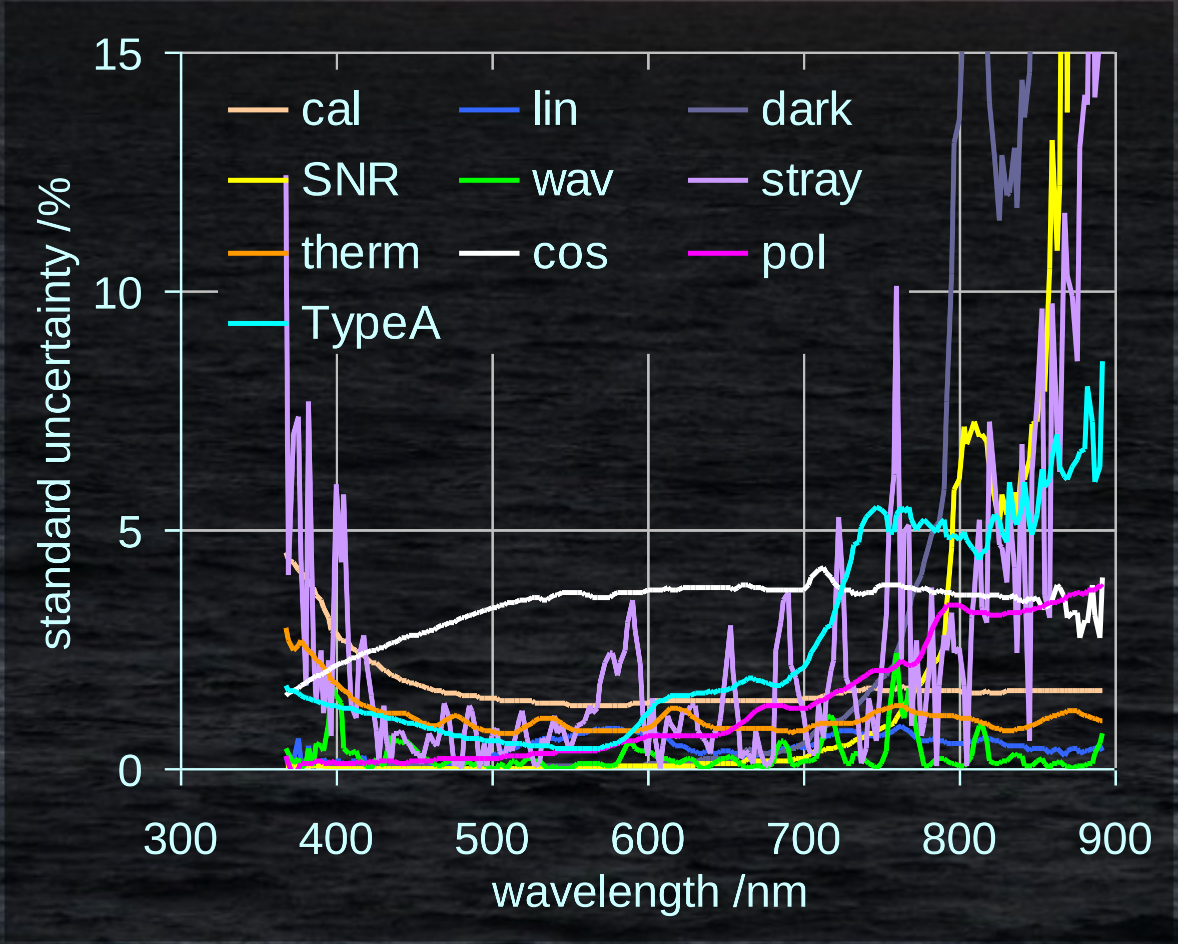

without and with corrections

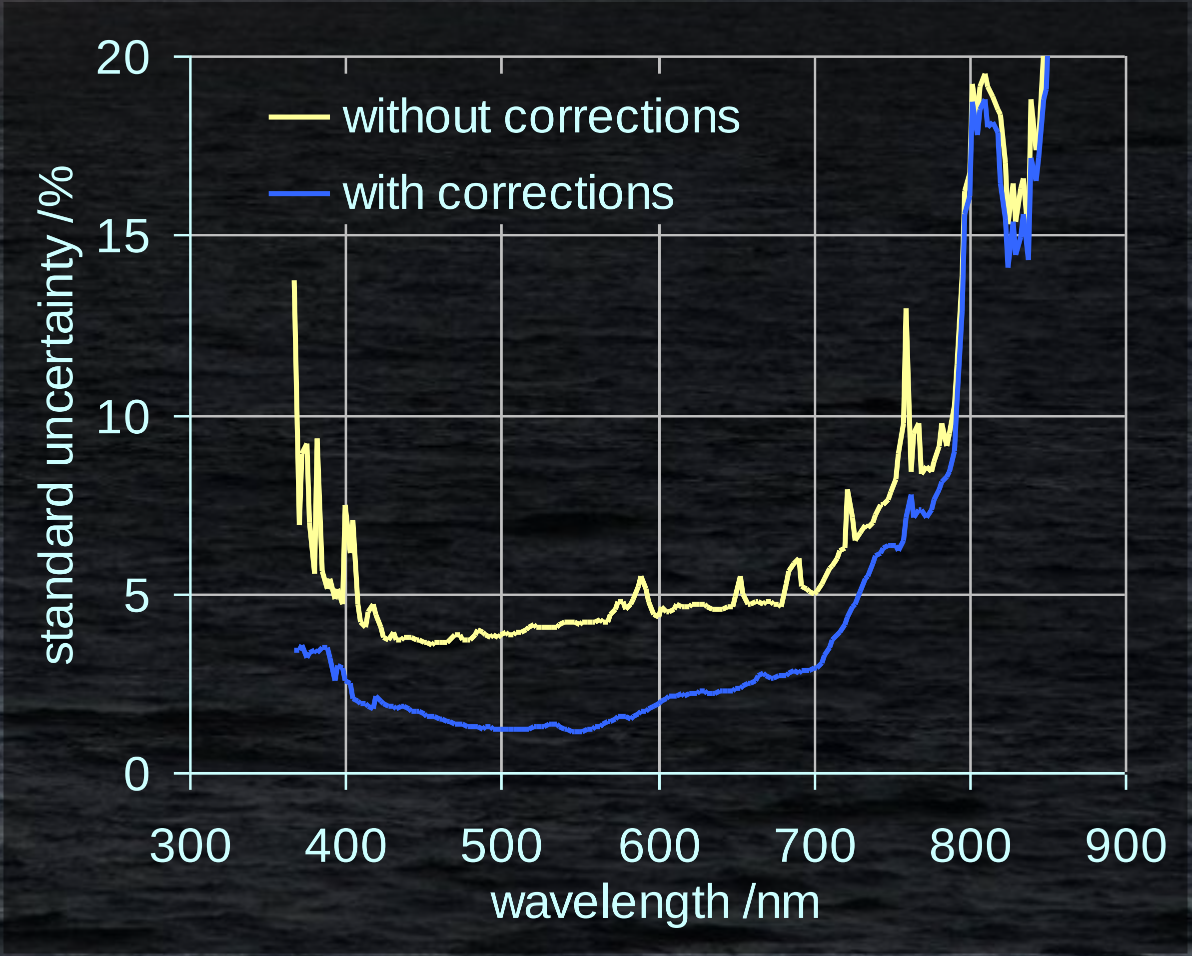

Uncertainty budget of R_{rs}

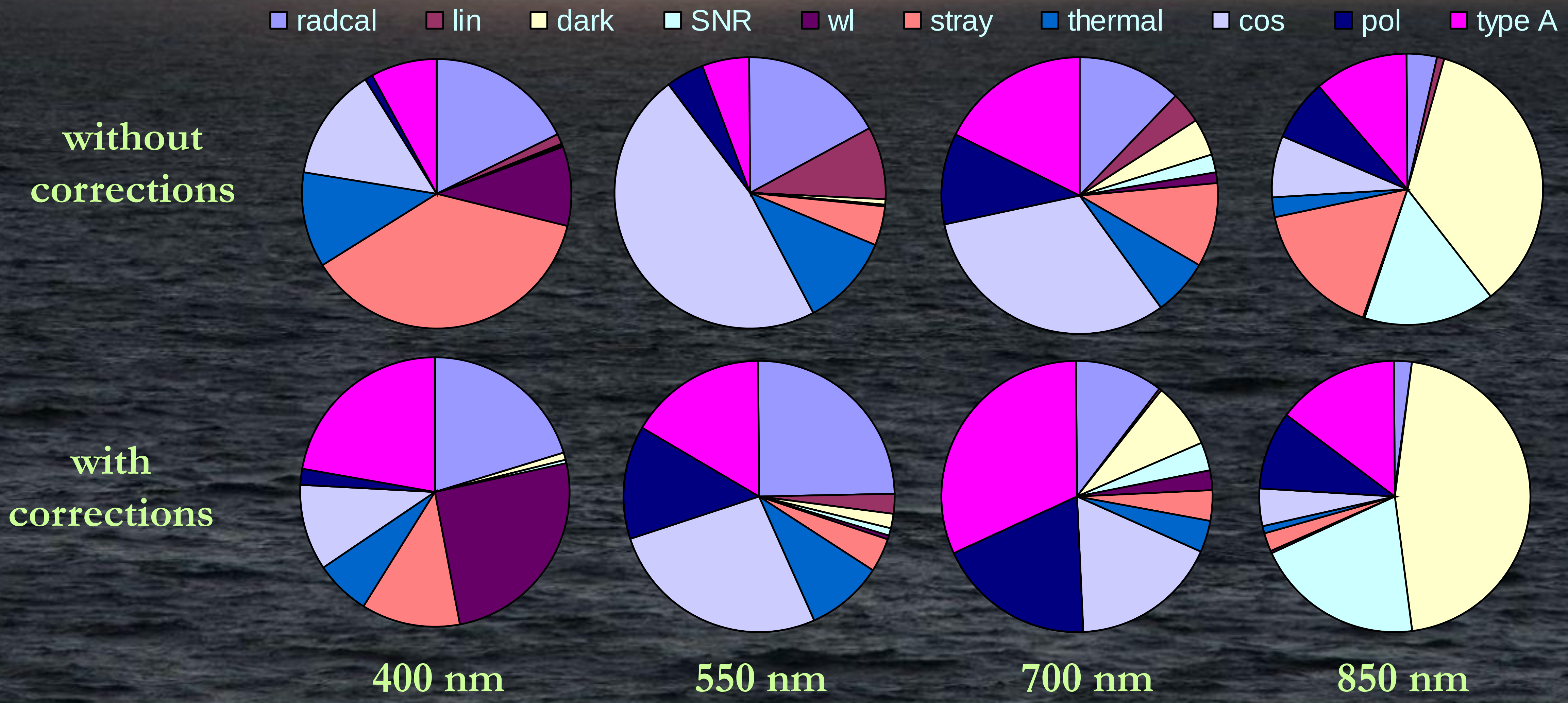

On the importance of calibration

During the FRM4SOC LCE2 experiment, participating radiometers were used to measure stable sources in laboratory environment.

Measurement geometry was close to the one during calibration.

Results were evaluated by using "legacy" (provided by the users) and the fresh "uniform" responsivity coefficients.

"Disagreement" was calculated as standard deviation of the results over ≈40 participating radiometers.

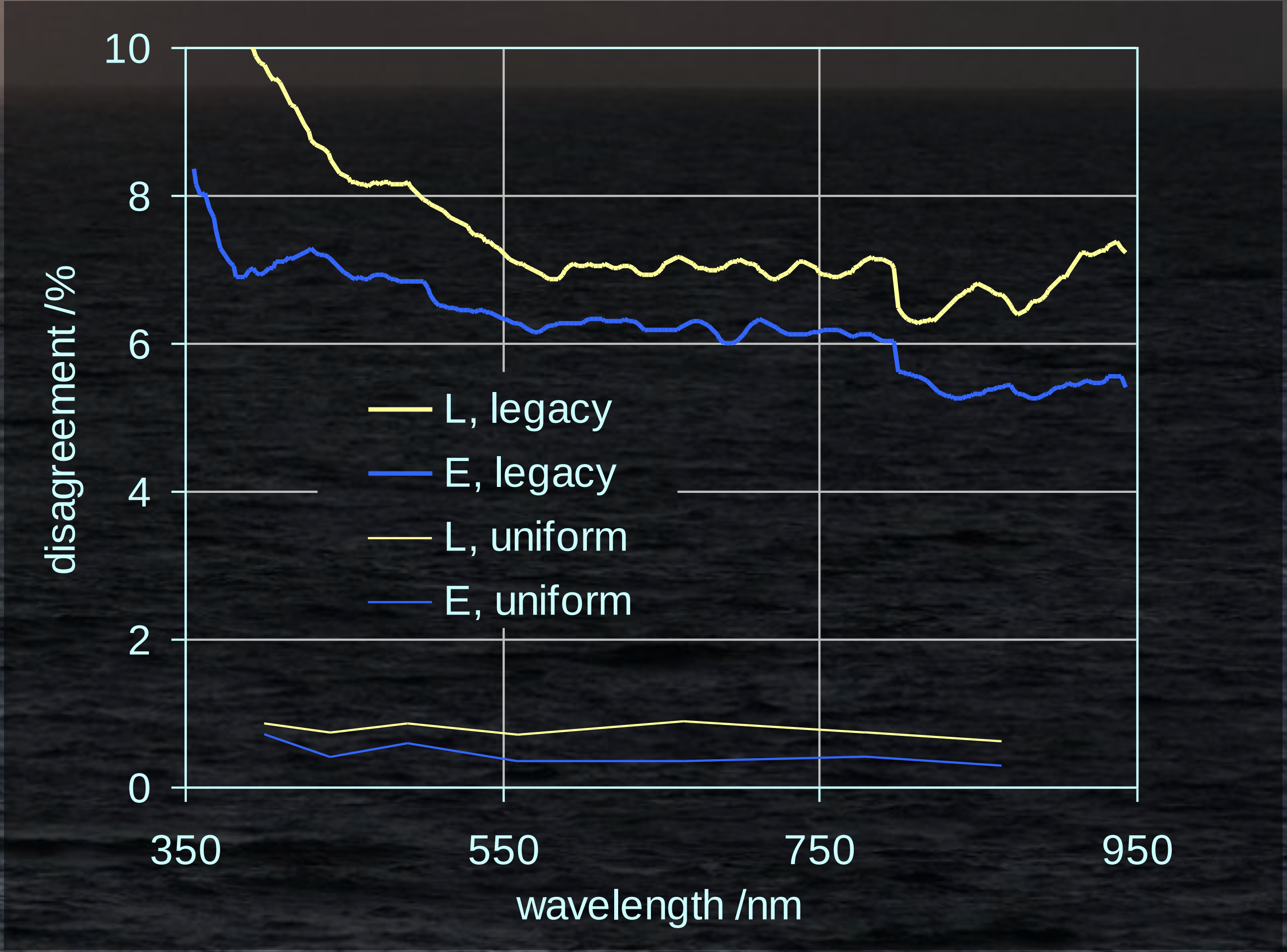

On the importance of characterization

During the FRM4SOC LCE2 experiment, freshly calibrated radiometers were taken to the field to measure radiance and irradiance of the natural objects.

Conclusion: radiometric calibration alone is not sufficient, we need characterization as well.

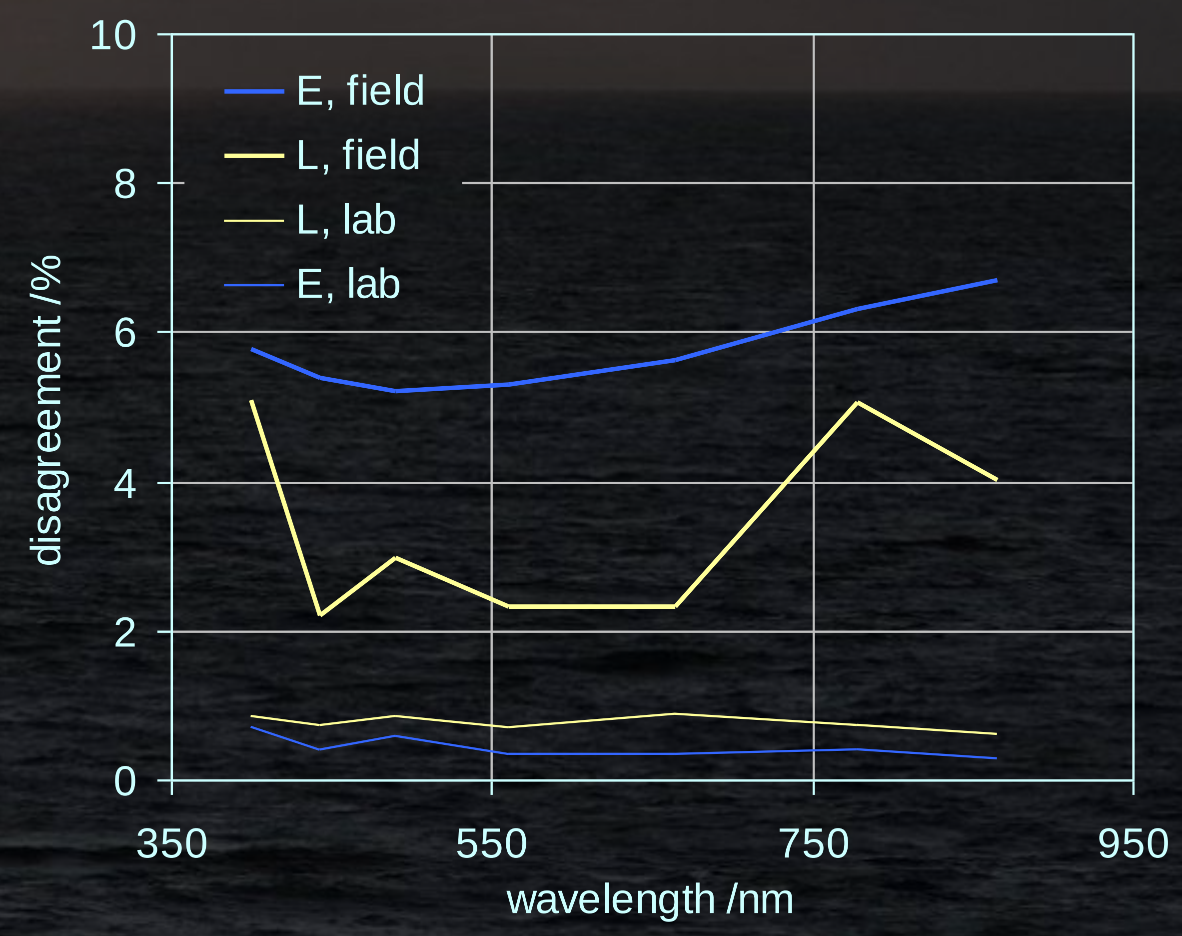

Conclusions

The instrument characterization results cannot be directly converted into the uncertainty of the OC products as the measurement conditions and properties of the measurand affect the result.

Radiometric calibration, linearity, angular and thermal sensitivity contribute the most to the uncertainty budget.

The number and the motivation of the labs regarding the opto-electronical characterizations are insufficient.

TODO: better cooperation with manufacturers to improve the instrumental parameters.

TODO: develop a reference radiometer.